Research on Engine Speed Tracking and NOx Emission Reduction of Diesel Engine by Modified Guaranteed Cost Control and MPC

Ge YU

December 2019

Waseda University Doctoral Dissertation

Research on Engine Speed Tracking and NOx Emission Reduction of Diesel Engine by Modified Guaranteed Cost Control and MPC

Ge YU

Graduate School of Information, Production and Systems
Waseda University

December 2019

Abstract

Internal combustion (IC) engines have become the most important power source for automotive during the last 140 years. Diesel engine shows most efficient performance among internal combustion engines including gasoline engines. Thus the diesel engines have been widely applied in heavy-duty applications such as big trucks on the road and electric generators off the road. With the challenges of fuel economy and emission legislation, the performance of diesel engine should be further improved.

In order to satisfy the increasing requirement of fuel efficiency and strict emission standard, the advanced technologies of diesel engine have been well developed. Modern diesel engine is normally equipped with two systems including exhaust gas recirculation (EGR) system and common-rail injection system. These two systems work together to reduce the exhaust emissions, particularly NOx with optimal fuel efficiency guaranteed. The control parameters in the system consist of the fuel quantities of injection, injection timing and injection pressure during different injection period by common rail. And the variables also include EGR valve opening, temperature of the engine cylinder, the engine load, etc. All these setting variables have influence on the engine performance such as engine speed, fuel consumption, and emissions.

The complication of control will increase the development effort and cost. Furthermore the traditional method by manual calibration is time consuming and does not lead to optimal results. Thus the model-based control method becomes attractive since it can solve such complicated problems efficiently.

The traditional study of engine behavior which influence combustion efficiency and exhaust emission has only been concentrated on the steady-state based on pre-calculated maps. But the real driving usually consists of many transient actions of engine such as change of speed and load. Furthermore comparing with the steady states, the fuel consumption and emissions are much worse during transient conditions. Thus so as to further improve the performance of diesel engine, the research during transient operation has much potential. Thus this study will concentrate on two topics: 1. dynamic model for control purpose; 2. robust control algorithm in consideration of model uncertainty for real-time application.

As for the above-mentioned topics, the dynamic model-based control of diesel engine has been developed. The real process is described by dynamic model with uncertainty. Then the guaranteed cost control method is studied which could guarantee a certain cost

under model uncertainty. Furthermore in consideration of input constraints, modified model predictive (MPC) is proposed to make the steady error zero by disturbance model which could describe the model mismatch. The proposed control systems have been successfully implemented on an one cylinder diesel engine. The dissertation consists of six chapters which are organized as follows:

Chapter 1 briefly describes the research background. Developing more effective system is essential for improvement of fuel efficiency and reduction of exhaust emissions for diesel engine. After emphasizing the importance of dynamic model-based methods during transient condition, the motivation and objective of this research are presented.

Chapter 2 describes the current status of studies on model-based control methods of diesel engine. It analyzes various MBCs according to their different models and control algorithms. The main challenges and strategies of this dissertation are expressed.

Chapter 3 introduces the experimental device and dynamic model of diesel engine by linear state space equation. In our test bench, the YANMAR TF70V-E diesel engine is modified for research application by the MicroAutoBox of dSPACE system. The data of inputs and outputs for modeling is obtained from this system. Furthermore the models for control purpose of diesel engine are described. In consideration of computation speed, linear state space equation is selected for modeling. Firstly the engine models are defined including the inputs and outputs. Engine speed and NOx value are chosen as the control targets. Accurate and fast tracking of engine speed will increase the fuel efficiency. NOx is the main emission of diesel engine when lean burn mode is applied to ensure other emissions such as particular matter, CO in a low level. Then the general binary noise (GBN) signals are designed to excite the engine system to get the data for modeling. At last the models are identified by the prediction-error minimization (PEM) method. (The second modeling fit for engine speed and NOx is 77.4% and 80.3%.)

Chapter 4 presents the extended guaranteed cost control of the diesel engine system with input constraints. The combustion uncertainties and nonlinear behavior of diesel engine are expressed by parameter uncertainties based on linear state space equations obtained in Chapter 3. The uncertainties are presented by variation on parameter matrices. The idea of confidence interval is proposed to describe this variation. The uncertainty matrices designed in our paper will ensure the confidence interval 75.45% for the engine speed model and 87.03% for the NOx emission model. For controller design, the quadratic performance with uncertainty, the inputs constraints and the demand of tracking are guaranteed by three augmented linear matrix inequalities (LMIs). The

gains of control and state estimate are obtained simultaneously. Then the real-time test by the proposed approach is done in our test bench. Comparing with traditional method LQR, for case 1 in the defined linear working range(2300 2500rpm), the tracking error for engine speed by the proposed method decreases by 37.2% and NOx emission value decreases by 19.2%. For case 2 with bigger working region(2200 2600rpm), the overshoot for engine speed by the proposed method decreases by more than 68.8% and NOx emission value decreases by 38.3%. For case 3 with the biggest working range (2100 2700rpm), the tracking error for engine speed by proposed method decreases by more than 34.0% and NOx emission value decreases by 33.7%. The experimental results prove that the designed cost guaranteed cost algorithm is effective and applicable.

Chapter 5 raises a modified model predictive control of diesel engine with no steady error. Since the application of input constraints in the prior chapter is not so convenient (initial state in the LMI need to be calculated each time), the MPC method becomes an attractive choice. Facing the model uncertainty and mismatch, the disturbance model is used in MPC. Based on this disturbance model, the condition for no steady error has been obtained. In details, in order to get the parameter B_d and D_d in disturbance model, dynamic observer has been built in which the cost function is optimized under H_∞ norm. The solution of this H_∞ has been proposed by the satisfaction of one LMI. A two-step algorithm has been proposed to search the optimal value of two parameters α and γ in LMI. The first step is to optimize γ under the assumption that $\alpha = 1$; the second step is to search the suitable α to satisfy the condition of zero offset. Then the state observer could be obtained based on the parameter B_d and D_d. Finally the obtained disturbance model and state observer are applied in the solver (qpOASES) of quadratic programming (QP) problem, which is the core of MPC problem. The real-time test by the proposed approach is also done in our test bench. The experimental results prove that the designed control system can achieve the reference tracking control of engine speed precisely, meanwhile the emissions can be reduced feasibly. For case 1 in the defined linear working range (2300 2500rpm), the tracking error for engine speed by the proposed method MPC 3 decreases by 61.2 % and NOx emission value decreases by 35.1% comparing with MPC 1 which is designed by normal MPC method. For case 2 with bigger working range (2150 2650rpm), comparing with MPC 1,the tracking error for engine speed by the proposed method decreases by 95.3% and NOx emission value decreases by 11.8%.

Chapter 6 gives the conclusions and future work.

Acknowledgements

First and foremost, I would like to express my deepest appreciation and gratitude to my dedicated supervisor, Professor Harutoshi Ogai, for giving me the opportunity to pursue my PhD degree, for his patience guiding me around all the research topics. His wide knowledge and his attitude and academic style have been great value to me.

Grateful thanks to Professor Li and Professor Tateno for their patiently review of my dissertation and lots of valuable comments.

Moreover I would like to thank all the group members in Diesel Engine group of Ogai Lab. Many thanks to Haoyang Deng for his constructive discussions all through my research. I would also like to acknowledge the other members and office staffs for their friendship and kind helps. The whole life here will always be in my memory.

Finally, I would like to appreciate my loving parents, Aijun Yu and Hong Qi, my wife Wenjing Cui for their love. Without their support and understanding, I can not continue my education life. This thesis is dedicated to them.

Kitakyushu, Japan

Ge Yu

December 2019

Contents

List of Figures

List of Tables

Chapter 1

Introduction

1.1 Research background

After Nikolaus Otto (1876) firstly applied 4-cycle internal combustion (IC) engines successfully and Rudolf Diesel (1892) proposed the idea of compression ignition, IC engines have been the main power source of automotive which pushed the development of society during the last 140 years [1]. In recent decade, the other power sources of vehicles such as electric, natural gas and bio-fuels have been developing. However the wide application of such alternative power sources has the limitation due to high cost and short of power storage [2]. Meanwhile, in order to satisfy the increasing requirement of fuel efficiency and strict emission standard, the advanced technologies of modern automotive engines have been well developed. Thus there is still a bright future for the development of IC engines for vehicles in the 21st century [3].

1.1.1 Society problems of fuel crisis and air pollution

With the growth of the global population and an increasing number of vehicles, the concern about fuel crisis and air pollution caused by automotive has been raised. The study showed that there will be an increasing demand for energy consumption from road transportation in the next twenty years. It is shown in Figure1.1. Although there is some small development for other energy supplies, fossil fuels including gasoline and diesel will still be main sources. As we know, the fossil fuels are precious resources which can not be renewable.

In order to meet the growing demand of energy consumption from road transportation, it is an essential issue to improve the fuel efficiency for the automotive industry.

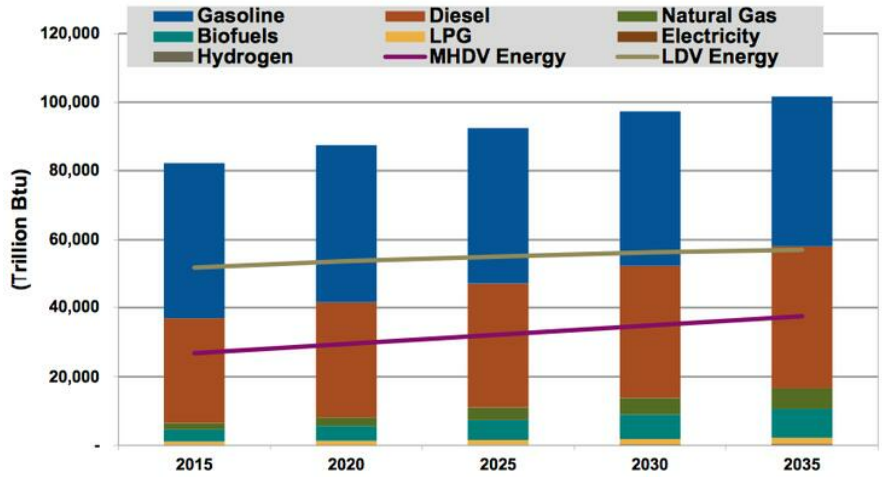

FIGURE 1.1: Energy consumption from road transportation (Navigant Research 2014)

On the other hand, the environment problems caused by emissions from vehicles have been widely concerned by the society in recent years. The well-known emission regulation from the European Union was firstly introduced in 1992. It included the limits for exhaust emissions such as carbon dioxide (CO), hydrocarbon (HC), nitrogen oxide (NOx) and particulate matter (PM). With the increasing concern about the environment problems caused by the emissions, the regulation has become stricter and stricter. The emission regulation by EU for heavy-duty diesel engines is shown in Figure 1.2. We can see that limits for all emissions have been reduced in a great amount, i.e. the critical value on NOx has been reduced by 97% [4]. And we believe that the regulation will be further enforced in the near future (by Figure 1.3). Thus in order to satisfy the tighter requirement, the performance improvement of diesel engine which is concentrated on reducing exhausted emissions is really necessary and important.

Stage	Date	CO(g/kWh)	HC(g/kWh)	NOx(g/kWh)	PM(g/kWh)
Euro 1	1992	4.5	1.1	8.0	0.612
Euro 2	1996	4.0	1.1	7.0	0.25
Euro 3	2000	2.1	0.66	5.0	0.10
Euro 4	2005	1.5	0.46	3.5	0.02
Euro 5	2008	1.5	0.46	2.0	0.02
Euro 6	2013	1.5	0.13	0.40	0.01

FIGURE 1.2: EU emission standards for heavy-duty diesel engines

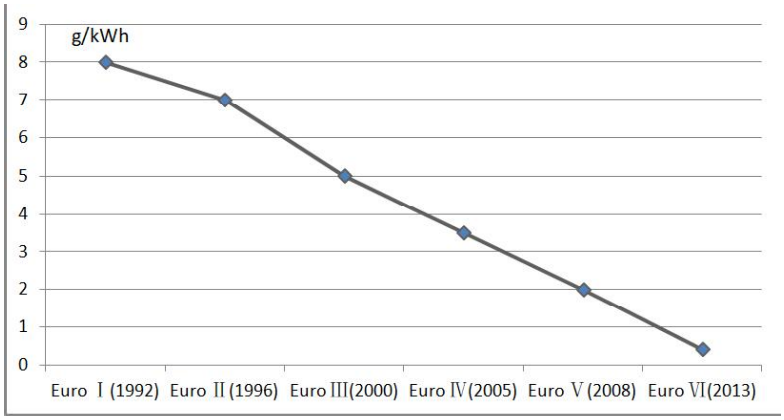

FIGURE 1.3: Trend of standard for NOx

1.1.2 Development of technologies for diesel engine

The diesel engine shows most efficient and powerful performance among internal combustion engines including the gasoline engine. It has been widely used in heavy-duty applications such as big trucks on the road and some generators off the road. The early diesel engine is very big, heavy and noisy. With the persistent efforts of researchers and engineers through many generations, the modern diesel engine has been well developed.

In last section, we discussed the main challenges for IC engines. The target is to satisfy the increasing requirement for fuel efficiency and stricter emission standards. Especially in the last decade, many advanced technologies have been developed and successfully implemented in the diesel engine.

Common-rail injection system is one important technology that is made up of three parts. The first one is a pump which can be controlled. The second part is the common rail that the fuel can go through. And the last part is the injectors that can be electronically controlled. The pressure of injectors are more than l00MPa and the fuel quantities of the injections are really precise in small scale [5].The injection strategy such as the pressure of fuel injection, the timing of fuel injection, and the quantity of fuel injection can be flexibly organized to contributes to the highly efficient combustion. But higher NOx is produced inevitably. EGR (Exhaust gas recirculation) is another advanced technology recirculating the exhaust gas into intake manifold driven by the motor. It will reduce peak temperature of combustion when the exhaust gas is inserted into the cylinder. Consequently the formation of NOx will be suppressed [5–7]. But high EGR levels reduce the amount of fresh air, which will cause an increase in particulate matter and possibly visible smoke. The particulate matter is emitted because of uncompleted combustion of diesel or lacking of oxygen. It is now reduced

by turbocharger, diesel particulate filter (DPF)[8], or by applying the lean burn which may cause engine damage and high level of NOx[9]. Last but not least, in order to govern all these components, a powerful engine control unit (ECU) is needed. With an increasing number of setting variables and more sophisticated structure, algorithms that can optimize the control parameters should be well developed. The control parameters of diesel engines in recent generations is shown in Figure 1.4. We can clearly see that the number of control parameters is growing. As a result, it is critical and difficult to operate modern diesel engine properly.

Year	Number of actuators	Description of control parameters
2001	1	Injector valve
2004	3	Injector valve EGR valve VGT
2007	6	2Injector valves EGR valve VGT Inlet throttle HC doser
2010	7	2Injector valves EGR valve VGT Inlet throttle HC doser Turbo-compound engagement Urea doser
2015+	10+	2Injector valves EGR valve VGT Inlet throttle HC doser Turbo-compound engagement Urea doser VVT

FIGURE 1.4: Control parameters of diesel engine

1.1.3 Model based control method

The complication of control will increase the development effort and cost. Furthermore the traditional method by manual calibration is time consuming and does not lead to optimal results. Thus the model-based control method become an attractive option due to its ability of dealing such complicated problems efficiently. The advantage of model-based control method is shown as follows:

- Decrease the number of experiments
- Increase the efficiency of development procedure
- Improve the response and effect of control

The model for control purpose consists of static model and dynamic model. The static model-based control method uses mass experiment data to acquire the regression model and combines the mathematical optimization theory with control parameters [10–17]. Control inputs could be obtained in each static operating point. One example of optimized results by TOYOTA is shown as follows in Figure 1.5. In each static operating point defined by engine speed and load, the corresponding optimal control inputs (such as injection quantity, timing and pressure) are obtained.

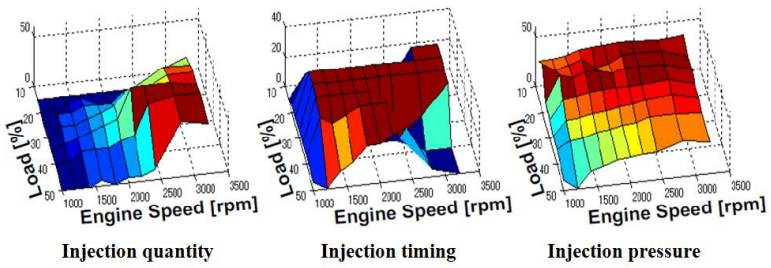

FIGURE 1.5: One example of optimized results by TOYOTA

The dynamic model-based control method is used to calculate the control inputs in each sampling time. Dynamic model can predict the process. And the control algorithm will optimize the inputs to satisfy the cost function (Target). The most representative structure of dynamic model-based control is shown in Figure 1.6. Different kinds of dynamic models and control algorithms are introduced in Chapter 2. The better performance during transient condition makes dynamic model-based control a hot topic in last two decades.

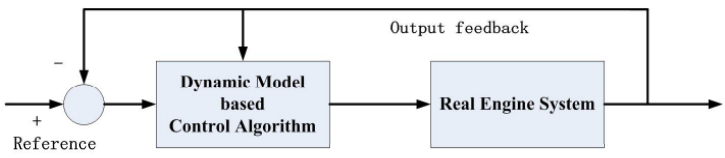

FIGURE 1.6: Dynamic model-based control structure

1.2 Motivation and objective

The traditional study of engine behaviour which influence combustion efficiency and exhaust emission has only been concentrated on the steady-state. But the real driving usually consists of many transient actions of engine. Furthermore comparing with the steady states, the fuel consumption and emissions are much worse during transient conditions [18]. Thus in order to further improve the performance of diesel engine, the research during transient operation has much potential. Motivation is listed as follows:

- Desire to improve the fuel efficiency and reduce the emissions of diesel engine, especially during the transient condition.
- The requirement for real-time application which could be used in the vehicle driving test.

In this study, a modern diesel engine was applied. It was equipped with a common rail injection system and EGR system. Our objective is to design the transient model-based control that satisfies the above requirement for real-time application of diesel engine. Furthermore the control system is modified for the challenge of nonlinear fast engine process with input constraints. As for the research objective, the detailed work is shown as follows:

- Analyzing the characteristics of engine during the transient condition of engine speed.
- Constructing a linear dynamic model with high computation speed based on the experimental data.
- Modification of two control algorithms based on the obtained model suitable for the nonlinear fast engine process with input constraints.
- Implementing the control algorithms into a real engine and validating the control strategies in the real-time application.

1.3 Organization of the dissertation

This thesis shows the cumulative works over my doctor career through six chapters. Chapter 1 laid the the fundamental background and story that connects the whole thesis. In Chapter 2, the previous research has been reviewed. The experimental engine and modeling of diesel engine for online control purpose are introduced in Chapter 3. Based on the identified model, Chapter 4 proposed a extended guaranteed cost controller design method. And Chapter 5 develops an offset-free model predictive control method by combined design of disturbance model and observer. Finally, our findings and future study are summarized in Chapter 6. Figure 1.7 shows the thesis outlines.

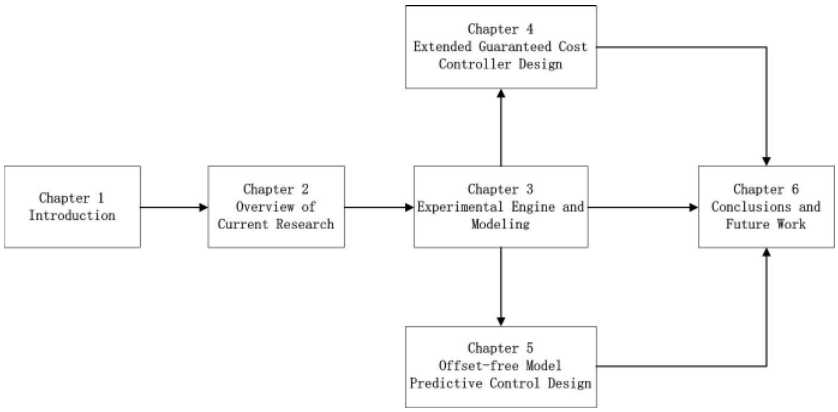

FIGURE 1.7: A diagram of the thesis outlines

The general theme of this thesis is to apply dynamic model-based control method for real-time application on diesel engine for satisfying the driver's demand and reducing the exhaust emission.

The overview of current researches is described in Chapter 2. The current status of studies on model-based control method of diesel engine is introduced. It analyzes various MBCs according to their different models and control algorithms; discusses current problems; and then expresses the main approaches of this dissertation.

In Chapter 3, the experimental engine setup is introduced firstly. Then the model is identified for control purpose. The procedure of the linear system identification of engine model is proposed. At first the inputs and outputs of the model are selected for control purpose. Then the stair tests are performed to ensure the linear working region and inputs constraints. And the general binary signals (GBN) are designed based on the step-responses. Finally the linear state space models of diesel engine process are

identified based on the data of inputs and outputs from real-time experiments by the PEM method.

In Chapter 4, the extended guaranteed cost state-feedback control of diesel engine with input constraints is presented. The engine process is fast and uncertain. In order to achieve the real-time application, the combustion uncertainties and nonlinear behavior are expressed by parameter uncertainties based on linear state space equations obtained in Chapter 3. For controller design, the quadratic performance with uncertainty, the inputs constraints and the demand of speed tracking are guaranteed by three augmented linear matrix inequalities (LMIs). The gains of control and state estimate are obtained simultaneously. Then the real-time test by the proposed approach is done in our test bench. The experimental results prove that the designed control system achieves a satisfied performance. The main contributions related to this chapter are shown as follows:

- The process of diesel engine through both air and fuel loop is expressed by linear state space equations with parameter uncertainties based on the idea of confidence interval;
- Compared with traditional guaranteed cost control, the state feedback and estimate gains are given from feasible solution of an augmented LMI simultaneously;
- To deal with tracking problem and physical constraints, more LMI conditions are discussed.

Chapter 5 raises a modified model predictive control of diesel engine with no steady error. Since the application of input constraints in the prior chapter is not so convenient, the MPC method becomes an attractive choice. As MPC itself has robustness to uncertainties, the main problem is the steady error in real-time application. In order to solve this problem, the definition of disturbance model and state estimate is firstly given. Then the parameters of disturbance model and state estimate are obtained from a combined design based on H_∞ theory. For the solution to H_∞ problem, there will be two challenges. Firstly for general application of H_∞ theory, the general solution is put forward. Secondly with the dimension of the model increasing, the reduced-order design for H_∞ problem is needed. Then a two-step algorithm is presented for the reduced-order solution which is suitable in general case. Finally the obtained disturbance model and state estimate gain are applied in the solver (qpOASES) of quadratic programming (QP) problem, which is the core of MPC problem. The real-time test by the proposed approach is also done in our test bench. The experimental results prove

that the designed control system can achieve the reference tracking control of engine speed precisely and affectively, meanwhile the emissions can be reduced feasibly. The main contributions related to this chapter are shown as follows:

- Compared with traditional offset-free tracking control, the disturbance model and state estimate are given from a combined design based on H_∞ theory.
- The general solution of H_∞ problem is put forward for the condition of tracking control without steady error.
- With the dimension of the model increasing, the reduced-order design for H_∞ problem is discussed.
- A two-step algorithm is presented for the reduced-order design problem which is suitable for the above additional condition.

Chapter 6 summarizes the thesis and gives suggestions for potential future research.

Chapter 2

Overview of Current Researches

2.1 Introduction

This chapter describes the current status of studies on model-based control method of diesel engine. With the purpose of increasing fuel efficiency and reducing emissions, researchers have developed many MBCs with different models and control algorithms. Instead of traditional methods based on look-up tables, the MBCs can ease the burden of calibration work when setting variables in diesel engine grow. As discussed in the prior chapter, we can categorized MBCs according to their models and control algorithms (including optimization algorithms). To discuss the existing MBCs in detail, this chapter is organized in the following: section 2.2 discusses different optimization algorithms based on different static models. Section 2.3 focuses on different control strategies based on different dynamic models. Section 2.4 summarizes the current MBCs and gives the conclusion.

2.2 Static model-based control

The static model-based control which is also called static model-based calibration is well developed by researchers in universities and companies. It could be easily applied in real-time application of diesel engine, because the solutions are obtained off-line which is shown in Figure 2.1 [19]. Afterwards, these optimal values are verified on the test bench. If the verification was successful, then the engine operation maps are

generated and stored on the ECU. The static model and the optimization method are introduced and compared in this section.

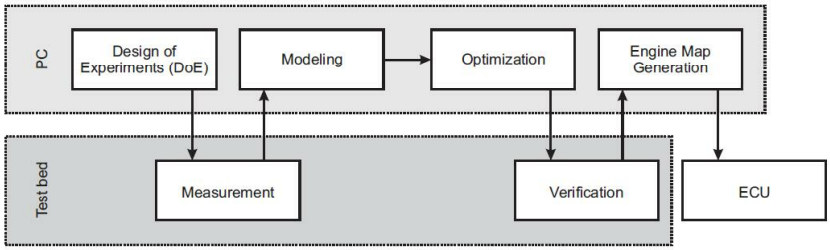

FIGURE 2.1: Static model-based calibration

2.2.1 Static model

The static model mainly consists the following three types:

polynomial model

The polynomial regression model used for engine calibration are mainly with first and second order. That with first order is in the following form [20, 21]:

$$y = \sum_{i=1}^{n}(a_i x_i) + c_i \tag{2.1}$$

That with second order is in the following form [22–26]:

$$y = \sum_{i=1}^{n}(b_i x_i) + \sum_{i}\sum_{j}(b_{ij} x_i x_j) + \sum_{i=1}^{n}(b_{ii} x_i^2) + c_i \tag{2.2}$$

where x_i are the inputs, y is the outputs. The polynomial model expresses the relationship between the inputs and outputs of diesel engine. A number of regression analysis are done to get coefficients$(a_i, b_i, b_{ij}, b_{ii})$ so that the models can be used to describe the responses.

redial basis function

Redial basis function (RBF) can be applied to build a regression model. RBF is suitable for building functions for such a target: diesel engine[27]. RBF is widely applied in nonlinear usage. Comparing with other modeling methods, it has rapid convergence [28, 29]. RBFs are radially symmetric functions that can be used to model complex surfaces with limited data [30]. A radial basis function can be written as

$$z(x) = f(||x - c||) \tag{2.3}$$

where f is the radial basis kernel. ||...|| means the Euclidian distance between input x and center c. The kernel function f can be of many different forms. Some examples of kernel functions and RBFs can be seen in Figure 2.2.

Type	Profile Function/ Kernal	Radial Basis Function
Gaussian	$f(r) = e^{\frac{r^2}{\sigma^2}}$	$z(x) = \exp\left(\frac{\|x-\mu\|^2}{\sigma^2}\right)$
Multiquadric	$f(r) = \sqrt{r^2 + \sigma^2}$	$z(x) = \sqrt{\|x-\mu\|^2 + \sigma^2}$
Reciprocal Multiquadric	$f(r) = \frac{1}{\sqrt{r^2 + \sigma^2}}$	$z(x) = \frac{1}{\sqrt{\|x-\mu\|^2 + \sigma^2}}$
Linear	$f(r) = -r$	$z(x) = -\|x-\mu\|$
Cubic	$f(r) = r^3$	$z(x) = \|x-\mu\|^3$
Logistic	$f(r) = \frac{1}{1 + \exp\left(\frac{r}{\sigma}\right)}$	$z(x) = \frac{1}{1 + \exp\left(\frac{\|x-\mu\|}{\sigma}\right)}$
Thin Plate Spline	$f(r) = r^2 \log(r)$	$z(x) = \|x-\mu\|^2 \log(\|x-\mu\|)$

† - σ is standard deviation of profile function

FIGURE 2.2: Types of Radial Basis Functions

Then the entire system is modeled as a linear combination of N radial basis functions with N centers. The RBF network is given by

$$y(x) = \sum_{i=1}^{N} \beta_i z_i(x) \tag{2.4}$$

where β is a weight factor for RBF centered at c_i and y is the output.

neural network

The linear modeling techniques suffer from several limitations since the engine process is nonlinear. The multi-layer perceptron (MLP)neural network which is the general form of RBF can be used as a kind of nonlinear regression model. It has been the most commonly used nonlinear modeling technique in engine calibration. As is well know, the schematic structure of the MLP network is shown in Figure 2.3.

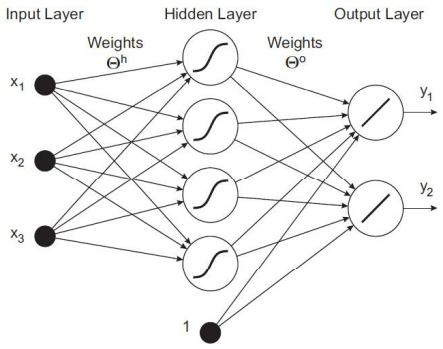

FIGURE 2.3: Schematic structure of the MLP network

The data of inputs and outputs of diesel engine in the static operating point is collected for training the neural network [19, 31–34]. Based on enough data from real test of engine, neural networks are able to learn the complicated nonlinear relationships between each setting variables.

2.2.2 Optimization method

With the model obtained in the section 2.2.1, the optimal settings of the parameters can be found by numerical optimization. Depending on different types of model and objective function, different suitable optimization algorithms can be applied.

response surface method

The response surface method (RSM) includes three parts: modeling, analysis and optimization. The model here is usually the polynomial regression model introduced in the prior part. Then the response surfaces of each inputs are generated. The trade-off between setting variables is analyzed.

Finally the optimal values of engine operating parameters were evaluated by using the desirability based approach of RSM. The RSM has been applied to diesel engine optimization [21, 24–26, 35]. In [21], T. Lee showed a good result of RSM in a high-speed diesel engine that equipped with common rail injection system and EGR valve. In the experiment, the manipulated variables such as injection quantity,injection pressure,injection timing, and EGR are decided. In [35], EGR and injection pressure are selected as manipulated variables. The linear polynomial model was chosen. They also defined an objective function considering NOx, PM. The results proved that it successfully reduced NOx and PM, meanwhile maintained fuel efficiency of a single cylinder direct injection (DI) diesel engine. However, RSM method has a disadvantage of often trapping into a local optima.

genetic algorithm

GA is adaptive heuristic search algorithm based on the evolutionary ideas of natural selection and genetics, which is proposed by John Holland[36]. It belongs to a part of evolutionary computing that has been widely experimented and applied to the fields of artificial intelligence.

Due to the advantage of GA, it has been fully used to emission and fuel efficiency optimization problems of diesel engine [24, 34, 37–41]. In [24], the second-order polynomial model was used to describe emissions(CO, HC, NOx, PM) by injection timing, load torque and engine speed. Comparing with the traditional RSM, GA has less work burden of procedure of trial and error. In [34, 37], the neural network was trained to predict the emissions and fuel efficiency with the ability of solving complex multiple relations. GA was applied in the optimization process to get the optimal AFR (air to fuel ratio), injection quantity and injection timing in each static operating point define by engine speed and load. In [38–41], T.Hiroyasu has done a great job applying and modifying the GA to calibration of diesel engine. In his research, the engine process was described by phenomenological model using HIDECS. Emission and fuel efficiency are selected as optimization target. An extended GA called “Neighborhood Cultivation GA” was applied to solve the problem in [38]. Simulation results proved the effectiveness of the proposed GA algorithm for diesel engine. In [40] T.Hiroyasu extended the former research [38] to multiple injection pattern including EGR.

particle swarm optimization

PSO is a stochastic population-based optimization method which was firstly proposed by Kennedy and Eberhart [42]. PSO is a kind of evolutionary computation. It is based on genetic algorithm and evolutionary programming with particle's velocity and position inside. PSO was integrated with diesel engine experiments to reduce emissions while maintaining high fuel efficiency [20, 23, 43, 44]. In [23], Wahono applied PSO algorithm to a second-order model to find the optimal operating conditions for low emissions. In [20], PSO was modified by Wu with better convergence performance. The objective includes NOx, PM and fuel efficiency. The simulation results prove that the modified PSO show a sufficient solution to satisfy the multiple objectives. In [43, 44], PSO was directly to generate the manipulated variables including EGR, start of injection (SOI) and injection pressure without modeling. The application was implemented in different cases including single- and double-injection. In each static operating point, favorable inputs were obtained.

2.3 Dynamic model-based control

As discussed in Chapter 1, the study of engine behaviour including combustion efficiency and exhaust emission has only been concentrated on the steady-state. But the real driving usually consists of many transient actions of engine. Furthermore comparing with the steady states, the fuel consumption and emissions are much worse during transient conditions [18]. Thus the dynamic model-based control suitable for transient condition has become hot topic last two decades.

The structure of dynamic model-based control has been mentioned in Chapter 1. The dynamic model and the control algorithm are introduced and compared in this section.

2.3.1 Dynamic model

The dynamic model mainly consists the following three types:

thermodynamic model

The thermodynamic modelling for diesel engine is usually based on physical first principles. This kind of models can be found in [45–49]. They can be applied in the performance simulation and prediction, but still too complicated for control purpose.

Thus the so-called mean-value model (MVM) was introduced by some simplification and approximation [6, 50–55]. The mean-value diesel engine models usually consist of a series of first-principles models. In the models, the dynamics inside engine including the intake manifold, the exhaust manifold, the compressor and turbocharger are chosen as state variables. MVMs with a minimum set of differential equations show superiority for control design. It will reduce the computation burden in a certain level. The difference between MVM and other physical models of diesel engine is that time is chosen as the independent variable. Meanwhile the time scale in MVM is considered as one engine cycle. And there are also many literatures about the control method based on the mean-value model.

In [55], the time-based equations of mean-value model is transformed into the engine cycle domain. But the dynamics of turbocharger are not directly related to the combustion behaviour of the diesel engine. They are different from the phenomenon in the intake manifold and exhaust manifold. Therefore the process in turbocharger is better modelled not in cycle domain but in time domain. So as to make the controller solvable, the engine model is simplified with three state equations.

In [52], the mean-value based robust control has been investigated. It focuses on the parameterisation of the turbocharger which is the challenging point of the paper. In order to design the controller for extended operating region, the nonlinear models are simplified and converted into linear parameter-varying (LPV) form.

In [53] the physical MVMs of diesel engine is discussed in details which are used in the dynamic optimization process. Six differential equations were built, which represent the dynamic processes in different engine's blocks (the intake manifold, the exhaust manifold, the cylinder and the variable geometry turbo-compressor). From the above literatures, we know that this kind of method requires much work of parameterization. It is not easy to apply the resulting nonlinear models directly for controller design. Furthermore the mean-value model is often not suitable for modeling of fuel-loop dynamics.

nonlinear parametric identification model

Thus it is really attractive to describe the process of combustion engines by parametric identification models for control purpose. There are two types of model: linear and nonlinear.

With the development of computer technology, the computation ability make the application of nonlinear model available for fast engine process. Two types of model are well developed: NARMAX and neural network.

In [56], a NARMAX model representing the process of diesel engine was raised. The model is in the following form of differential equation.

$$\begin{aligned} y(t) = &-a_0 + a_1 y(t-1) + a_2 u(t) + a_3 u(t-1) + a_4 y^2(t-1) \\ &+ a_5 y(t-1)u(t) - a_6 y(t-1)u(t-1) - a_7 u^2(t) - a_8 u^2(t-1) \end{aligned} \tag{2.5}$$

Here u describes the input which is fuel rack position in the study. y is the output which is engine speed. a_i are the coefficients obtained by the system identification based on data of dynamic experiments.

Aside of NARMAX models, neural network models are another option for nonlinear modeling of diesel engine. The NN models here is dynamic which differs from the static ones mentioned in the prior part. The dynamic NN models are built to make the prediction in [57–61]. The data of former states (inputs and outputs) is needed for building NN model. It makes the model has dynamic characteristics and prediction ability.

In [58, 61], the dynamic NN models of spark ignition (SI) engine were proposed. The Figure 2.4 in [61] shows the structure of dynamic NN model. The fuel injection, throttle angel and air-fuel ratio in former time are selected as the inputs of the NN, the current air-fuel ratio as output. This kind of model could be applied in predictive algorithms.

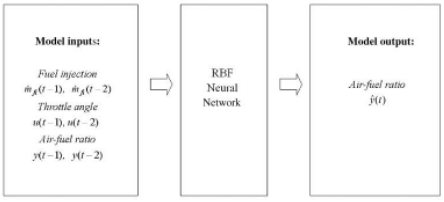

FIGURE 2.4: Structure of dynamic NN model

linear parametric identification model

Because of the nonlinear behavior of a diesel engine in the wide operating region (for example, engine speed changes from 800 rpm to 4500 rpm), obtaining a unique linear model becomes impossible with high precision. To deal with this problem, the entire operation region of engine is then segmented into several sub-zones. [54, 62–65]. One example is shown is Figure 2.5. Within each sub-zone, a linear model is identified.

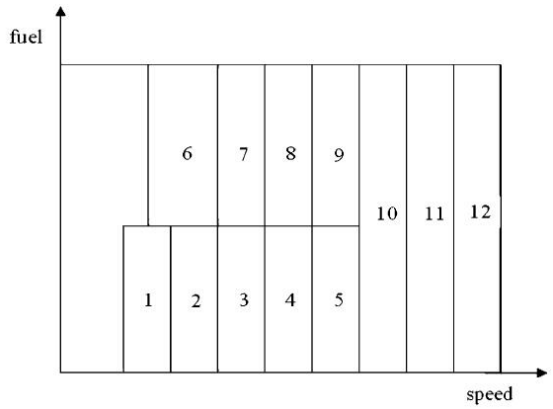

FIGURE 2.5: One example for segmentation of the engine operation region

There are two types of linear model: transfer function and state space equation. State space equation has become the common choice in recent research [54, 62–65]. After the inputs and outputs of the model are determined, the pseudo-random binary sequence (PRBS) signal is implemented to generate data for system identification. It is proved that the state space equation could play a significant role in real-time application in diesel engine because of its simplicity and fast computation.

2.3.2 Control strategy

Many control strategies based the above dynamic models have been developed for diesel engine. As discussed in the previous part, the control during transient condition is the key of performance improvement for diesel engine. The representative control strategies are introduced in the following part.

neural network control

Neural network is mentioned three times in the dissertation. As presented in the previous part, neural networks have been used to describe the relationship between inputs

and outputs of diesel engine in static and dynamic condition. Based on the strong ability of learning, the neural network has also been used as controller of diesel engine.

Optimal control using neural networks is applied in [53]. At first, the optimization algorithm was conducted for searching the optimal control action during transient condition. Then the neural network was trained based on the database of optimal control action. The NN controller is implemented in real time simulations on the ETC cycle. From the results it can seen that a better performance is obtained than the traditional method.

An adaptive critic learning controller for engine control based on neural networks was studied in [66]. The structure of controller is shown in Figure 2.6. The commanded values are the reference including air-fuel ratio (AFR) and torque (TRQ). $Q(t)$ is the critic network outputs function which is also the cost function of the controller. The simulation results prove that the proposed self-learning control is effective in tracking the TRQ and AFR in SI engine.

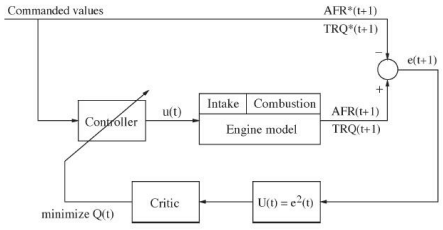

FIGURE 2.6: Structure of the adaptive critic learning engine controller

nonlinear MPC

As we talk about the model-based control method, the model predictive control (MPC) is a inevitable topic. MPC is a beneficial approach for MIMO control and performance optimization with adjustment of constraints.

A control structure for a turbo-charged diesel engine based on nonlinear model predictive control (NMPC) is illustrated in [67]. The process of diesel engine is described using the differential equation with nonlinearities and constants from MVMs. Then a NMPC with quasi-infinite horizon is applied. The improved transient behaviour could be seen in the simulation. But it is not possible to apply the NMPC system directly in real-time test since the time of computing will be a huge burden.

In [68], the nonlinear model predictive control (NMPC) of an air-loop of a diesel engine based on a LPV model is shown. The LPV model is identified based on real data from

an engine test bench. The software package qpOASES is used to solve the nonlinear QP problem. An excellent tracking performance by nonlinear MPC is shown in the simulation. But computation burden is a huge problem. As a consequence, it proves that nonlinear MPC cannot be used for real-time application at that time in 2009.

explicit linear MPC

As we just discussed, the concern for control of diesel engine in real-time is computation speed. Explicit MPC is a method to apply the MPC algorithm to fast process such as diesel engine. In [54, 63–65], the solver such as active set method for the QP problem of MPC requires much computation effort. As a result, the application of MPC has been restricted for slow processes. Thus for every possible initial state, each affine control law is precalculated and stored in look-up tables. With this method the MPC could be applied in fast process such as diesel engine. The procedure is shown in Figure 2.7.

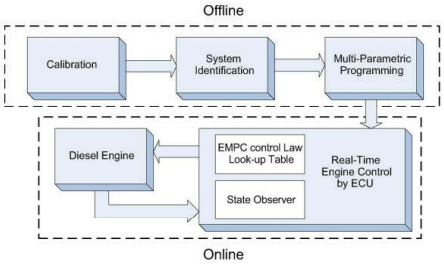

FIGURE 2.7: Implementation procedure of EMPC on the diesel engine

online linear MPC

Comparing with above strategies, a more efficient method to deal with the problems of quadratic programming of MPC is given in [62]. The condition of applying this method which is called online strategy is that there is not too much change for the active set of QP between each sampling time. However this kind of method is different from conventional techniques for warm starting. In this way the online calculation in a given sampling time becomes possible. And in our thesis, this method of QP solving is applied in the MPC design. Above all any calibration work was not required. This system has been tested in real-time application, but the dynamic behavior of fuel loop is not discussed.

linear quadratic regulator

It is common to apply LQR as an optimal algorithm to solve control problems. LQR is superior due to its advantage of easy implementation and fast computation speed. LQR is widely used in engine control for reduction of emissions [69–71].

In [69], the EGR and injection timing are selected as manipulated variables. The target is to solve the NOx-soot trade-off problems. The real-time experiment on a six-cylinder engine proves its effectiveness not only in stationarity but also in transients. Linear optimal control approach of LQR has been applied to an advanced diesel engine with EGR and turbocharger in [70]. The control is focuses on the air loop of the engine. The objective is to regulate oxygen fractions and pressures in manifolds by EGR and VGT (variable geometry turbocharger). The tracking performance in the simulation is satisfied.

2.4 Summary

In summary, the overview of current researches focuses on model-based control methods of diesel engine. With the purpose of increasing fuel efficiency and reducing emissions, researchers have developed many MBCs with different models and control algorithms. Through the review of literature, main results are discussed as follows:

1. The static model based calibration is well developed and implemented into real-time application of production diesel engine. But the performance during transient condition is the main source of air pollution. It makes the transient control based on dynamic model an attractive choice.

2. The modeling of engines has a long story. And the model is very important in the design of control strategies. In consideration of real-time application including air and fuel loop of diesel engine, it motivates us to use linear state space equation for modeling because of its simplicity and fast computation.

3. Many control strategies have been developed to improve the performance during transient condition. As we know the simulation results are satisfied. But the real-time experimental results are lack. In another word, the real-time controller of diesel engine which is easily implemented is desired. Among the existing methods, MPC and LQR have been proven a good choice.

Chapter 3

Engine Test Bench and Modeling

3.1 Introduction

The experimental experiments described in this thesis were performed in a diesel engine test bench at the Laboratory of Ogai, at the graduate school of information production and system, Waseda University. The engine applied in the test bench was an one-cylinder YANMAR TF70V-E. Then it was modified for research purpose. Two computer systems were inserted, which could be used for the measurement, data acquisition and the engine control.

The requirement of an engine model that will predict the plant behaviour and can be used inside the controller has been declared. The behavior of a diesel engine usually involves air-path and fuel-path loop, which is easily captured simultaneously by state space equation introduced in previous chapter. Meanwhile the engine combustion is a real fast process. In consideration of on-line computation burden, it motivates to use linear state space equation to describe the diesel engine system.

Thus this chapter describes the engine test bench and the model for control purpose. The rest of this chapter is organized as follows: Section 3.2 describes the detailed setup of the engine test bench. In section 3.3, the procedure of linear system identification for diesel engine model is conducted. And finally Section 3.4 summarizes the conclusions.

3.2 Engine test bench

The engine test bench is shown in Figure 3.1. And the schematic view of the engine test bench is shown in Figure 3.2.

FIGURE 3.1: Diesel engine test bench

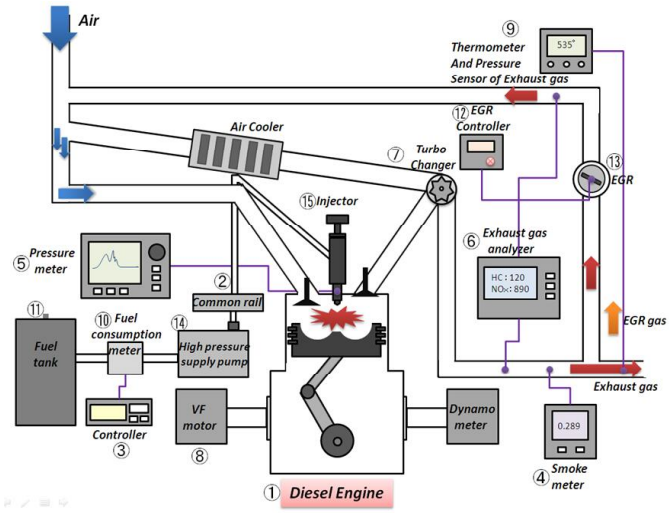

FIGURE 3.2: The schematic view of engine test bench

3.2.1 Diesel engine

The heart of the test bench is the YANMAR TF70V-E diesel engine, modified for advanced research applications. The main specifications of the investigated diesel engine are described in Table 3.1. The engine in its commercial form is mainly used for shipboard electric power generation and small ship propulsion.

TABLE 3.1: Specifications of diesel engine

Name	YANMAR TF70V-E
Type	4-cycle, 1 cylinder, DI
Bore × Stroke	78mm × 80mm
Compression ratio	21.4
Displacement	382cc
Maximum power	5.5/2600 kW/min^{-1}
Rated power	4.8/2600 kW/min^{-1}
Fuel type	Diesel
Fuel tank capacity	7.1 liter
Size	640×330.5×474 mm^3
Drying quantity	78.5 kg

In the experimental setup, the engine is coupled to an electric dynamometer, VLC134-100kg. The connection between the engine and the dynamometer is realized via a shaft and a flexible coupling (⑧ in Figure 3.2). The dynamometer typically works in two modes:

Constant speed mode In this mode, engine is kept at a constant speed. This is achieved by a feedback loop, for example, using Proportional-Integral-Derivative (PID) controller to control the engine speed by adjusting the load on the engine.

Constant load mode In this mode, a constant load generated by the dynamometer is set to the engine. The constant load mode is set in this thesis.

3.2.2 Instrumentation

Each instrumentation of the engine test bench with marked number is shown in Figure 3.2. Table 3.2 provides the identification of sensors and actuators. Just as the descriptions about sensors in Table 3.2, the information about measurement instrumentation

for exhausted emissions, pressures and temperatures could be found from the manufacturer, which are not described in details here. The devices for monitoring exhausted emissions (④,⑥), pressures (⑤,⑨) and temperatures (⑨) are shown in Figure 3.3.

TABLE 3.2: Sensors and actuators at test bench

No.	Name	Model	Manufacturer
①	Engine	TF70V-E	YANMAR
②	Common rail system	/	Common rail: Bosch Controller: Denso Fuel pump: Bosch
④	Soot sensor	MEXA-600SW	Horiba
⑥	NOx sensor	MEXA-720NOx	Horiba
⑥	CO, HC, CO_2 sensor	MEXA-584L	Horiba
⑧	Dynamometer	VLC134-100kg	VMC
⑩	Flow rate sensor	FD-SS02A	KEYENCE
⑬	EGR valve	25620-46090 135000-8081	Toyota

FIGURE 3.3: Operation platform

3.2.3 Data acquisition and control system

The engine data acquisition system (DAQ) acquires and stores measured data from sensors and actuators during test runs. Meanwhile the control system sends commands to actuators.

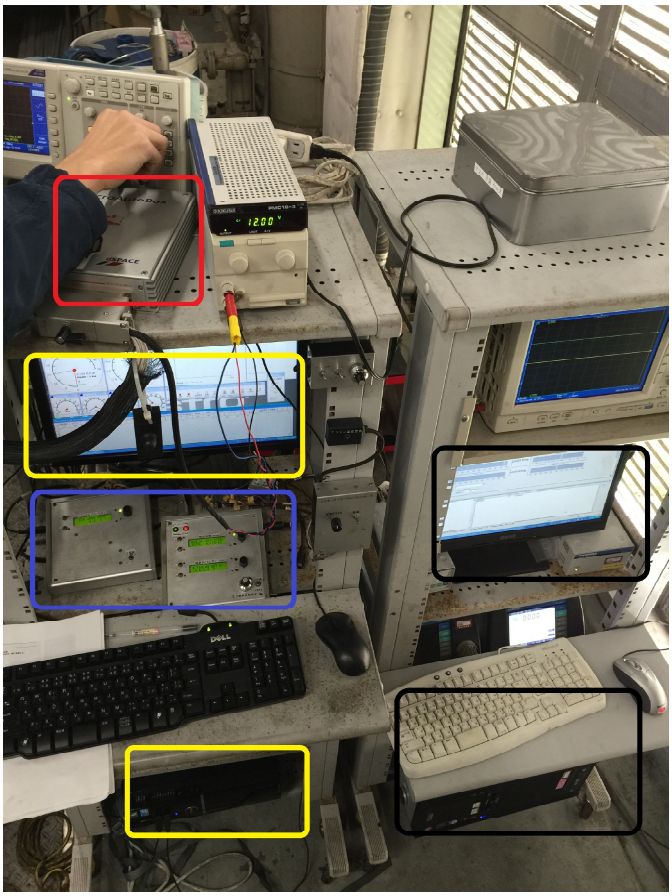

FIGURE 3.4: Modified operation platform with two computer systems

FC-design system

The original diesel engine was modified by the FC-design company. FC-design is a company focused on the development of engine control. As shown in the Figure 3.4, the computer with the provided software in the yellow frame on the left side processes and collects the data from all the sensors and measurement devices. The information of engine speed, output power, fuel efficiency, exhausted emissions, pressures and temperatures can be shown on the display. The controller panel in the blue frame is used to send and display the commands to actuators such as EGR valve opening and fuel injection parameters. But these input variables including EGR, injection quantity, injection timing and injection pressure can only be set manually. The detailed information about the communication configuration of FC-design system is omitted here.

dSPACE system

dSPACE is one of the world's leading providers of tools for developing electronic control units (ECU). In recent years, the dSPACE system is widely applied in area of automobile industry. The heart of the dSPACE system in out test bench is the MicroAutoBox 1401 shown in red frame in Figure 3.4. MicroAutoBox is a real-time system for performing fast function prototyping. It can operate without user intervention, just like an ECU in the vehicle. MicroAutoBox is running at 800MHz. The SIMULINK in Matlab could be used to program for fast prototyping.

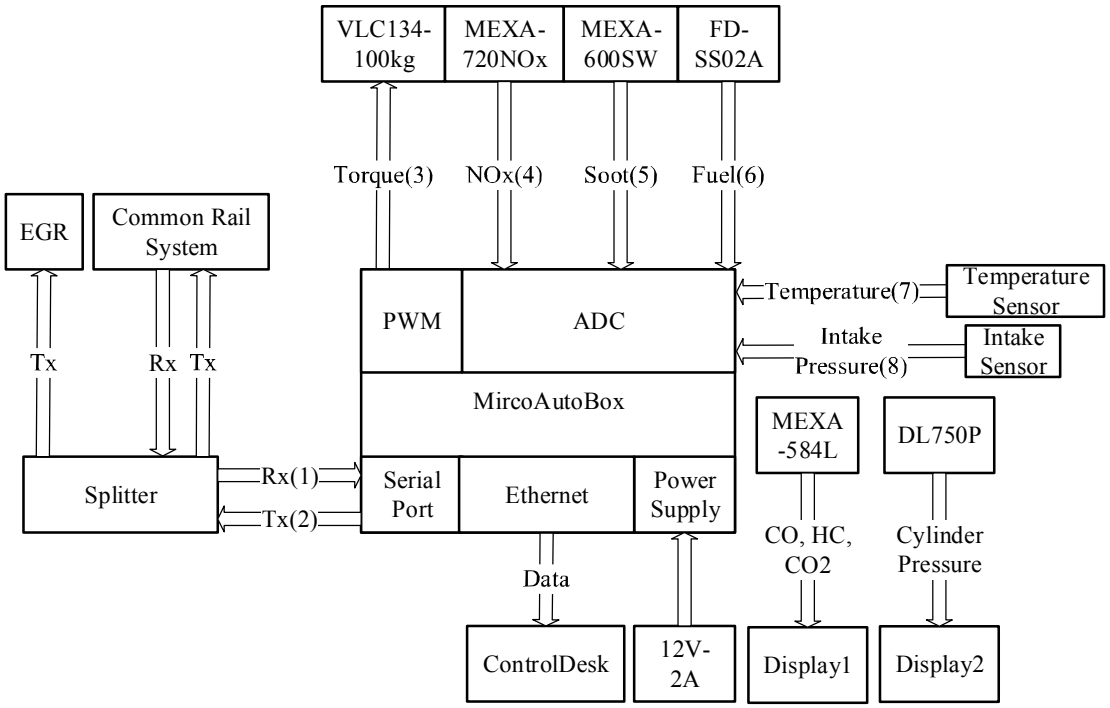

FIGURE 3.5: Connections with MicroAutoBox

The dSPACE system in our test bench was developed by our diesel engine group of the Ogai lab. And the detailed work will be introduced in the following parts. The hardware connection in the system is depicted in Figure 3.5.

There are four kinds of communication interfaces in MicroAutoBox. The communication between the MicroAutoBox and the controller panel of EGR and common real system is by the interface of serial port. The detailed information about the serial port protocol is shown in Table 3.4 and 3.5. The communication of dynamometer is by the interface of pulse-width modulation (PWM). The communication of all the other sensors and measurement device is by the interface of analog-to-digital converter (ADC).

T .3: Description of communication protocols and data acquisition interfaces

Index	Name	I/O	Interface	Value	Unit
(1)	Engine Speed	I	Serial port	See Table. 3.4	RPM
(1)	Rail Pressure	I	Serial port	See Table. 3.4	MPa
(2)	EGR	O	Serial port	See Table. 3.5	%
(2)	Injection Parameters	O	Serial port	See Table. 3.5	/
(3)	Torque	O	PWM	Period: 2ms Duty ratio 0.001 for 0.225N.m	N.m
(4)	NOx	I	ADC	$Voltage(V)\times 400$	ppm
(5)	Soot	I	ADC	$V\times 10$	1/m
(6)	Fuel	I	ADC	$(V-1)\times 3000$	cc/h
(7)	Temperature	I	ADC	$V\times 40$	°C
(8)	Intake Pressure	I	ADC	$(V-1)\times 233.2+0.44$	KPa

TABLE 3.4: Serial port receiving protocol

Description	R: engine speed(RPM)×1 P: measured rail pressure(MPa)×10 Checksum: sum from byte 1 to 38 E: Error							
Byte[0:7]	0xFF	0x01	0x41	R[8:15]	R[0:7]	P[8:15]	P[0:7]	E[8:15]
Byte[8:39]	E[0:7]	$0\cdots 0$						Checksum

T

Description	T_n: nth injection timing([0 720]degree)×2 T_n-$T_{n-1}\geq 8$ Q_n: nth injection quantity([0 30000]us)× 1 E: EGR rate([0 100]%) ×10 P: rail pressure set-point([0 200]MPa)×10 Checksum: sum from byte 1 to 38							
Byte[0:7]	0xFF	0x01	0x64	T1[8:15]	T1[0:7]	T2[8:15]	T2[0:7]	T3[8:15]
Byte[8:15]	T3[0:7]	Q1[8:15]	Q1[0:7]	Q2[8:15]	Q2[0:7]	Q3[8:15]	Q3[0:7]	P[8:15]
Byte[16:23]	P[0:7]	E[8:15]	E[0:7]	T4[8:15]	T4[0:7]	T5[8:15]	T5[0:7]	T6[8:15]
Byte[24:31]	T6[0:7]	T7[8:15]	T7[0:7]	Q4[8:15]	Q4[0:7]	Q5[8:15]	Q5[0:7]	Q6[8:15]
Byte[32:39]	Q6[0:7]	Q7[8:15]	Q7[0:7]	0	0	0	0	Checksum

The communication protocols and the data acquisition interfaces between sensors, actuators and MicroAutoBox are depicted in Table 3.3. The communication between the MicroAutoBox and the computer is by the interface of ethernet. The computer is shown in the black frame in Figure 3.4.

ControlDesk is a software from dSPACE experiment package installed in this computer for ECU development. All the necessary tasks could be performed in it. The simple and efficient working environment is given from the start of experimentation to the end. One example for operation interface built by ControlDesk is shown in Figure 3.6.

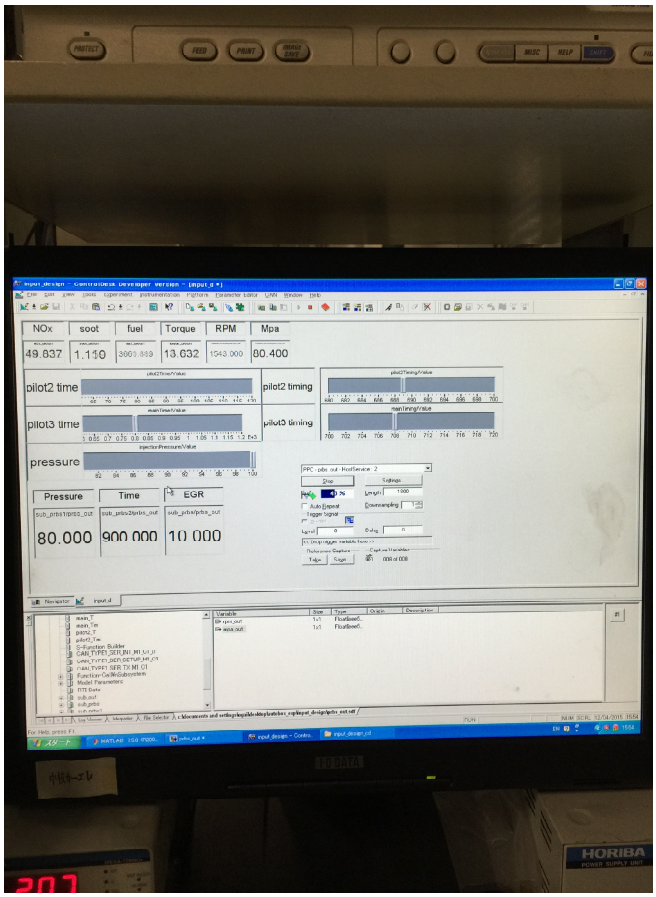

FIGURE 3.6: Operation interface built by ControlDesk

3.3 Modeling

With this setup, experiments were designed and conduct to obtain experimental data which could be used for system identification. Identification and derivation of dynamic models for control purpose are the subjects of the section.

The derivation of such an engine model is based on system identification. For system identification, there are mainly five parts depicted in Figure 3.7 including experiment design, the preprocessing of data, the selection of model structure, the estimation of unknown parameters and validation.

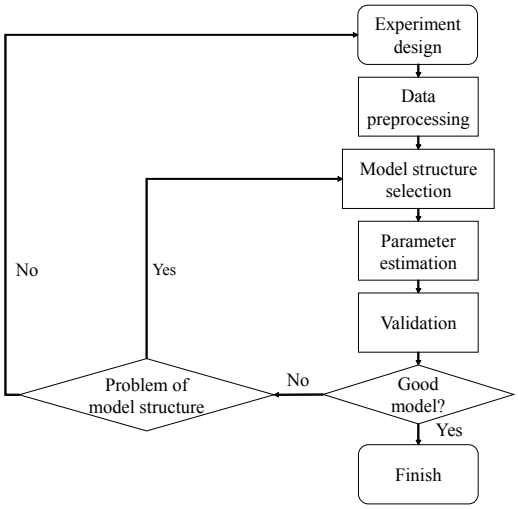

FIGURE 3.7: System identification procedures

Models obtained following the above procedure are often called black box models. As an advantage, they are relatively easy to obtain and more importantly are simple enough to make dynamic model-based control system design mathematically and practically tractable.

3.3.1 Engine model definition

Since the behavior of a diesel engine is nonlinear in the wide operating region (for example, engine speed changes from 800 rpm to 4500 rpm), obtaining a unique linear model becomes impossible with high precision. To deal with this problem, the entire operation region of engine is then segmented into several sub-zones [54, 63]. Within each sub-zone, a linear model is identified.

The control objective in this thesis is to operate the engine to meet drivers speed demand and reduce NOx emission. As for the diesel engine we tested, lean-burn is applied. Thus the particular matter is not considered as the control target here. Figure 3.8 shows the structure of the model of whole engine system.

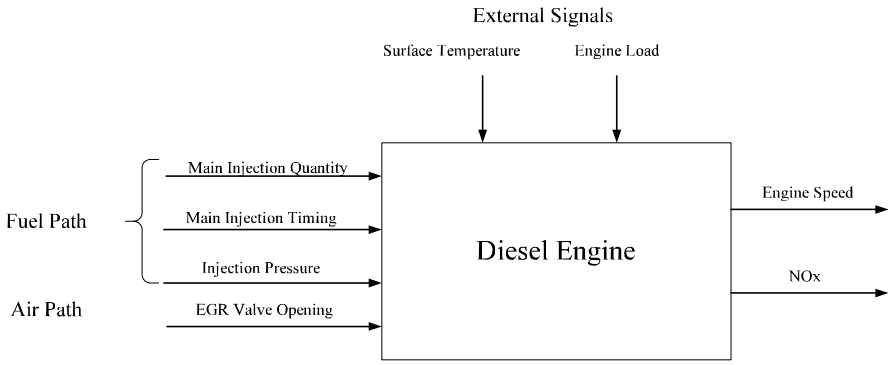

FIGURE 3.8: Identification structure of diesel engine

Traditionally, the values of NOx emission and engine speed are not directly selected as feedback variables. The reason is that direct measurements of such variables, which are so-called high-level objectives, have not been available in production engines. As the new sensor technic has been developed [72], there exists a chance to design the control system based on high-level values. In this thesis engine speed and NOx value are directly selected as the outputs (y) of the model. The engine speed is expressed by revolutions per minute (RPM). These two variables are influenced by many factors, but test results indicate that the main influences are main injection quantity, main injection timing, injection pressure and EGR valve opening. These manipulated variables are selected as the inputs (u) of the model. The surface temperature of engine cylinder and the engine load are the measured disturbances.

3.3.2 Data preparation

For system identification, it can be considered as the process of obtaining a model to describe the behavior of a plant. The parameters in the model are obtained based on inputs and outputs data [73–76].

The procedure of obtaining the data is normally performed in the following way. The predesigned signals are inserted into the systems as inputs. Then the resulting outputs are recorded. Thus the design of inputs signals is naturally very important. As a result, the data preparation is introduced in details in this section.

stair test

In this section, stair tests on diesel engine are performed to develop a linear working region. Since the linear model and linear system identification are applied, the engine should be ensured to work in a linear range. The constraints of inputs (lower bound $\underline{u}$ and upper bound $\overline{u}$) should be chosen according to the signal noise ratio (SNR) and the linearity. If the inputs range is too small, it could be easily influenced by the noise signal. On the contrary, if it is too big, there will be nonlinearity in the system and the linear system identification results might not be satisfied. Therefore, the lower and upper boundary of inputs should be chosen as wide as possible in the linear zone. The linearity of the working region could be checked by stair test (multi-step test).

Through the stair test for our diesel engine, the inputs boundaries are chosen by ourselves. In another word, the choice of input boundaries is very subjective. Among these groups of data, one selection is chosen in Table 3.6. In this region, if we do the stair test, the responses seem like linear relation.

TABLE 3.6: Inputs boundaries

Inputs	Lower boundary: $\underline{u}$	Upper boundary: $\overline{u}$	Unit
Injection quantity	680	700	us
Injection timing	710	712	degree
EGR	11	15	%
Injection pressure	100	110	MPa

Choice of input signal

The signal used for the experimental input is called the exciting signal. In identification test the system is usually excited with known impulse and step signal and the output is recorded. But the noise will distort the measured output. In this case the exciting signal should be applied repeatedly and persistently [73–76]. Persistence of excitation is the basic requirement for an informative experiment and guarantees the unique solution for the parameter estimation. Here open loop experiment is discussed.

Some representative persistent exciting signals are introduced in the literature [76]:

- **Pseudo random binary signal (PRBS)**: PRBS signal is a kind of binary signal switching between $\underline{u}$ and $\overline{u}$. PRBS signal could be generated from a shift register

with feedback. The binary signal is easy to be designed and implemented. PRBS signal has a wide spectrum just like the white noise. Therefore much information can be excited from the system. The disadvantage for binary signal is that the validation against nonlinearity can not be allowed. For example, if the true system has different steady-state gain, this could not be detected from this exciting signal. For this case the amplitude-modulated PRBS (APRBS) signal could be used.

- **General binary signal (GBN)**: Just like PRBS, GBN signal is another kind of binary signal switching between $\underline{u}$ and $\overline{u}$. But unlike PRBS, GBN signal is generated with a switching possibility and the spectrum is mainly in the lower and middle frequency domain. Usually it is better for the manipulated variables not to change rapidly and the spectrum of manipulated variables would be also lack of power in the high frequency domain. Using the GBN signal could be more likely to obtain a model for control purpose.

- **Filtered Gaussian white noise**: By filtering the Gaussian white noise, the signal with any spectrum could be achieved using different filter. The Gaussian noise signal is theoretically not bounded and it should be saturated with a certain amplitude.

- **Combination of sinusoids**: Several sinusoids with different frequencies are combined together. Using the combination of sinusoids will be unavoidably distorted by nonlinearities and the result may not be satisfied.

In this thesis, GBN signal is selected as the exciting signal for the following reasons:

- Easy to be designed and implemented.

- The lower and middle frequency domain of the true system is excited. Thus the model obtained is suitable for the control purpose.

- Comparing with PRBS, GBN signal has less possibilities to have multiple manipulated variables changing simultaneously, which is good for monitoring.

Design of GBN signal

GBN signal switches between the boundaries $\underline{u}$ and $\overline{u}$ with a possibility of p_{sw} in every minimum switching time T_{min}:

$$\begin{cases} P(u_k = -u_{k-1}) = p_{sw} \\ P(u_k = u_{k-1}) = 1 - p_{sw} \end{cases} \tag{3.1}$$

The parameters for designing a GBN signal are depicted in Table 3.7.

TABLE 3.7: GBN parameters

Upper and lower boundaries	$\overline{u}$ and $\underline{u}$
Switching possibility	p_{sw}
Minimum switching time	T_{sw}
Length	n

The power spectrum of GBN signal is:

$$\Phi_u(\omega) = \frac{(1-q^2)T_{min}}{1-2q\cos(\omega T_{min})+q^2} \tag{3.2}$$

where $q = 2p_{sw} - 1$.

The GBN signal depends on these parameters. The details of these parameters are depicted as follows:

- **Upper and lower boundaries $\overline{u}$ and $\underline{u}$**: As is described in section 3.3.2.
- **Switching possibility** p_{sw}: the power spectrum of the signal is decided by p_{sw} as depicted in Eq. (3.2). The methods for choosing p_{sw} is shown in [76] and [77].

  In [76], the mean switching time ET_{sw} is chosen as:

  $$ET_{sw} = \frac{T_{min}}{1-p_{sw}} = \frac{1}{3}t_s \tag{3.3}$$

  where t_s is 98% of the settling time. Then T_{min} can be chosen as sampling time and p_{sw} can be calculated.

  In [77], the optimal p_{sw} is chosen so that the power in the frequency interval $\omega_{min} \le \omega \le \omega_{max}$ is maximized.

  $$\omega_{min} = \frac{1}{\beta\tau_H} \le \omega \le \frac{\alpha}{\tau_L} = \omega_{max} \tag{3.4}$$

where β is the factor representing the settling time of the process and α is the factor representing the closed-loop speed of response as a multiple of the open-loop response time. τ_H and τ_L are the slowest and fastest time constants over all of the channels. Typically, β is chosen as 3 and α is chosen as 2.

The frequency interval $\omega_{min} \leq \omega \leq \omega_{max}$ is the frequency interval for control purpose. The GBN signal is designed to mainly excite for this interval. ω_{min} and ω_{max} can be obtained from the step response. The optimal p_{sw} is given as:

$$p_{sw} = 1 - \frac{1}{1 + \sqrt{\tan\frac{\omega_{min}T_{min}}{2}\tan\frac{\omega_{max}T_{min}}{2}}} \tag{3.5}$$

In this thesis, the method of [77] is employed, since it is reasonable to increase the power in the frequency interval for the control purpose.

- **Minimum switching time** T_{min}: T_{min} is usually chosen the same as the sampling time. Alternatively, one could choose T_{min} as the times of sampling time. Then p_{sw} can be calculated according to Eq.(3.5).

- **Length** n: As for the length , there is a trade-off between experiment cost and parameter estimation variance. n is usually chosen six to eight times the length of the settling times. As a matter of fact there exists distortion in the engine system. In order to reduce the effect of distortion, length could be chosen six to eight times longer than the settling times.

Therefore, the GBN signal parameters are chosen according to the procedures depicted in Figure 3.9. Step test is very important because it can give us an intuitive impression on the system. The parameters of GBN signal could be obtained according to the time constant and settling time by the step test. After doing the stair test, the inputs bound-a $\overline{u}$ and $\underline{u}$ are depicted in Table 3.6. The step responses from each input channel to each output channel are depicted in Figure 3.10.

Based on the step response tests, the sampling time is selected as 1 second. Settling time is depicted in Table 3.8. Time delay is depicted in Table 3.9. Time constant is depicted in Table 3.10.

For each input channel, two outputs are excited. Thus the time constant should be chosen as the biggest (slowest) and smallest (fastest) among all the outputs. For example in Table 3.10 , for injection quantity, τ_L is chosen as 5.83 and τ_H as 8.57.

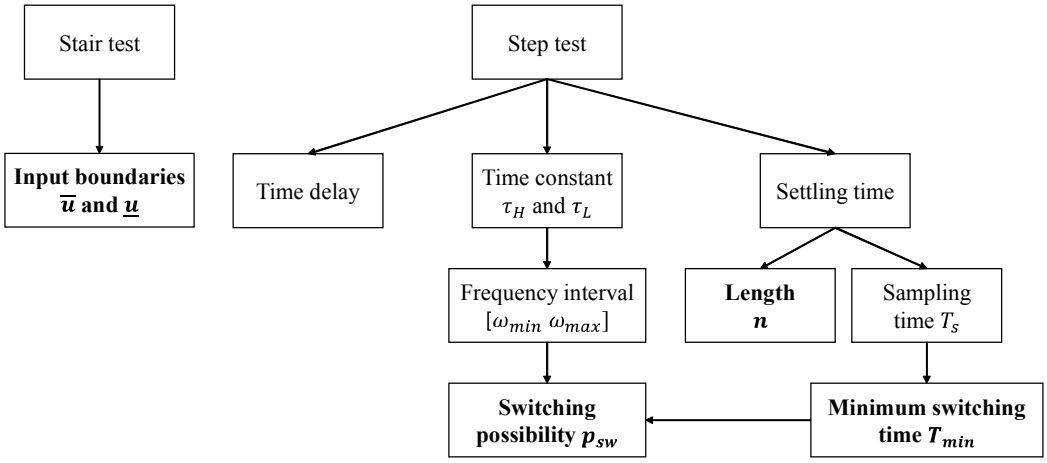

FIGURE 3.9: GBN signal design procedures

TABLE 3.8: Settling time

Settling time									
	Injection quantity		Injection timing		EGR		Injection pressure		Unit
	Up	Down	Up	Down	Up	Down	Up	Down	
RPM	17	16	16	38	25	30	16	8	s
NOx	23	13	12	16	23	21	16	13	s

TABLE 3.9: Time delay

Time delay									
	Injection quantity		Injection timing		EGR		Injection pressure		Unit
	Up	Down	Up	Down	Up	Down	Up	Down	
RPM	1	1	1	1	1	1	0	0	s
NOx	1	3	0	0	0	0	0	0	s

T

Time constant								
	Injection quantity		Injection timing		EGR		Injection pressure	
	Up	Down	Up	Down	Up	Down	Up	Down
RPM	7.00	8.00	4.00	8.63	8.79	17.79	4.20	1.84
NOx	5.83	8.57	1.36	1.96	2.45	2.47	6.20	5.50

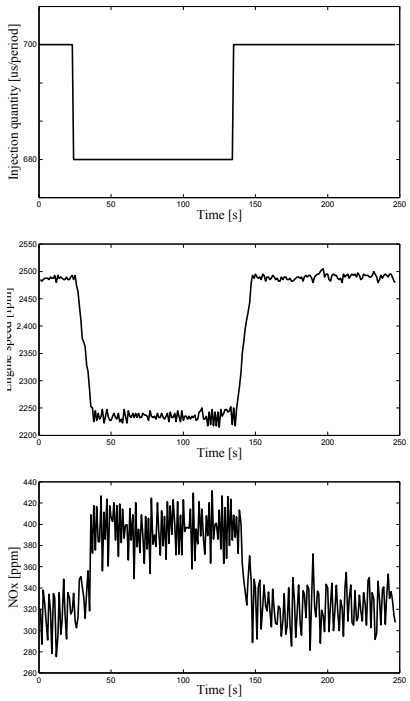

(a) Injection quantity and its responses

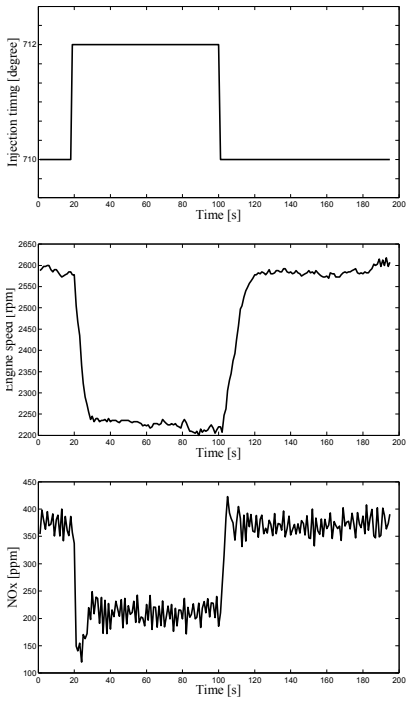

(b) Injection timing and its responses

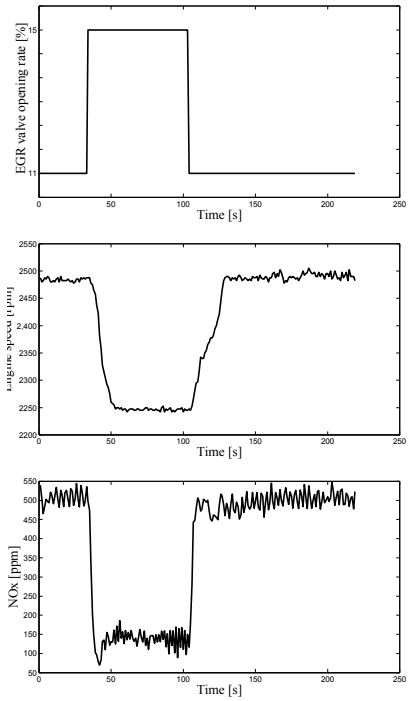

(c) EGR valve opening and its responses

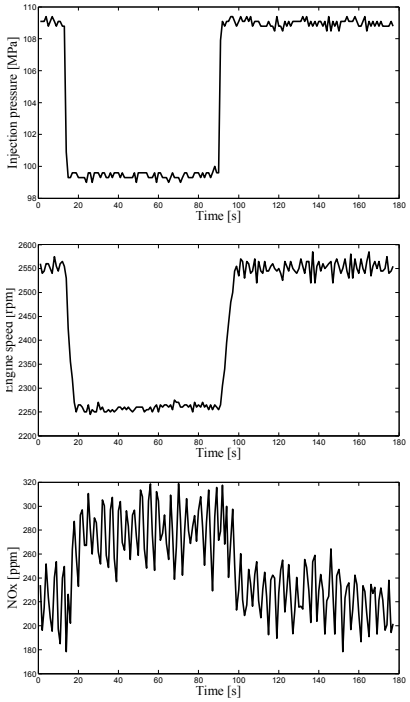

(d) Injection pressure and its responses

FIGURE 3.10: Step responses

T

	τ_L	τ_H	ω_{min}	ω_{max}	p_{sw}	T_{min} (s)	Length (s)
Injection quantity	5.83	8.57	0.0389	0.3431	0.0549	1	575
Injection timing	1.36	8.63	0.0386	1.4706	0.1167	1	575
EGR	2.45	17.79	0.0187	0.8163	0.0598	1	575
Injection pressure	1.84	6.20	0.0538	1.0870	0.1130	1	575

Through the procedure shown in Figure 3.9, the parameters are chosen as Table 3.11.

Then the GBN signal can be designed and applied to the test bench. The diesel engine system is excited for almost thirty minutes. The signals of main injection quantity, main injection timing, injection pressure and EGR valve opening are designed as Figure 3.11 shows (a part of the total collected data). The engine load is chosen as 50 N. The surface temperature of the engine stays around 90 degrees. In Figure 3.11 the constraints of identification signals is designed to ensure the tested diesel engine is working in the linear sub-zone where the engine speed changes from 2250 to 2550 rpm. The engine speed and NOx responses are also shown in Figure 3.11. Then the data for system identification can be obtained.

3.3.3 Parameter estimation

After the data of inputs and outputs being obtained, the linear system identification is then implemented. In linear system identification, a certain structure of model should be firstly determined. Then the parameter estimation is needed. The parameters inside are optimized to minimize the error (specified distance) between the measured and model outputs.

There are several common-used model structures for linear models:

- **Polynomial model** The general form of polynomial model is:

$$A(q)y(k) = \sum_{i=1}^{m} \frac{B_i(q)}{F_i(q)} u_i(k - nk_i) + \frac{C(q)}{D(q)} e(k) \tag{3.6}$$

  where A, B, C, D and F are unknown polynomials expressed in the time-shift operator q^{-1}. m is the number of inputs, nk_i is the input delay and e is the disturbance. The common linear polynomial model structures include ARX, ARMAX, OE and BJ [78].

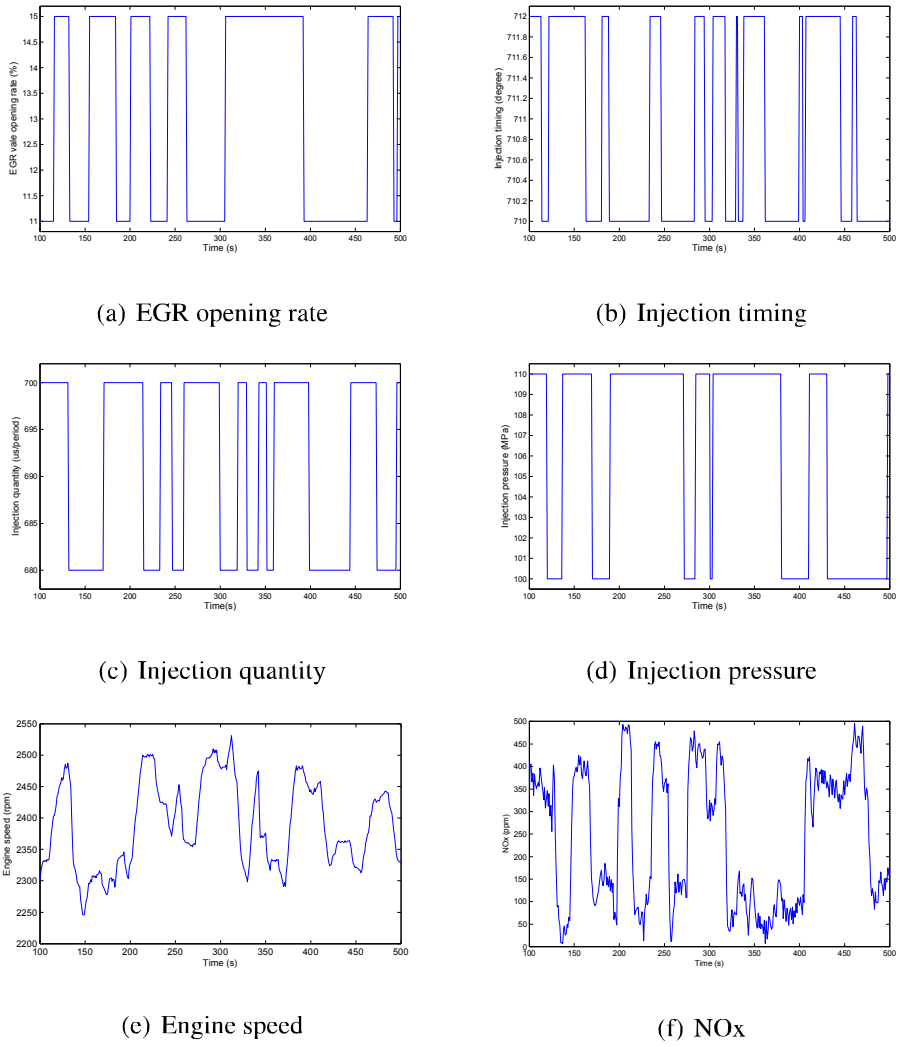

(a) EGR opening rate (b) Injection timing

(c) Injection quantity (d) Injection pressure

(e) Engine speed (f) NOx

FIGURE 3.11: Identification signals for the linear model

- **State space model** The state space model can be defined in continuous-time form and in discrete-time form. The discrete-time state space model structure that is applied in this thesis is often written in the following form:

$$\begin{cases} x(k+1) = Ax(k) + Bu(k) \\ y(k) = Cx(k) + Du(k) \end{cases} \tag{3.7}$$

Therein $x(k)$ denotes the states of the identified model, $u(k)$ the manipulated variables. And $y(k)$ denotes the controlled variables. A, B, C and D are the unknown parameter matrices to be identified.

- **Transfer function** For the discrete time system, transfer function is a special form of polynomial model structure. Transfer function describes the relationship between input and output.

As for the linear system identification, prediction-error minimization (PEM) is often chosen as the method of parameter estimation. The basic idea behind PEM is described as follows:

For convenience, here θ is used to represent all of the unknown parameters.

- Describe the one-step prediction function of output using Eq. (3.7) as:

$$\hat{y}(k|k-1) = f(Z^{k-1}, \theta) \tag{3.8}$$

- Define the distance $V_N(\theta)$ between predicted output $\hat{y}(1|0)$,..., $\hat{y}(N|N-1)$ and measured output $y_m(1)$,...,$y_m(N)$. The distance can be chosen as the assumed probability density function, which will be the maximum likelihood estimate, or the Euler distance.

- Find θ to minimize the distance function.

$$\hat{\theta} = \arg\min V_N(\theta) \tag{3.9}$$

  The distance function may have several local solution. The method of damped Gauss-Newton is usually used to search for the solution..

In this thesis, the diesel engine is modelled by linear discrete state space equation.

$$\begin{cases} x_p(k+1) = A_p x_p(k) + B_p u(k) \\ y_p(k) = C_p x_p(k) \end{cases} \tag{3.10}$$

Therein $x_p(k) \in R^n$ denotes the states of the identified engine model, $u(k) \in R^m$ the manipulated variables including main injection quantity, main injection timing, injection pressure and EGR valve opening. And $y_p(k) \in R^p$ denotes the controlled variables including engine speed and NOx value at the kth sampling instant respectively. A_p, B_p and C_p are the parameter matrices that can be obtained by PEM method using the MATLAB System Identification Toolbox [78].

3.3.4 Validation results

Based on the data of inputs and outputs in section 3.3.2, the state space model and the parameter estimation method of PEM described in section 3.3.3, the system identification could be finished. For different application in model-based controller design in the following chapters, models with different orders are obtained. The order discussed here is the dimension of parameter matrix A_p.

For Chapter 4, the models of engine speed and NOx emission have been identified separately. By comparing the fitting values and mean square error (MSE), a fourth-order model with the best fit is chosen as the engine speed model and a fourth-order model as the NOx emission model. The modeling fit for engine speed and NOx is 69.7% and 81.2%. Then two multiple-input single-output (MISO) models are augmented into one multiple-input multiple-output (MIMO) model with eighth order. Especially in this form, the uncertainty matrices will be easily added to each model to influence each output respectively. The validation results and superiority of this form will be explained further in Chapter 4.

For Chapter 5, since the order discussion is really important in the offset-free condition and reduced-order H infinity control problem, the second-order and fourth-order MIMO models of the engine system have been identified in this part. For the second-order model, the parameter matrices are as follows:

$$A_p = \begin{pmatrix} 0.6930 & -0.0259 \\ -0.2679 & 0.8305 \end{pmatrix}$$

$$B_p = \begin{pmatrix} 0.00019765 & -0.0150 & -0.0126 & 0.00073984 \\ -0.00042114 & -0.0070 & -0.0129 & -0.00042944 \end{pmatrix}$$

$$C_p = \begin{pmatrix} 1188.1 & -851.2876 \\ 1237.1 & 1101.4 \end{pmatrix}$$

For the forth-order model, the parameter matrices are as follows:

$$A_p = \begin{pmatrix} 0.7996 & 0.0698 & 0.1726 & 0.2252 \\ -0.2506 & 0.8381 & -0.1044 & 0.2343 \\ -0.3622 & -0.2608 & -0.0982 & 0.0608 \\ -0.1569 & -0.3859 & 0.0238 & -0.0246 \end{pmatrix}$$

$$B_p = \begin{pmatrix} -0.00019828 & -0.0085 & -0.0017 & -0.00019962 \\ 0.0023 & -0.0274 & -0.0299 & 0.0042 \\ 0.0110 & -0.0928 & -0.0976 & 0.0195 \\ -0.0056 & 0.0353 & 0.0183 & -0.0090 \end{pmatrix}$$

$$C_p = \begin{pmatrix} 1283.3 & -889.7686 & 245.5906 & 21.5544 \\ 1081.8 & 1352.9 & -359.1263 & -68.4600 \end{pmatrix}$$

The validation results with data not used for identification are shown in Figure 3.12. The figures indicate that the models with two kind of orders is similar in tracking the measured outputs of engine speed and NOx value. The second modeling fit for engine speed and NOx is 77.4% and 80.3%. And the forth modeling fit is really similar. Main dynamics are captured well. These models are suitable for operation of the model-based controller design, as this is formulated and further implemented in the next chapters.

3.4 Summary

In this chapter, the test bench with experimental diesel engine was described. Information on the structure of the test bench and each component was provided. With this setup, experiments were designed and conduct to obtain experimental data which could be used for system identification. And the proposed control algorithm in chapter 4 and 5 can be applied for real-time application on the engine test bench.

Then as for diesel engine system, the procedure of the linear system identification is conducted. At first the setting variables of the model are selected for control purpose. Then the stair tests are performed to ensure the linear working region and inputs constraints. And the general binary signals (GNB) are designed based on the step-responses. Finally the linear state space engine models of the engine process through

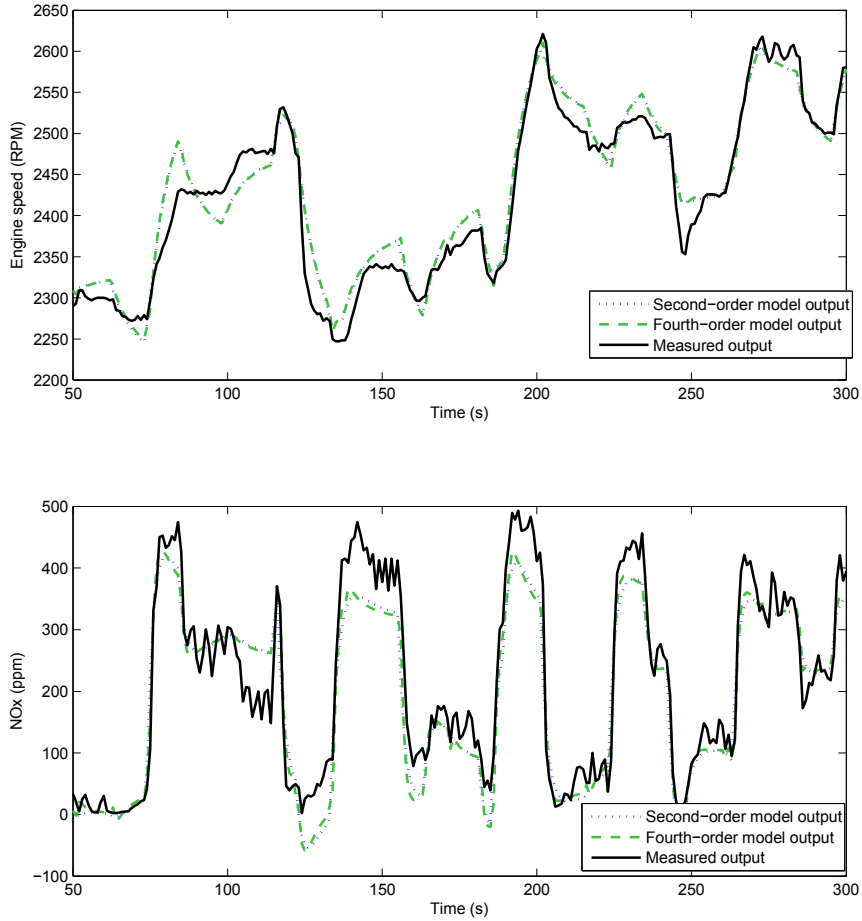

FIGURE 3.12: Validation results of the model

both air and fuel loop are identified based on the data of inputs and outputs from real-time experiments by the PEM method. The validation results show that the identified dynamic model could be used for the controller design in the next chapters.

Chapter 4

Extended Guaranteed Cost Controller Design

4.1 Introduction

As was discussed in Chapter 2, various model-based control approaches for diesel engine have been proposed. Although the aforementioned studies provide model-based methods to construct controllers, unfortunately, the problem of system uncertainties was not discussed. Meanwhile in real-time application, there must be uncertainties in the linear model identified in the staff-defined linear working region. The uncertainties of diesel engine control system include nonlinearities, some unmodeled dynamics and unknown parameters [79]. In consideration of guaranteeing the closed-loop stability of this uncertain system, the so-called guaranteed cost approach is proposed. Furthermore a certain quality of control performance can be guaranteed at the same time. In the last few years, the method of linear matrix inequalities (LMI) has been widely applied in the controller design for its advantage of analysis of uncertain system. Meanwhile solving methods of LMI have been well developed [80]. This chapter is mainly contribute to building an extended guaranteed cost controller of diesel engine system with input constraints via LMI approach. The control target is to track the engine speed and reduce the exhaust emissions. The quadratic performance with uncertainty, the inputs constraints and the demand of tracking are guaranteed by two augmented LMIs. The main contribution is the diesel engine model expressed by linear state space equations obtained in Chapter 3 with parameter uncertainties. And the control laws and state estimate gains are given from feasible solution of an extended LMI simultaneously.

The rest part of this chapter is written as follows: A diesel engine model with parameter uncertainties is built in Section 4.2. Section 4.3 focuses on the design of a extended guaranteed cost controller with input constraints. The real-world experimental results are given in Section 4.4. Finally, conclusions are summarized in Section 4.5.

4.2 Model with norm-bounded parameter uncertainties

The nonlinear characteristic of the diesel engine system is represented by linear models of state space equations in Chapter 3. Due to the subjective decision of the linear working region by experimental staff, the linear models may include large parameter uncertainty. In this chapter, the parameter uncertainty in the system is assumed to be norm-bounded and time-varying. Then the diesel engine system is described in the following form:

$$\begin{cases} x_p(k+1) = (A_p + \Delta A)x\ (k) + (B_p + \Delta B)u(k) \\ y_p(k) = C_p x_p(k) \end{cases} \tag{4.1}$$

where A_p,B_p,C_p are the certain matrices by linear system identification in Chapter 3.

$$A_p = \begin{bmatrix} 0.9516 & -0.2089 & -0.1021 & -0.0132 & 0 & 0 & 0 & 0 \\ 0.3226 & 0.0163 & 0.5249 & -0.1890 & 0 & 0 & 0 & 0 \\ 0.0147 & -0.2844 & 0.2810 & -0.6033 & 0 & 0 & 0 & 0 \\ -0.0407 & -0.0764 & -0.3110 & 0.1084 & 0 & 0 & 0 & 0 \\ 0 & 0 & 0 & 0 & 0.6293 & 0.3655 & 0.0328 & 0.1063 \\ 0 & 0 & 0 & 0 & -0.4477 & 0.0432 & -0.6806 & 0.3366 \\ 0 & 0 & 0 & 0 & -0.1234 & -0.4062 & 0.5196 & 0.5551 \\ 0 & 0 & 0 & 0 & 0.0387 & -0.0688 & 0.0682 & 0.1960 \end{bmatrix}$$

$$B_p = \begin{bmatrix} -1.5856*10^{-4} & -2.4805*10^{-4} & -0.0014 & -3.2707*10^{-4} \\ -0.0071 & 0.0830 & -0.0203 & -0.0122 \\ 0.0058 & -0.0345 & 0.0404 & 0.0078 \\ 0.0062 & -0.0298 & 0.0411 & 0.0083 \\ 2.3178*10^{-5} & -0.0116 & -0.0035 & 1.0763*10^{-4} \\ 9.4971*10^{-4} & -0.0260 & -0.0535 & 0.0030 \\ 0.0011 & -0.0161 & -0.0201 & 0.0027 \\ -5.7088*10^{-4} & 0.0058 & -0.0054 & -0.0013 \end{bmatrix}$$

$$C_p = \begin{bmatrix} 1.5851*10^3 & -79.6091 & -144.6003 & 110.4044 & 0 & 0 & 0 & 0 \\ 0 & 0 & 0 & 0 & 1.6819*10^3 & 259.9515 & -681.8811 & -142.3450 \end{bmatrix}$$

Δ

[80–86].

$$\begin{bmatrix} \Delta & \end{bmatrix} = DF \begin{bmatrix} E_a & E_b \end{bmatrix} \tag{4.2}$$

where F is an unknown matrix that satisfies

$$F^{\mathrm{T}} F \leq I \tag{4.3}$$

D, E_a, E_b are the defined constant matrices with appropriate dimensions. I denotes the identity matrix.

When the system uncertainty is expressed in this form, it is usually applied in numerical examples such as [81–84]. It is challenging to apply in the real process. In [85], this kind of uncertainty description is applied in the motion control system of the robot prototype. But in the article, the uncertainty matrices are defined randomly without physical meaning. [86] mainly talks about tracking control for autonomous homing phase of spacecraft rendezvous. The uncertainty matrices in this article are defined for 4 cases. But the uncertainty matrices are determined only to ensure the system stability, also without physical meaning. In [80], the control of a boiler-turbine unit with reference tracking is discussed. Especially the state variables in the model have the real physical meaning. Thus the uncertainty matrices could be determined according to the constraints of these state variables.

In this thesis, the idea of confidence interval is applied to obtain the uncertainty matrices from the experimental data. The confidence interval express the possibility that

the measured outputs lie within the lower and upper bound defined by the uncertainty matrices. The uncertainty matrices D, E_a, E_b are designed in the form of diagonal parameter uncertainty. Thus the augmented MIMO models with eighth order is suitable in this case. With bigger uncertainty matrices, the confidence level that the measured outputs lie within the lower and upper bound will increase. But the optimization problem by LMI is unsolvable if the uncertainty matrices are too big.

Remark 4.1 *The constant matrices D, E_a, E_b must be determined by two requirement. The first one is to ensure the max level of the confidence interval. The confidence interval is the possibility that the measured outputs of engine speed and NOx value lie within the representation area of the uncertain models. The second one is that the optimization problem by LMI in the following section must have feasible solution.*

In this chapter, D, E_a, E_b are given by

$$D = diag\{0.1, 0.1, 0.1, 0.1, 0.1, 0.1, 0.1, 0.1\}, \tag{4.4}$$

$$E_a = diag\{0.001, 0.001, 0.001, 0.001, 0.001, 0.001, 0.001, 0.001\}, \tag{4.5}$$

$$E_b = \begin{pmatrix} diag\{0.004, 0.004, 0.004, 0.004\} \\ diag\{0.015, 0.015, 0.015, 0.015\} \end{pmatrix} \tag{4.6}$$

A validation result for the system model by Eq. (4.1) with data not used for identification can be seen in Figure 4.1. The solid lines describe the nominal models which are linear state space equations with parameter matrices A_p,B_p,C_p identified by the method in Chapter 3. $F = I$ is chosen as the upper bound of parameter uncertainties, and $F = -I$ as the lower bound. The dashed lines show the representation area of the uncertain models. The uncertainty matrices D, E_a, E_b designed here will ensure the confidence interval 75.45% for the engine speed model and 87.03% for the NOx emission model. We can see that most parts of the measured outputs of engine speed and NOx value lie within the lower and upper bound. Main dynamics are captured well.

Here is on thing we should pay attention to. As for the calculation of confidence interval, we need more data of real outputs. And average value should be used for the calculation of confidence interval.

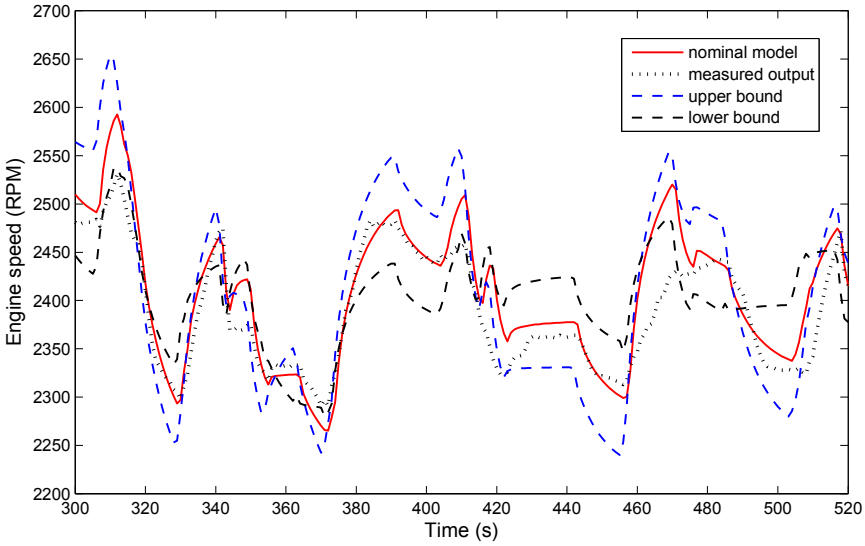

(a) engine speed

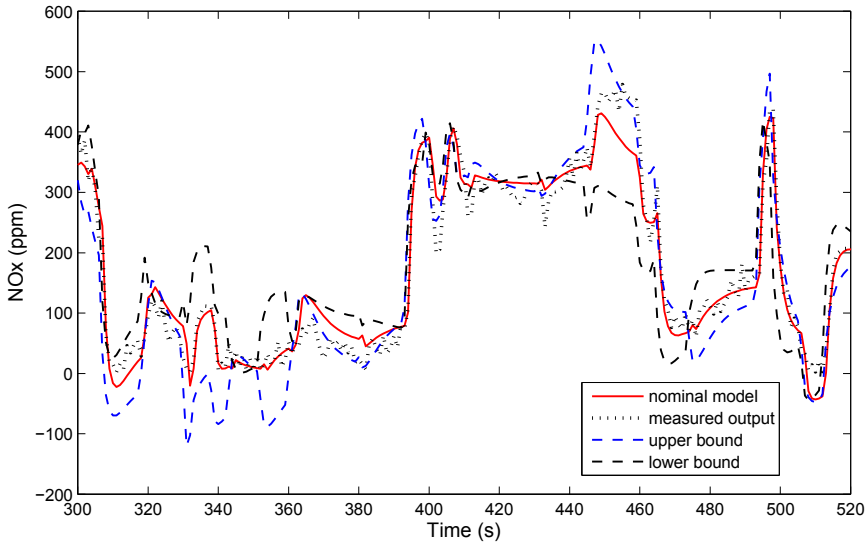

(b) NOx

FIGURE 4.1: Validation results of model by Eq.(4.1)

4.3 Controller design

4.3.1 Extended guaranteed cost state feedback control

The controller described in this section is based on the idea of guaranteed cost control technique [81]. The control goal is to achieve the output reference tracking with input constraints. Associating with the system by Eq. (4.1), the quadratic performance which is also called cost function is defined as follows:

$$J = \sum_{k=0}^{\infty} \left[x_p^{\mathrm{T}}(k) Q x_p(k) + u^{\mathrm{T}}(k) R u(k) \right] \tag{4.7}$$

where Q and R are the defined weight matrices to make the performance of the controller satisfied.

But unlike [80–83], the state variables in engine uncertain model have no physical meaning, which means they are unmeasured. Thus state estimate is needed. A Luenberger observer [87] for state estimate is given by

$$\begin{cases} \hat{x}\ (k+1) = A_p \hat{x}_p(k) + B_p u(k) + L\left[y_p(k) - \hat{y}_p(k) \right] \\ \hat{y}_p(k) = C \hat{x}_p(k) \end{cases} \tag{4.8}$$

where $\hat{x}_p$ is the estimation of the state x_p, $\hat{y}_p$ the observer output, L the observer gain. The control law is designed in the following form with state feedback.

$$u(k) = -K \hat{x}_p(k) \tag{4.9}$$

Then the resulting extended closed-loop system could be obtained.

$$\begin{cases} x_p(k+1) = A_x x_p(k) + B_x K e(k) \\ e(k+1) = A_e x_p(k) + B_e e(k) \end{cases} \tag{4.10}$$

Then the objective is to get a suitable K making the closed-loop system in Eq. (4.10) asymptotically stable for the uncertain matrices. Meanwhile the value of the cost function in Eq. (4.7) satisfies $J \leq J^*$, where J^* is some specified constant. Due to the existence of state observer, the original system is augmented. $e(k) = x_p(k) - \hat{x}_p(k)$ is the

estimated error.

$$\begin{cases} A_x = A_p + \Delta A - B_p K - \Delta BK \\ B_x = B_p K + \Delta BK \\ A_e = \Delta A - \Delta BK \\ B_e = A_p - LC_p + \Delta BK \end{cases} \tag{4.11}$$

In order to make the proof of the final conclusion, the following lemma is introduced.

Lemma 4.1 *The inequality*

$$Y + HFE + E^{\mathrm{T}} F^{\mathrm{T}} H^{\mathrm{T}} < 0 \tag{4.12}$$

where the matrix Y is symmetric and the matrices inside should have the appropriate dimensions. It could be transferred to the following form for all F satisfying $F^{\mathrm{T}} F \leq I$,

$$Y + \varepsilon HH^{\mathrm{T}} + \varepsilon^{-1} E^{\mathrm{T}} E < 0 \tag{4.13}$$

if the scalar ε *is bigger than* 0.

Theorem 4.1 $u(k) = -K\hat{x}_p(k)$ *is the control law for system by Eq. (4.10) and satisfies the guaranteed cost condition of* $J \leq J^*$ *if the following matrix inequality is satisfied.*

$$\begin{pmatrix} A_x^{\mathrm{T}} PA_x + A_e^{\mathrm{T}} TA_e - P + Q + K^{\mathrm{T}} RK & A_x^{\mathrm{T}} PB_x + A_e^{\mathrm{T}} TB_e \\ B_x^{\mathrm{T}} PA_x + B_e^{\mathrm{T}} TA_e & B_x^{\mathrm{T}} PB_x + B_e^{\mathrm{T}} TB_e - T \end{pmatrix} < 0 \tag{4.14}$$

where P, T are the matrices that are symmetric and positive-definite.

Proof. The proof procedure is similar to ref. [81]. Suppose we have the matrices P, T that are symmetric and positive definite, then the Lyapunov function candidate

$$V(k) = x_p^{\mathrm{T}}(k) P x_p(k) + e^{\mathrm{T}}(k) T e(k) \tag{4.15}$$

is positive definite. Consequently the corresponding difference of the Lyapunov function candidate based on the closed-loop system by Eq. (4.10) is given by

$$\begin{aligned}
\Delta V &= V(k+1) - V(k) && (4.16)\\
&= x_p^{\mathrm{T}}(k+1)Px_p(k+1) + e^{\mathrm{T}}(k+1)Te(k+1) \\
&\quad - x_p^{\mathrm{T}}(k)Px_p(k) - e^{\mathrm{T}}(k)Te(k) && (4.17)\\
&= (A_x x_p(k) + B_x e(k))^{\mathrm{T}} P(A_x x_p(k) + B_x e(k)) \\
&\quad + (A_e x_p(k) + B_e e(k))^{\mathrm{T}} T(A_e x_p(k) + B_e e(k)) \\
&\quad - x_p^{\mathrm{T}}(k)Px_p(k) - e^{\mathrm{T}}(k)Te(k) && (4.18)\\
&= \begin{pmatrix} x_p^{\mathrm{T}}(k) & e^{\mathrm{T}}(k) \end{pmatrix} \begin{pmatrix} A_x^{\mathrm{T}}PA_x + A_e^{\mathrm{T}}TA_e - P & A_x^{\mathrm{T}}PB_x + A_e^{\mathrm{T}}TB_e \\ B_x^{\mathrm{T}}PA_x + B_e^{\mathrm{T}}TA_e & B_x^{\mathrm{T}}PB_x + B_e^{\mathrm{T}}TB_e - T \end{pmatrix} \\
&\quad \begin{pmatrix} x_p(k) \\ e(k) \end{pmatrix} && (4.19)
\end{aligned}$$

From condition in Eq. (4.14), we can get

$$\Delta V(k) < -x_p^{\mathrm{T}}(k)(Q + K^{\mathrm{T}}RK)x_p(k) \tag{4.20}$$

Thus we can see that the Lyapunov stability theory is satisfied. And obviously the system by Eq. (4.10) is asymptotically stable. Furthermore, form Eq. (4.20) we can get

$$-\Delta V(k) > x_p^{\mathrm{T}}(k)(Q + K^{\mathrm{T}}RK)x_p(k) \tag{4.21}$$

The following inequality could be obtained by adding both sides of the above inequality from 0 to ∞,

$$J \leq x_p^{\mathrm{T}}(0)Px_p(0) + e^{\mathrm{T}}(0)Te(0) \tag{4.22}$$

We can see that the guaranteed cost form is established. The upper bound of the cost function is connected with the initial state in Eq. (4.10).

$$J^* = x_p^{\mathrm{T}}(0)Px_p(0) + e^{\mathrm{T}}(0)Te(0) \tag{4.23}$$

The proof of the theorem is completed. □

In the next part, the sufficient condition for the existence of guaranteed cost controller and corresponding state observer is given if the extended LMI in Eq.(4.24) has a feasible

solution.

Theorem 4.2 *Theorem 4.1 holds if there exist scalar* $\varepsilon_1 > 0, \varepsilon_2 > 0$ *, matrices W, U and symmetric matrix M which is positive-definite in order to make the LMI in Eq. (4.24) satisfied.*

$$\begin{pmatrix} -M+\varepsilon_1 DD^{\mathrm{T}} & 0 & 0 & A_pM-U & 0 & 0 & 0 & 0 \\ 0 & -M+\varepsilon_2 DD^{\mathrm{T}} & A_pM-B_pW & B_pW & 0 & 0 & 0 & 0 \\ 0 & (A_pM-B_pW)^{\mathrm{T}} & -M & 0 & (E_aM-E_bW)^{\mathrm{T}} & (E_aM-E_bW)^{\mathrm{T}} & M^{\mathrm{T}} & W^{\mathrm{T}} \\ (A_pM-U)^{\mathrm{T}} & (B_pW)^{\mathrm{T}} & 0 & -M & (E_bW)^{\mathrm{T}} & (E_bW)^{\mathrm{T}} & 0 & 0 \\ 0 & 0 & E_aM-E_bW & E_bW & -\varepsilon_1 I & 0 & 0 & 0 \\ 0 & 0 & E_aM-E_bW & E_bW & 0 & -\varepsilon_2 I & 0 & 0 \\ 0 & 0 & M & 0 & 0 & 0 & -Q^{-1} & 0 \\ 0 & 0 & W & 0 & 0 & 0 & 0 & -R^{-1} \end{pmatrix} < 0 \quad (4.24)$$

F , if matrix inequality in Eq. (4.24) can be solved, the solution variables ε_1, ε_2, *W, U, M could be obtained. Then the control law based on extended guaranteed cost theory with the state feedback is as follows*

$$u(k) = -WM^{-1}\hat{x}_p(k) \quad (4.25)$$

and the observer gain is given by

$$L = U(C_pM)^{-1} \quad (4.26)$$

Proof. Matrix inequality in Eq. (4.14) can be written as

$$\begin{pmatrix} A_e^{\mathrm{T}}TA_e - P + Q + K^{\mathrm{T}}RK & A_e^{\mathrm{T}}TB_e \\ B_e^{\mathrm{T}}TA_e & B_e^{\mathrm{T}}TB_e - T \end{pmatrix} + \begin{pmatrix} A_x^{\mathrm{T}} \\ B_x^{\mathrm{T}} \end{pmatrix} P \begin{pmatrix} A_x & B_x \end{pmatrix} < 0 \quad (4.27)$$

The above inequality is equivalent to the following form using the theory of Schur complement.

$$\begin{pmatrix} -P^{-1} & A_x & B_x \\ A_x^{\mathrm{T}} & A_e^{\mathrm{T}}TA_e - P + Q + K^{\mathrm{T}}RK & A_e^{\mathrm{T}}TB_e \\ B_x^{\mathrm{T}} & B_e^{\mathrm{T}}TA_e & B_e^{\mathrm{T}}TB_e - T \end{pmatrix} < 0 \quad (4.28)$$

Then by similar procedure, we can solve the matrices with respect to T

$$\begin{pmatrix} -T^{-1} & 0 & A_e & B_e \\ 0 & -P^{-1} & A_x & B_x \\ A_e^{\mathrm{T}} & A_x^{\mathrm{T}} & -P+Q+K^{\mathrm{T}}RK & 0 \\ B_e^{\mathrm{T}} & B_x^{\mathrm{T}} & 0 & -T \end{pmatrix} < 0 \tag{4.29}$$

By substituting Eq. (4.2) and Eq. (4.11) in the above inequality, it can be rewritten as

$$\begin{aligned} &\begin{pmatrix} -T^{-1} & 0 & 0 & A_p - LC_p \\ 0 & -P^{-1} & A_x & B_x \\ 0 & A_x^{\mathrm{T}} & -P+Q+K^{\mathrm{T}}RK & 0 \\ (A_p - LC_p)^{\mathrm{T}} & B_x^{\mathrm{T}} & 0 & -T \end{pmatrix} \\ &+ \begin{pmatrix} D \\ 0 \\ 0 \\ 0 \end{pmatrix} F \begin{pmatrix} 0 & 0 & E_a - E_bK & E_bK \end{pmatrix} \\ &+ \begin{pmatrix} 0 & 0 & E_a - E_bK & E_bK \end{pmatrix}^{\mathrm{T}} F^{\mathrm{T}} \begin{pmatrix} D \\ 0 \\ 0 \\ 0 \end{pmatrix}^{\mathrm{T}} < 0 \end{aligned} \tag{4.30}$$

By applying the method of Lemma 4.1 and Schur complement, under the condition of any admissible uncertain matrices F, the inequality in Eq. (4.30) could be transferred into the following LMI if there exists a scalar ε_1.

$$\begin{pmatrix} -T^{-1} + \varepsilon_1 DD^{\mathrm{T}} & 0 & 0 & A_p - LC_p & 0 \\ 0 & -P^{-1} & A_x & B_x & 0 \\ 0 & A_x^{\mathrm{T}} & -P+Q+K^{\mathrm{T}}RK & 0 & (E_a - E_bK)^{\mathrm{T}} \\ (A_p - LC_p)^{\mathrm{T}} & B_x^{\mathrm{T}} & 0 & -T & (E_bK)^{\mathrm{T}} \\ 0 & 0 & E_a - E_bK & E_bK & -\varepsilon_1 I \end{pmatrix} < 0 \tag{4.31}$$

By the similar procedure, matrices A_x and B_x can be solved.

$$\begin{pmatrix} -T^{-1}+\varepsilon_1 DD^{\mathrm{T}} & 0 & 0 & A_p - LC_p & 0 & 0 \\ 0 & -P^{-1}+\varepsilon_2 DD^{\mathrm{T}} & A_p - B_pK & B_pK & 0 & 0 \\ 0 & (A_p - B_pK)^{\mathrm{T}} & -P+Q+K^{\mathrm{T}}RK & 0 & (E_a - E_bK)^{\mathrm{T}} & (E_a - E_bK)^{\mathrm{T}} \\ (A_p - LC_p)^{\mathrm{T}} & (B_pK)^{\mathrm{T}} & 0 & -T & (E_bK)^{\mathrm{T}} & (E_bK)^{\mathrm{T}} \\ 0 & 0 & E_a - E_bK & E_bK & -\varepsilon_1 I & 0 \\ 0 & 0 & E_a - E_bK & E_bK & 0 & -\varepsilon_2 I \end{pmatrix} < 0 \tag{4.32}$$

Then the above inequality is pre-multiplied and post-multiplied in both sides by

$$\begin{pmatrix} I & 0 & 0 & 0 & 0 & 0 \\ 0 & I & 0 & 0 & 0 & 0 \\ 0 & 0 & P^{-1} & 0 & 0 & 0 \\ 0 & 0 & 0 & T^{-1} & 0 & 0 \\ 0 & 0 & 0 & 0 & I & 0 \\ 0 & 0 & 0 & 0 & 0 & I \end{pmatrix} \tag{4.33}$$

Then we can obtain

$$\begin{pmatrix} -T^{-1}+\varepsilon_1 DD^{\mathrm{T}} & 0 & 0 & A_pT^{-1} - LC_pT^{-1} & 0 & 0 \\ 0 & -P^{-1}+\varepsilon_2 DD^{\mathrm{T}} & A_pP^{-1} - B_pKP^{-1} & B_pKT^{-1} & 0 & 0 \\ 0 & P^{-1}(A_p - B_pK)^{\mathrm{T}} & -P^{-1}+P^{-1}QP^{-1}+P^{-1}K^{\mathrm{T}}RKP^{-1} & 0 & P^{-1}(E_a - E_bK)^{\mathrm{T}} & P^{-1}(E_a - E_bK)^{\mathrm{T}} \\ T^{-1}(A_p - LC_p)^{\mathrm{T}} & T^{-1}(B_pK)^{\mathrm{T}} & 0 & -T^{-1} & T^{-1}(E_bK)^{\mathrm{T}} & T^{-1}(E_bK)^{\mathrm{T}} \\ 0 & 0 & E_aP^{-1} - E_bKP^{-1} & E_bKT^{-1} & -\varepsilon_1 I & 0 \\ 0 & 0 & E_a - E_bK & E_bKT^{-1} & 0 & -\varepsilon_2 I \end{pmatrix} < 0 \tag{4.34}$$

Finally the matrix inequality in Eq. (4.24) is obtained using the theory of Schur complement again. Where $M = P^{-1} = T^{-1}$, $W = KP^{-1}$, $U = LCT^{-1}$.

The proof of the theorem is completed. □

In order to solve the above LMI in Eq. (4.24), we use the LMI toolbox of Matlab in this dissertation. The LMI such as Eq. (4.24) can be written into the program by LMI toolbox of Matlab. The variables ε_1, ε_2 and matrices W, U, M are the solution variables. The solution variables could be obtained by two kinds of calculation function. The first one is '$feasp$' which can calculate the feasible solution that make the LMI satisfied. This function is used in this chapter. The other one is '$mincx$' which can optimize target function and make the LMI satisfied. This function is used in Chapter 5.

Remark 4.2 *The matrix inequality is extended by lines and rows through the existing matrix T in Eq. (4.34) for the solution of observer gain. It is even unsolvable due to this augmented portion. By the assumption P = T, the problem is transferred to final LMI formation Eq. (4.24) that can be solved by Matlab program.*

4.3.2 Input constraints

There are physical constraints on main injection quantity, main injection timing, injection pressure and EGR valve opening. The manipulated variables u in the system Eq.(4.1) are subjected the following constraints:

$$\underline{u_i} \leq u_i \leq \overline{u_i}, i = 1, 2, \cdots, m, \tag{4.35}$$

where u_i is the *ith* element in the manipulated variables u, $\underline{u}$ and $\overline{u_i}$ are known lower and upper bound. m is the number of the manipulated variables. The constraints can be normalized to the following form:

$$-1/2(\overline{u_i} - \underline{u_i}) \leq (u_i - 1/2(\overline{u_i} + \underline{u_i})) \leq 1/2(\overline{u_i} - \underline{u_i}), i = 1, 2, \cdots, m, \tag{4.36}$$

where the term $(\overline{u_i} - \underline{u_i})$ and term $(\overline{u_i} + \underline{u_i})$ are known constants.

By defining the set λ using Lyapunov function [88],

$$\lambda = \left\{ \begin{pmatrix} x_p(k) \\ e(k) \end{pmatrix} \middle| \begin{pmatrix} x_p(k) \\ e(k) \end{pmatrix}^{\mathrm{T}} \begin{pmatrix} P & 0 \\ 0 & T \end{pmatrix} \begin{pmatrix} x_p(k) \\ e(k) \end{pmatrix} \leq 1 \right\} \tag{4.37}$$

Where λ is positive invariant set.

As discussed in [88], $x_p(0)$ is a known value. The initial estimation error is assumed to be 0. Then in order to ensure

$$J^* = x_p^{\mathrm{T}}(0) P x_p(0) + e^{\mathrm{T}}(0) T e(0) \leq 1 \tag{4.38}$$

the following matrix inequality must hold [89]

$$\begin{pmatrix} P^{-1} & x_p(0) \\ x_p^{\mathrm{T}}(0) & 1 \end{pmatrix} > 0 \tag{4.39}$$

The control law can be written in the form of x and e as follows

$$\begin{aligned} u(k) &= -K\hat{x}_p(k) = -K(x_p(k) - e(k)) \\ &= -\begin{pmatrix} K & -K \end{pmatrix} \begin{pmatrix} x_p(k) \\ e(k) \end{pmatrix} \end{aligned} \tag{4.40}$$

Theorem 4.3 *If the matrix inequality in Eq. (4.24) holds for any admissible uncertainties and following three inequalities*

$$\begin{pmatrix} M & x_p(0) \\ x_p^{\mathrm{T}}(0) & 1 \end{pmatrix} > 0 \tag{4.41}$$

$$\begin{pmatrix} M & 0 & W^{\mathrm{T}} \\ 0 & M & -W^{\mathrm{T}} \\ W & -W & X \end{pmatrix} \geq 0 \tag{4.42}$$

$$X_{ii} \leq (1/2(\overline{u_i} - \underline{u_i}))^2, i = 1, 2, \cdots, m. \tag{4.43}$$

are satisfied, Then control law $u(k) = K\hat{x}_p(k)$ based on the extended guaranteed cost theory could be obtained. Furthermore the constraints in Eq. (4.36) of system by Eq. (4.1) are also guaranteed.

Proof. This theorem can be proved with the similar way in [82]. The difference is that this theorem computes the augmented matrix inequalities, but this does not affect the proof. The following matrix inequalities can be obtained easily,

$$\begin{pmatrix} P & 0 & K^{\mathrm{T}} \\ 0 & T & -K^{\mathrm{T}} \\ K & -K & X \end{pmatrix} \geq 0 \tag{4.44}$$

Based on the same assumption in Theorem 2. Then the above inequality is pre-multiplied and post-multiplied in both sides by

$$\begin{pmatrix} P^{-1} & 0 & 0 \\ 0 & T^{-1} & 0 \\ 0 & 0 & I \end{pmatrix} \tag{4.45}$$

Then the matrix inequalities in Eq. (4.41) and Eq. (4.42) are obtained. These LMIs guarantee that control law never saturates over λ.

The proof of the theorem is completed. □

4.3.3 Tracking control

The main control goal is to track the engine speed of diesel engine and reduce NOx emission. Consider the uncertain system by Eq. (4.1) and the desired tracking output is y_{ref}, then we can get the tracking error by [80]

$$z(k+1) = z(k) + y_p(k) - y_{ref} \tag{4.46}$$

Then the augmented system is given in the following form

$$\begin{aligned} \begin{pmatrix} x_p(k+1) \\ z(k+1) \end{pmatrix} &= \begin{pmatrix} A_p + \Delta & \\ & I \end{pmatrix} \begin{pmatrix} x_p(k) \\ z(k) \end{pmatrix} \\ &+ \begin{pmatrix} B_p + \Delta B \\ 0 \end{pmatrix} u(k) + \begin{pmatrix} 0 \\ -y_{ref} \end{pmatrix} \end{aligned} \tag{4.47}$$

or in a compact form

$$\tilde{x}(k+1) = (\tilde{A} + \Delta\tilde{A})\tilde{x}(k) + (\tilde{B} + \Delta\tilde{B})u(k) + \tilde{d}(k) \tag{4.48}$$

where

$$\begin{aligned} &\tilde{x}(k) = \begin{pmatrix} x_p(k) \\ z(k) \end{pmatrix}, \tilde{A} = \begin{pmatrix} A_p & 0 \\ C_p & I \end{pmatrix}, \tilde{C} = \begin{pmatrix} C & \end{pmatrix}, \\ &\tilde{B} = \begin{pmatrix} B_p \\ 0 \end{pmatrix}, \tilde{d}(k) = \begin{pmatrix} 0 \\ -y_{ref} \end{pmatrix} \end{aligned} \tag{4.49}$$

The augmented uncertainty matrices are also augmented in the following form

$$\begin{aligned} &\begin{bmatrix} \Delta\tilde{A} & \Delta\tilde{B} \end{bmatrix} = \tilde{D}F \begin{bmatrix} \tilde{E}_a & \tilde{E}_b \end{bmatrix} \\ &\tilde{D} = \begin{pmatrix} D & 0 \\ 0 & 0 \end{pmatrix}, \tilde{E}_a = \begin{pmatrix} E_a & 0 \\ 0 & 0 \end{pmatrix}, \tilde{E}_b = \begin{pmatrix} E_b \\ 0 \end{pmatrix} \end{aligned} \tag{4.50}$$

Thus the extended guaranteed cost tracking control can be obtained by Theorem 4.2 as $u^* = \tilde{K}\tilde{x}(k)$. $\tilde{K} = \begin{pmatrix} K & K_I \end{pmatrix}$ and observer gain as $\tilde{L} = \begin{pmatrix} L \\ 0 \end{pmatrix}$. K is the control matrix by state feedback and K_I is the integral action matrix.

4.4 Experimental results

For comparisons, the linear quadratic regulator (LQR) design is discussed. The cost function of LQR method and the proposed method is the same. And the state inside is the augmented one as follows:

$$J = \sum_{k=0}^{\infty} \left[\tilde{x}(k)^{\mathrm{T}}(k) Q \tilde{x}(k) + u^{\mathrm{T}}(k) R u(k) \right] \tag{4.51}$$

The closed-loop control performance is really influenced by the weighting matrices Q and R in the cost function. So the it is crucial to choose the value of weighting matrices. Here in this thesis, the weighting matrices is decided by the procedure of trial and error to get a satisfied result [80]. Through the trial and error method by the simulation, the following weighting matrices are obtained:

$$\begin{aligned} Q &= diag\{1,1,1,1,1,1,1,1,1,0.00001\}, \\ R &= diag\{1500,40000,15000,4000\} \end{aligned} \tag{4.52}$$

Meanwhile the weighting matrices Q and R in Eq. (4.7) is chosen the same as above. Then control inputs are subjected to the following constraints:

$$\begin{aligned} 680 \le u_1 \le 700, 706 \le u_2 \le 716, \\ 100 \le u_3 \le 110, 6 \le u_4 \le 20 \end{aligned} \tag{4.53}$$

where $u_i, i = 1,2,3,4$ imply the injection quantity, injection timing, injection pressure and EGR valve opening. The constraints of u_2 and u_4 are expanded from the original ones applied for linear system identification. Thus the tested diesel engine can work in a wider nonlinear operation region.

When we design the controller in considering of input constraints, Theorem 4.3 is applied. In Eq. (4.41), the initial state $x_p(0)$ should be given. In our experiment, we use the undisturbed switching between manual mode and automation mode. In all the cases of experiment, we choose the middle of the working range as 2400 *rpm*. So we choose the initial state by state observer when the output of engine speed is 2400 *rpm*. In our case, we select the average value in 5 sampling times before the switching. The initial states are shown as follows:

$$x(0) = [0, 0.013, -0.011, -0.0072, 0.0074, 0.0052, 0, 0.0016]^T \tag{4.54}$$

4.4.1 Simulation results

The simulation results in Matlab is shown in this section. The control system of LQR and Extended guaranteed cost are built in the simulink. The reference of engine speed make a step from 2300 rpm to 2500 rpm. The reference of NOx stays at 50 ppm.

In this case, the disturbance is added into the system in an uncertainty form (random with constraints) as Figure 4.2. There is some model mismatch between the model used for controller and target model (Figure 4.3). The simulation results of control variables and manipulated variables are shown in Figure 4.4 and Figure 4.5. From the results, we can see that under the influence of uncertain disturbance, the response time be the proposed method is shorter. And the overshoot by the method of LQR is bigger. With the better transient performance, the NOx value is lower by the proposed method. The comparison is shown is Table 4.1.

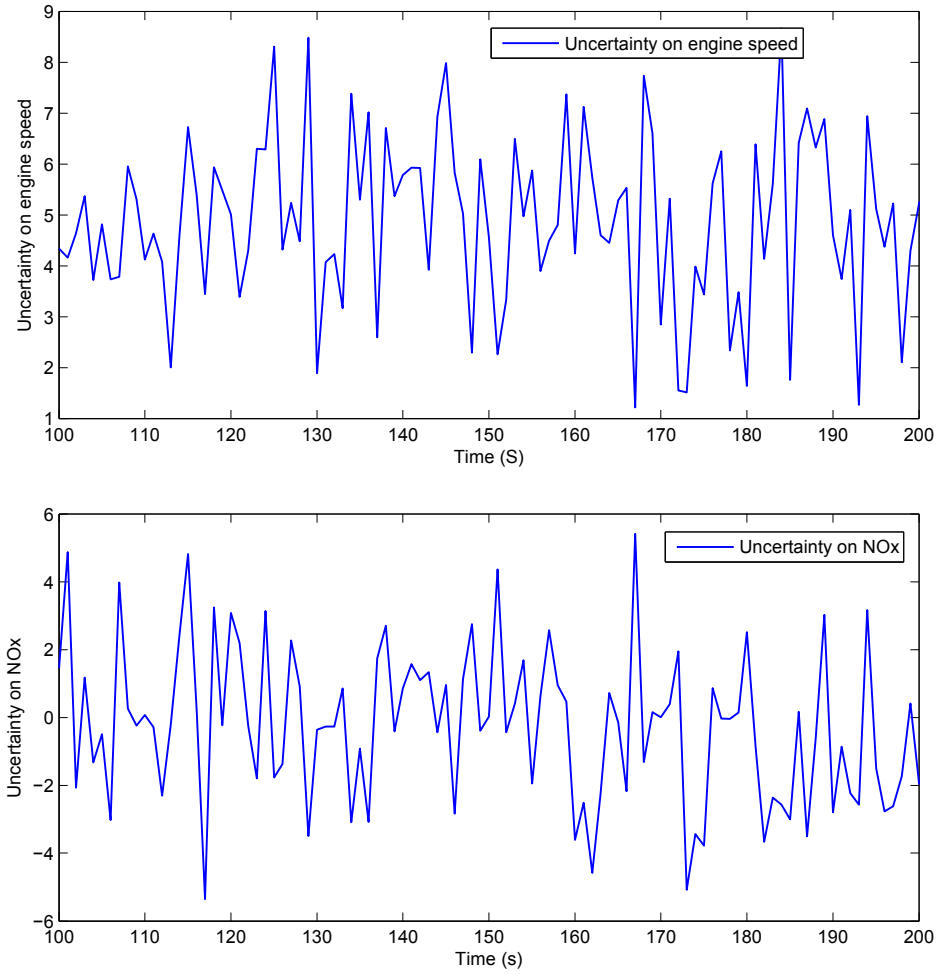

FIGURE 4.2: Uncertainty

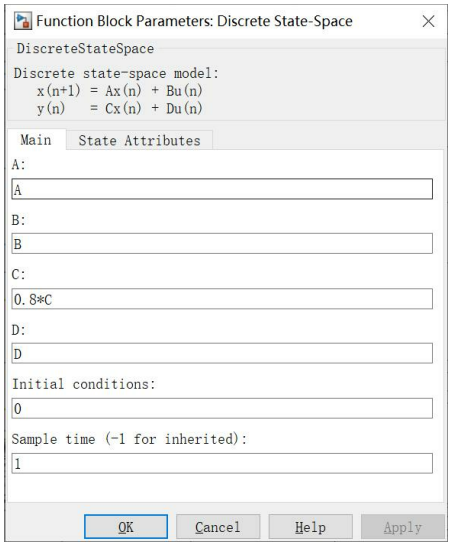

FIGURE 4.3: Condition of model mismatch

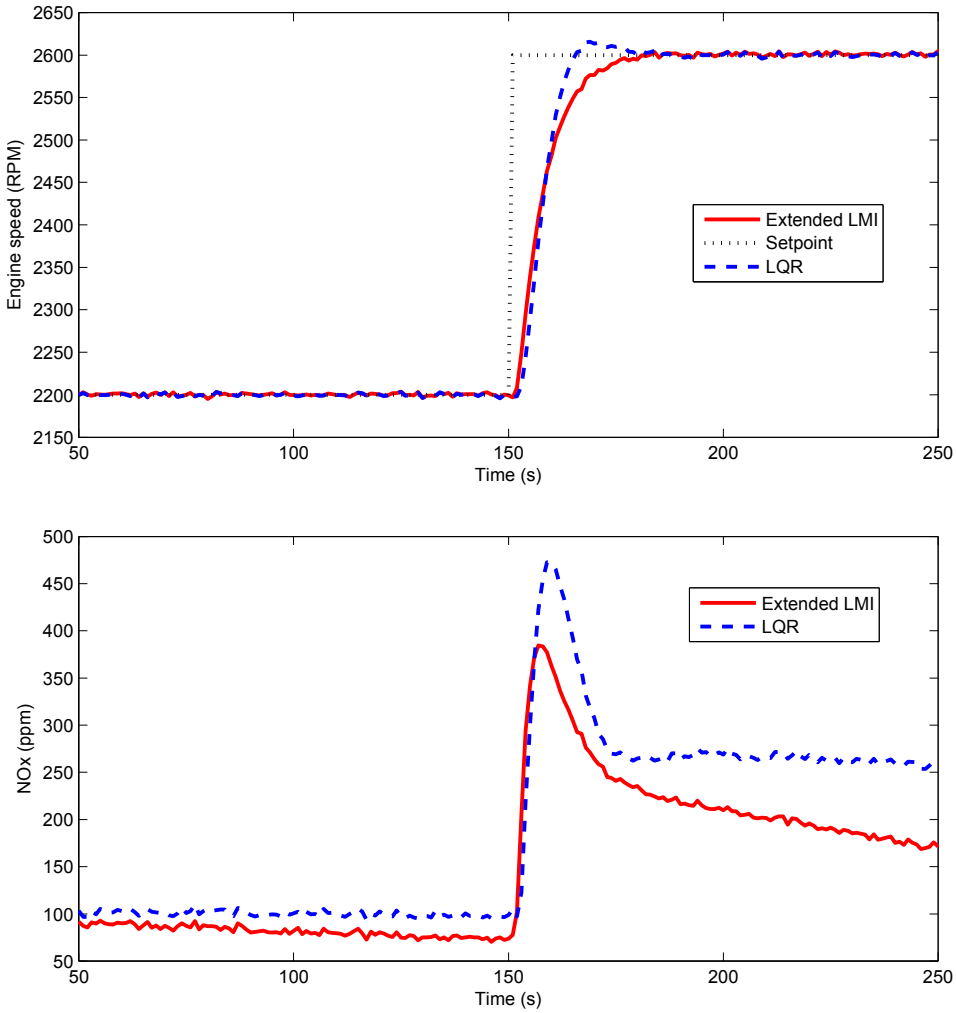

FIGURE 4.4: Control variables of simulation results

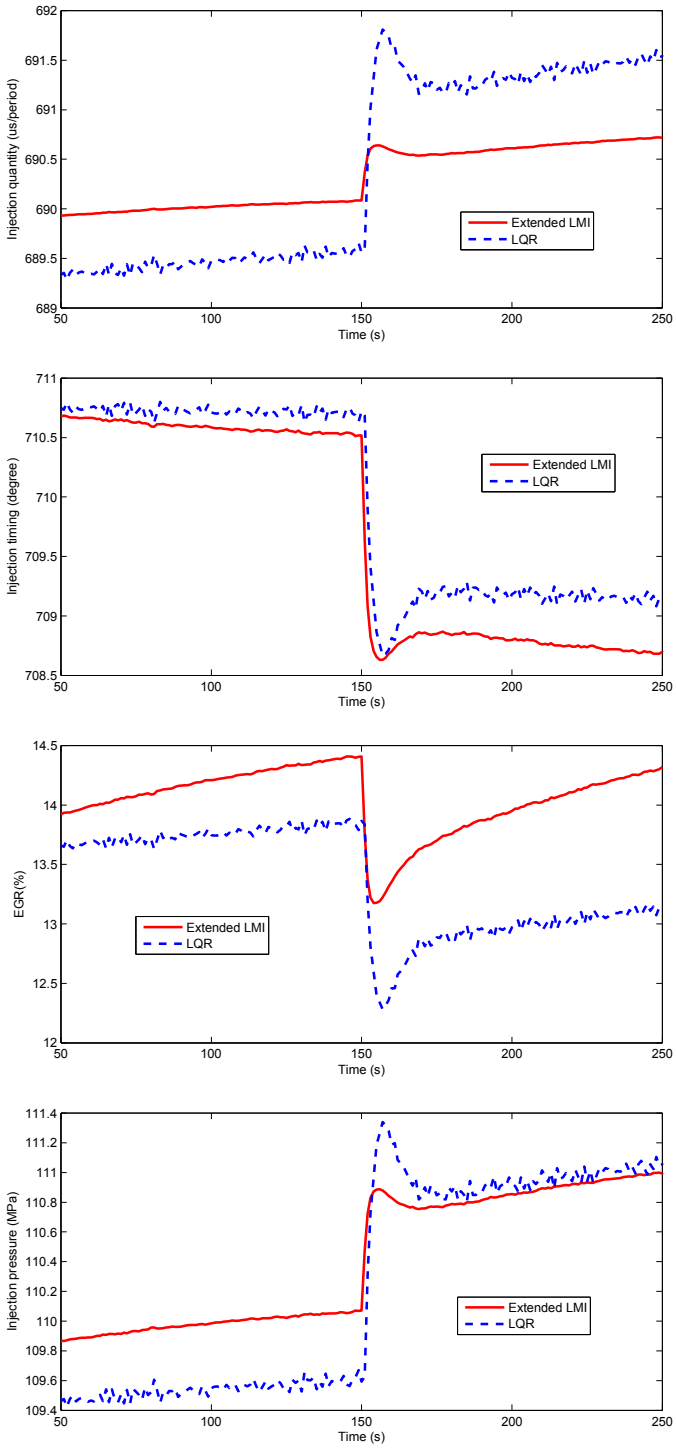

FIGURE 4.5: Manipulated variables of simulation results

T

	LQR	Extended LMI
Overshoot(rpm)	16	0
NOx value (ppm/point)	176.1242	148.3190

4.4.2 Real-time test results

The proposed control system is implemented in the dSPACE system. The control performance is evaluated in the real-time application. All the experiments are done in the test bench described in Chapter 3 which is fully warmed.

In this section three cases will be considered. In case 1 the engine speed reference changes in the working range where the system identification in Chapter 3 is done. Case 2 and 3 analyze how efficient the proposed control system could be during the working range of diesel engine expands. The NOx reference remains at 50 for each case. This is done to ensure the exhaust emission is as low as possible when the engine speed is changing.

$$Case1:$$

$$\begin{cases} y_1^{ref} = 2300, y_2^{ref} = 50, 0 \le t \le 10 \\ y_1^{ref} = 2500, y_2^{ref} = 50, 10 \le t \le 50 \\ y_1^{ref} = 2300, y_2^{ref} = 50, 50 \le t \le 90 \end{cases}$$

$$Case2:$$

$$\begin{cases} y_1^{ref} = 2200, y_2^{ref} = 50, 0 \le t \le 10 \\ y_1^{ref} = 2600, y_2^{ref} = 50, 10 \le t \le 70 \\ y_1^{ref} = 2200, y_2^{ref} = 50, 50 \le t \le 110 \end{cases}$$

$$Case3:$$

$$\begin{cases} y_1^{ref} = 2100, y_2^{ref} = 50, 0 \le t \le 10 \\ y_1^{ref} = 2700, y_2^{ref} = 50, 10 \le t \le 70 \\ y_1^{ref} = 2100, y_2^{ref} = 50, 50 \le t \le 110 \end{cases}$$

The experimental results of case 1, 2 and 3 are summarized in Figure 4.6, Figure 4.7, Figure 4.8,Figure 4.9, Figure 4.10 and Figure 4.11. In these figures, the control variables and manipulated variables are depicted. The red solid lines show the results of the proposed method, and the blue dashed lines show the results of the linear control method by LQR.

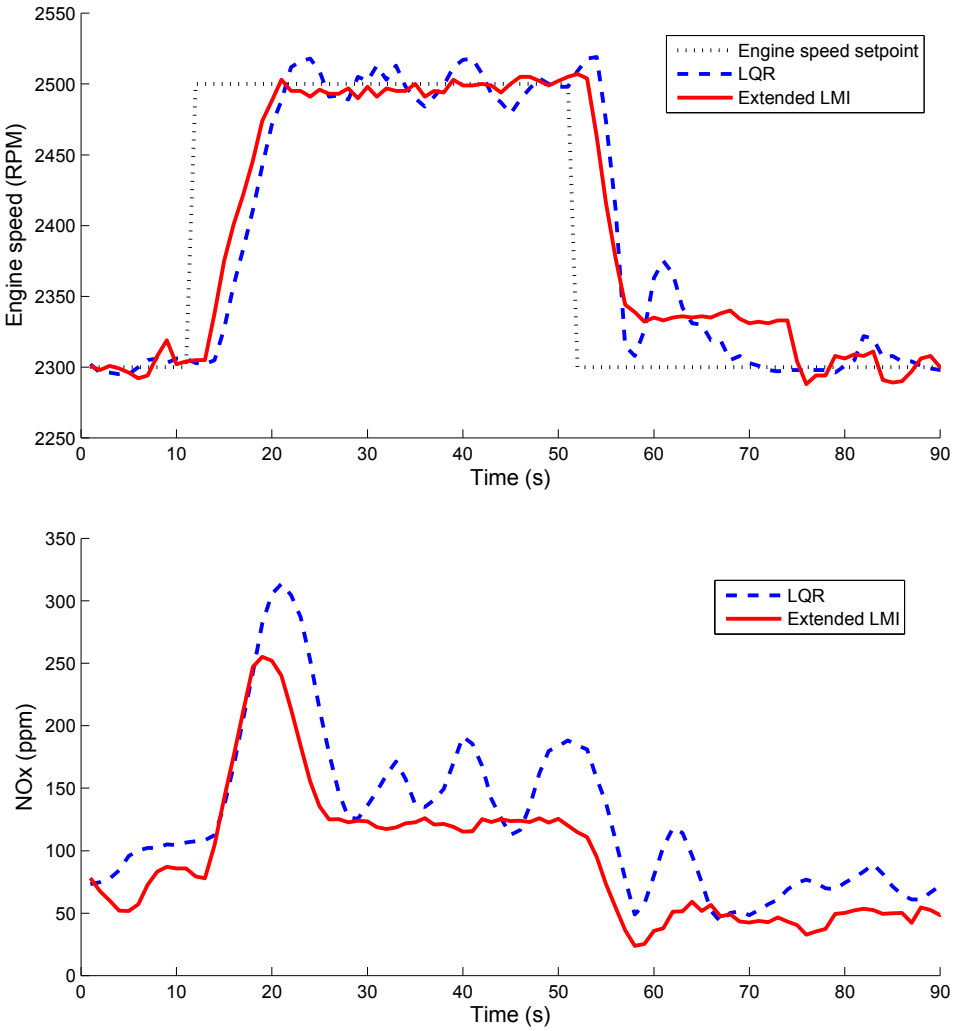

FIGURE 4.6: Control variables of case 1

For case 1, the tracking performance of engine speed by proposed method is similar to the linear control design. But the overshoot can be seen in linear control design with larger manipulated variables in Figure 4.6 and 4.7. Meanwhile the variation of inputs and outputs is bigger by the linear method of LQR. Also, the exhaust emission of NOx is higher than by proposed method.

For case 2, the working range expands as the nonlinearities and uncertainties increase. In Figure 4.8 and 4.9, the overshoot of engine speed is too large during speed up process by linear approach. Conversely, the system designed in this chapter shows a good performance in this case. Moreover the exhaust emission of NOx decreases much more than the linear approach.

For case 3, the working range expands larger. As a result the manipulated variables by the linear approach saturate the constraints occasionally. On the contrary the proposed

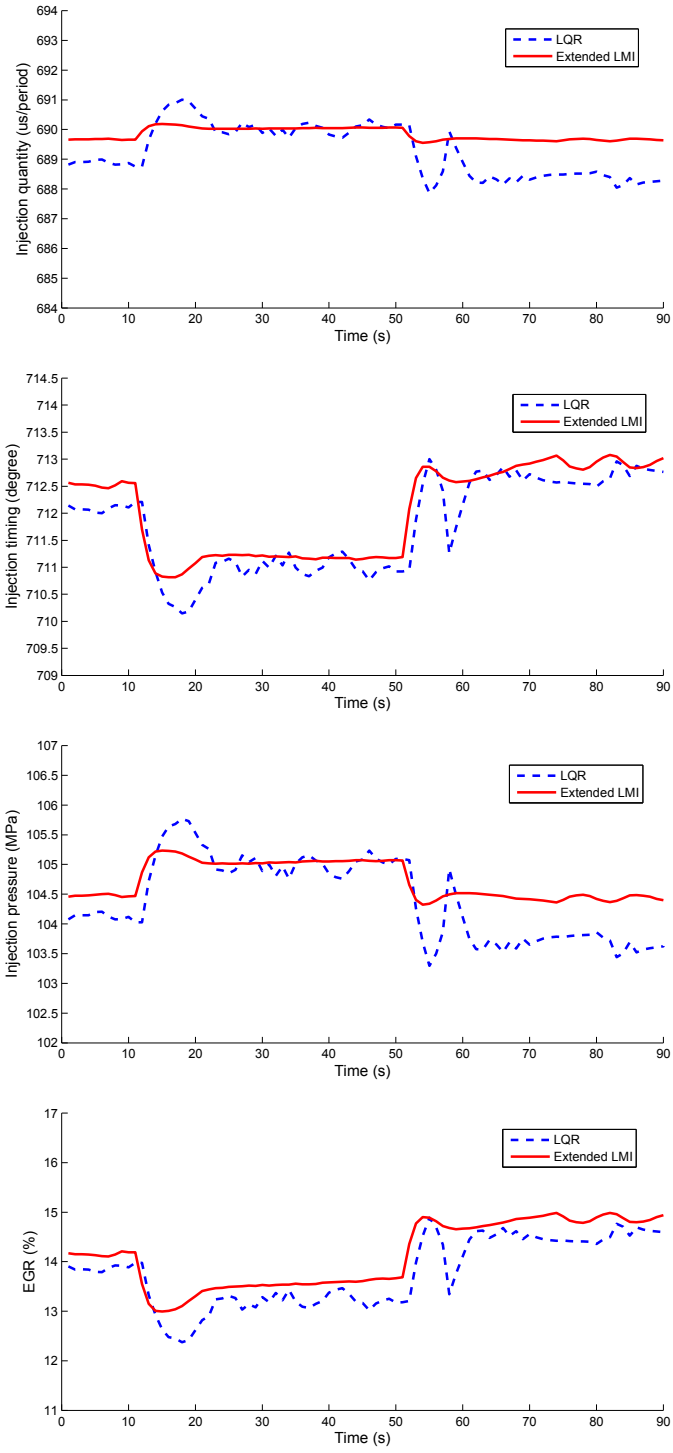

FIGURE 4.7: Manipulated variables of case 1

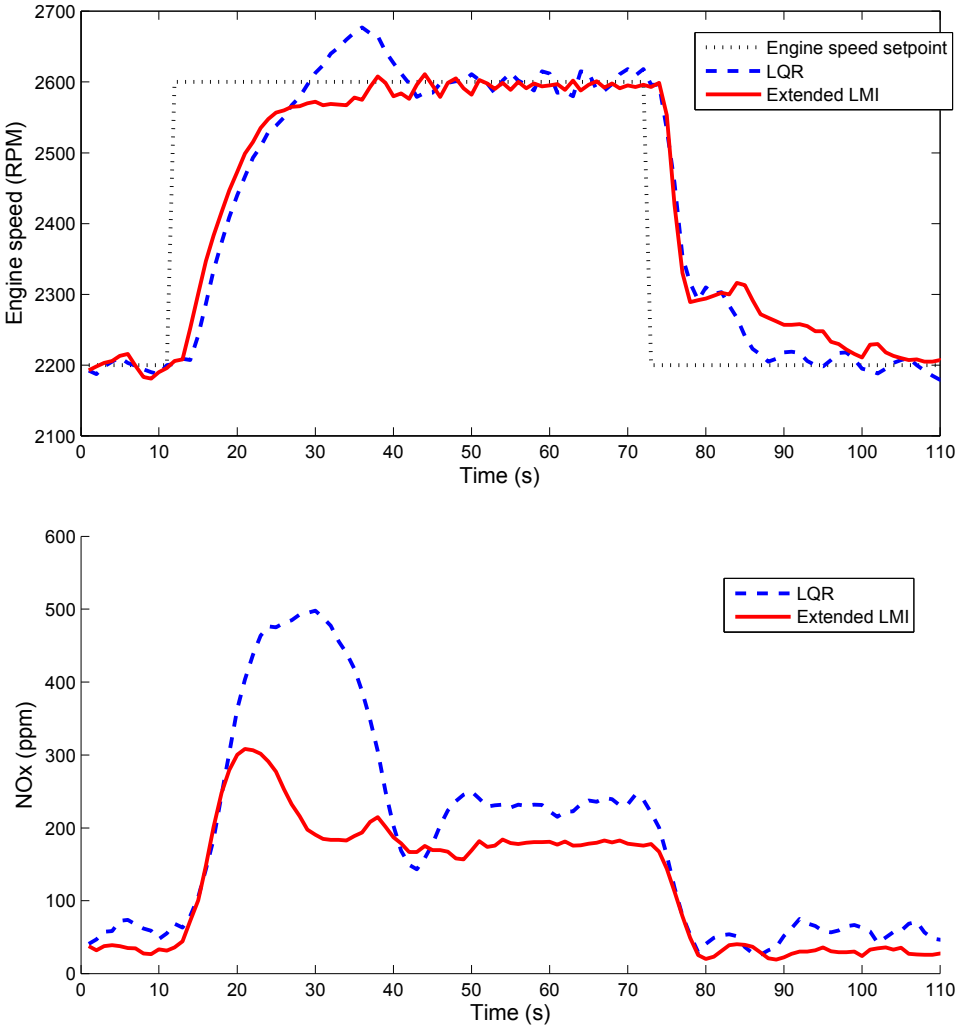

FIGURE 4.8: Control variables of case 2

method with superiority of dealing with the input constraints can achieve great control performance. Due to the constant load set to the tested engine, the sharp decrease can be seen when reference of engine speed is down in all cases. During the speed-down process, the load will have the direct prior influence on the diesel engine. After the sharp decrease of engine speed, linear approach shows faster response with bigger vibration. The engine speed tracking performance and the exhausted emission reduction are really satisfied by the proposed method.

In Chapter 3, it can be seen that the definition of linear working region is really time-consuming. With the proposed method, the designed model-based control system could be used in wider working region, which means that the time cost of the design for full working region will be reduced at the same time. The comparison of experiments results for each case is shown in Table 4.2.

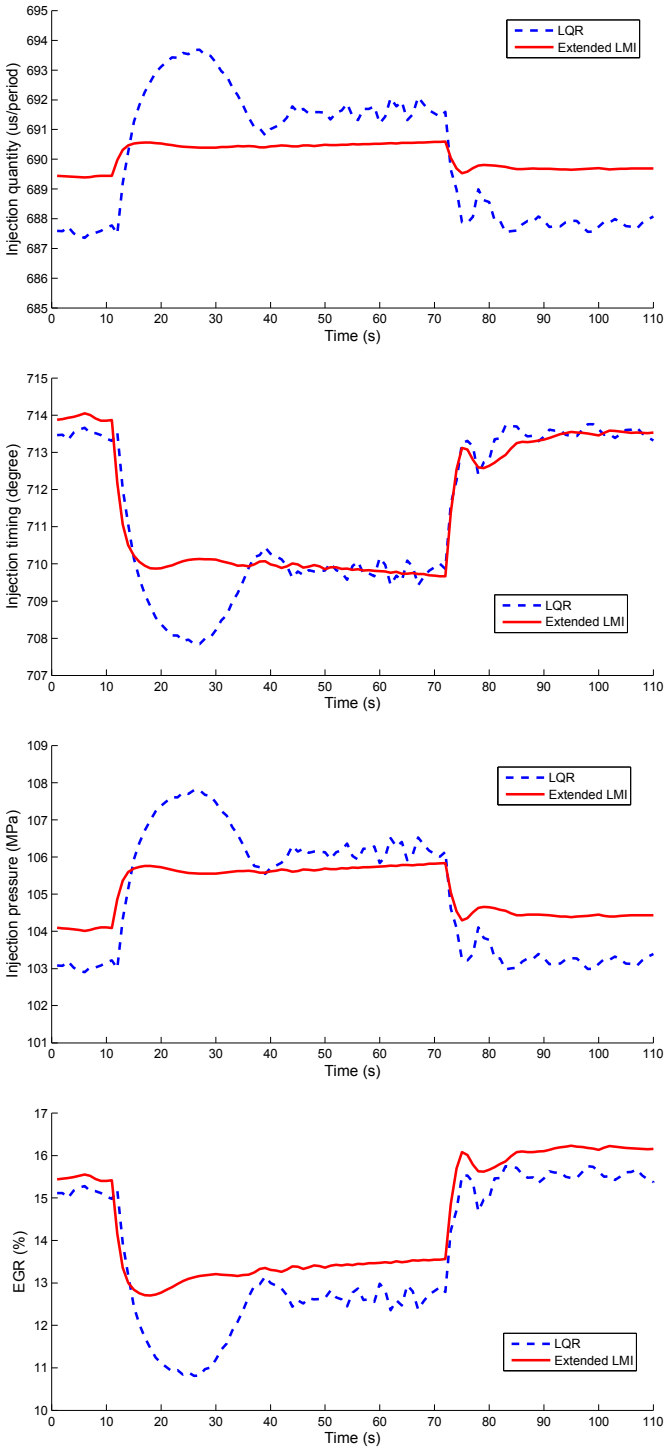

FIGURE 4.9: Manipulated variables of case 2

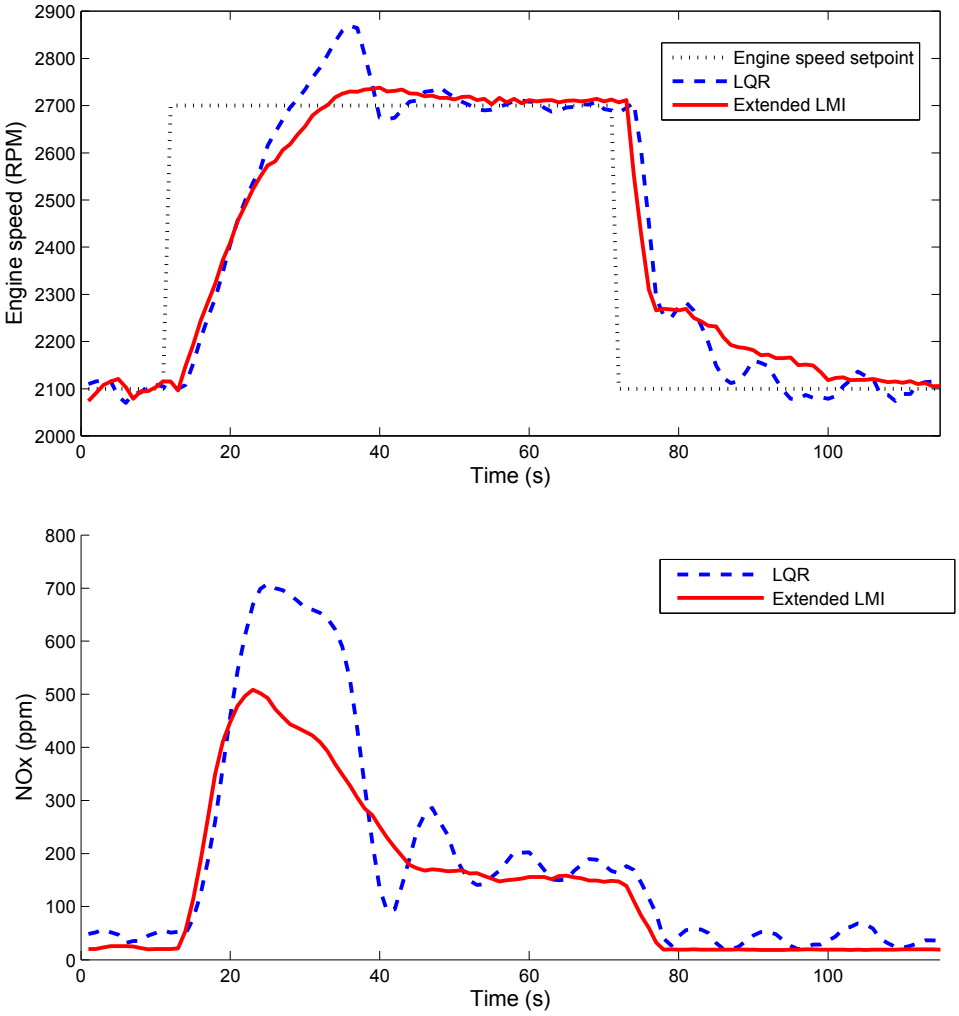

FIGURE 4.10: Control variables of case 3

*

4.4.3 Discussion about robustness

In order to discuss the robustness of the proposed method, we try to compare the experimental results from two different dates. Besides the experimental results in this section from 8th October 2016, here we show more results from 5th October 2016. In Figure 4.12 and Figure 4.13, it shows the control variables in case 1 and 2 on 5th October 2016. The detailed comparison of experimental results is shown in Table 4.3. From the results we can see that even in different experimental dates, the performance of the proposed method is similar. In another word, the extended guaranteed cost control can deal with the uncertainty very well. From the results in the above tables, we can see

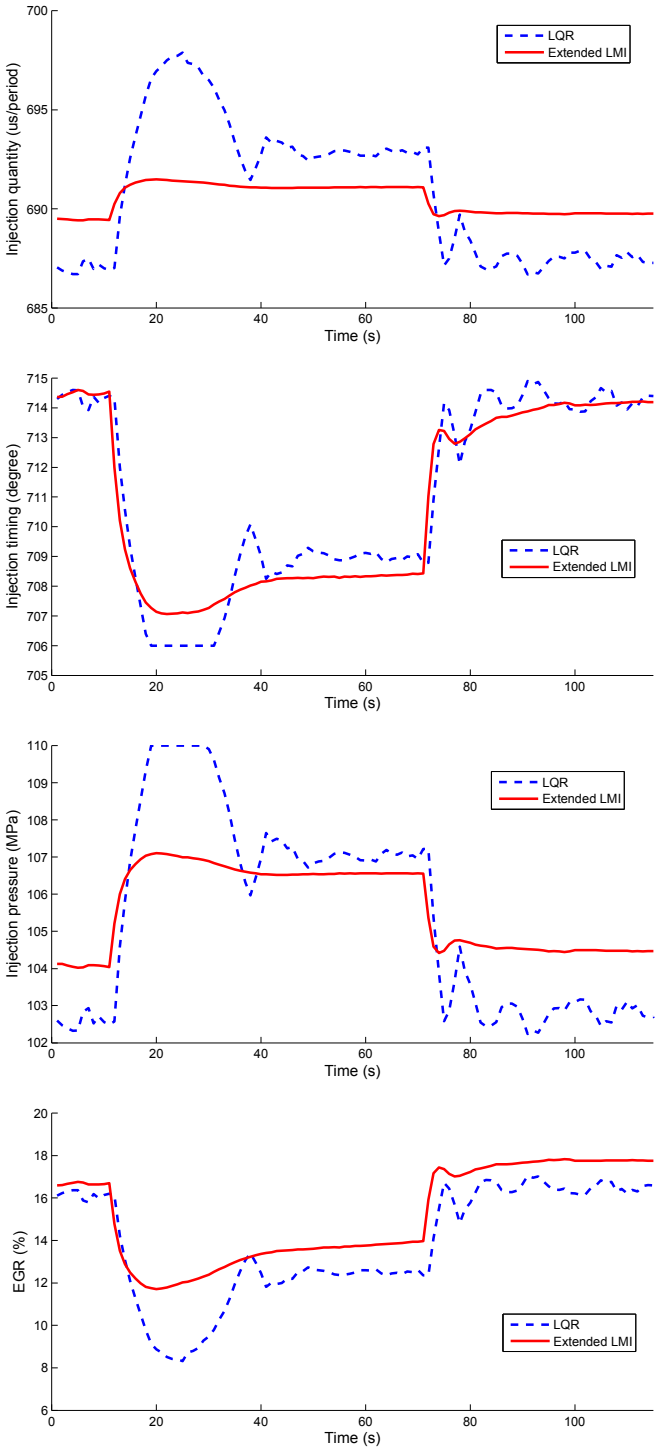

FIGURE 4.11: Manipulated variables of case 3

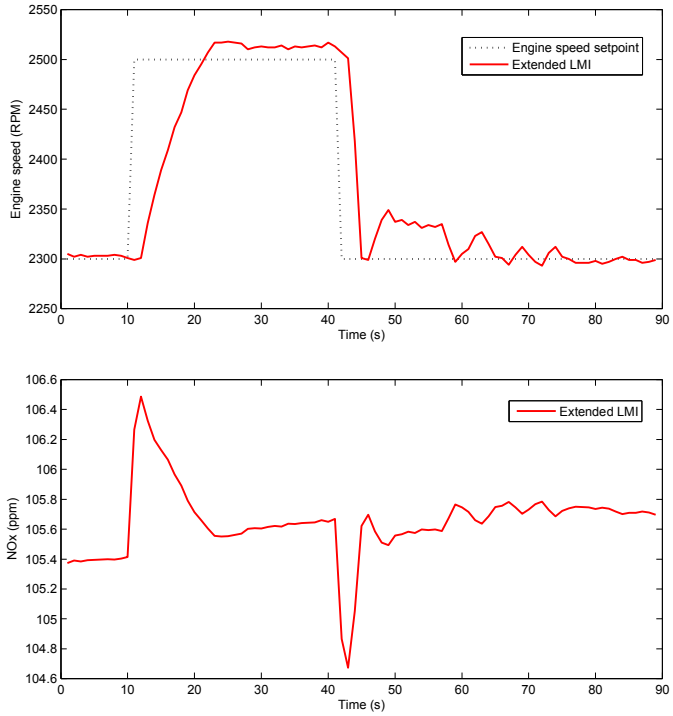

FIGURE 4.12: Control variables of case 1 on 10.05.2016

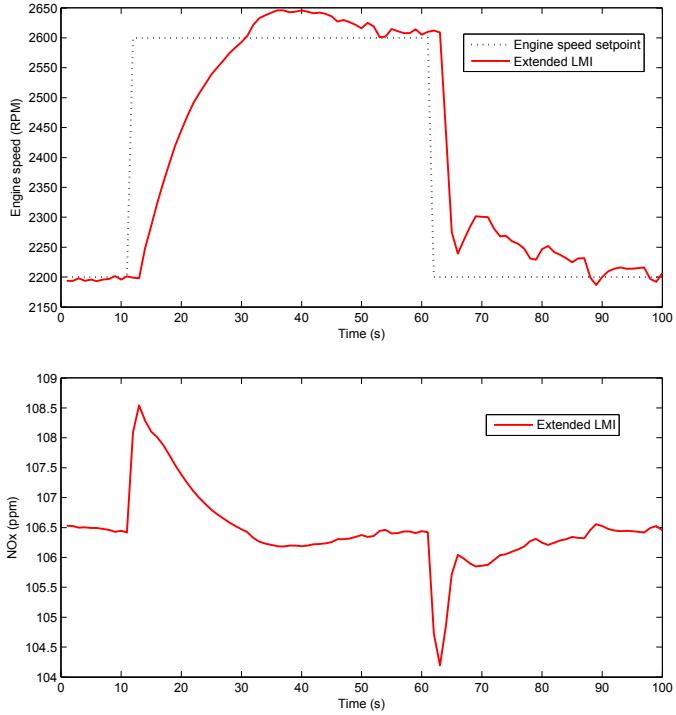

FIGURE 4.13: Control variables of case 2 on 10.05.2016

T -time results for 3 cases

Case 1	LQR	Extended LMI
Settling time(s)	15	11
Overshoot(rpm)	13	0
Steady tracking error (MSE from 25s to 50s)	106.9231	23.6923
NOx value (ppm/point)	117.0064	81.9605
Case 2		
Settling time(s)	32	29
Overshoot(rpm)	80	0
Steady tracking error (MSE from 42s to 70s)	135.5862	84.8276
NOx value (ppm/point)	181.7596	108.4164
Case 3		
Settling time(s)	38	39
Overshoot(rpm)	189	21
Steady tracking error (MSE from 49s to 70s)	146.5455	96.5909
NOx value (ppm/point)	186.0979	123.3580

T -time results from 2 different days

Case 1	Extended LMI (10.05)	Extended LMI (10.08)	Average value
Settling time(s)	15	11	13
Overshoot(rpm)	11	0	5.5
Steady tracking error (MSE in the middle of 20s)	86.7620	20.6923	53.7272
NOx value (ppm/point)	107.0155	81.9605	94.488
Case 2			
Settling time(s)	36	29	32.5
Overshoot(rpm)	50	0	25
Steady tracking error (MSE in the middle of 20s)	95.9673	64.3571	80.1622
NOx value (ppm/point)	121.4298	108.4164	114.9231

the improvement by the proposed method. One thing needs to be mentioned: in Table 4.2, the period of tracking error calculation is $25s$; in Table 4.3, the period of tracking error calculation is $20s$. In order to make comparison in the same situation, the average value of tracking error during 20 s need to be multiplied by 1.25. For case 3, there was only one group of experiment data on 8th October. So there is no comparison for case 3 in this research.

For case 1 in the defined linear working range, the average value of overshoot by

the proposed method decreases by 57.7% ((13-5.5)/13). The average value of tracking error for engine speed by the proposed method decreases by 37.2% ((106.9231-53.7272*1.25)/106.9231) and NOx emission value decreases by 19.2% ((117.0064-94.488)/117.0064) than LQR. For case 2 with bigger working region, the average value of overshoot for engine speed by the proposed method decreases by more than 68.8% ((80-5.5)/80) and NOx emission value decreases by 38.3% ((181.7596-114.9231)/181.7596). For case 3 with the biggest working range, the tracking error for engine speed by the proposed method decreases by more than 34.0% ((146.5455-96.5909)/146.5455) and NOx emission value decreases by 33.7% ((186.0979-123.3580)/186.0979).

4.5 Summary

This chapter presents an extended guaranteed cost tracking control of diesel engine with input constraints. Combustion uncertainties and nonlinear behavior of the system make the problem difficult to handle using classical control design methods. In this chapter, the process of diesel engine through both air and fuel loop is expressed by linear state space equations with parameter uncertainties. Compared with traditional guaranteed cost control, the state feedback and estimate gains are given from feasible solution of an augmented LMI simultaneously. To deal with tracking problem and physical constraints, more LMI conditions are discussed. The experimental results prove that the proposed control system achieve a better performance in precise reference tracking, meanwhile NOx is in a lower level as well.

From the Theorem 4.3, we can see that the solution to input constraints in this research is relative to the initial state of the system. As a result, the application of input constraints is not so convenient. Although the simple structure of state feedback control is very suitable for real-time application of diesel engine, it still motivates us to apply the model predictive control that can deal with the input constraints in MIMO systems in the next chapter.

Chapter 5

Modified Model Predictive Controller Design

5.1 Introduction

As described in Chapter 2, the fact that various model-based control methods for diesel engine has been ensured. As is well known, the diesel engine is a very complicated system. It is proved to be a highly coupled nonlinear multi-input multi-output (MIMO) system with input constraints. Among all these control strategies including the methods in Chapter 4, model predictive control (MPC) is one of the most attractive methods for the ability to deal with the input constraints in MIMO systems. In practice, modeling error, unmeasured disturbances and nonlinearity in the system can result into steady-state offset. For the real-time diesel engine control purpose, the offset-free control is needed. To achieve the reference tracking control of diesel engine with no offset, the disturbance model is introduced into MPC controller [62–65, 72, 90]. Unfortunately, the choice of disturbance model is not discussed in aforementioned studies. Many different researches [91–93] show that the closed-loop performance is extremely influenced by the choice of disturbance models. Still the importance of the state observer for the closed-loop performance is the same as the disturbance model itself. The method of design of the disturbance model and state observer at the same time was firstly proposed in [93]. The dynamic observer is designed based on the idea of H-infinity theory. The core of H-infinity theory is to minimize the effect from noise to the prediction error. This part of noise includes the unmeasured disturbances and model mismatch. However the H_∞ control problem of general solution and reduced order design were not discussed.

This chapter is mainly devoted to applying an offset-free MPC to the diesel engine system by combined design of disturbance model and state observer which are given from feasible solution of the linear matrix inequality (LMI). Furthermore the method of reduced-order design for H-infinity problem which satisfies the additional condition of offset-free tracking is addressed.

The rest of this chapter is organised as follows. Some preliminary results are described in Section 5.2. Section 5.3 focuses on the design of disturbance model and state observer. Furthermore the condition of offset-free tracking based on general solution of H_∞ problem is presented. The reduced-order design for H-infinity problem is addressed in Section 5.4. The MPC algorithm and experimental results including simulation and real-time application are given in Section 5.5 and 5.6. Finally, conclusions are summarized in Section 5.7.

5.2 Preliminary results

5.2.1 State space model

For the convenience, the diesel engine model in the form of discrete state space equations that was identified in Chapter 3 is introduced here again.

$$\begin{cases} x_p(k+1) = A_p x_p(k) + B_p u(k) \\ y_p(k) = C_p x_p(k) \end{cases} \tag{5.1}$$

Therein $x_p(k) \in R^n$ denotes the states, $u(k) \in R^m$ the manipulated variables, and $y_p(k) \in R^p$ the controlled variables.

5.2.2 Disturbance model

The model accuracy plays a important role in the design of model-based control system. It will really influence the closed-loop control performance. Especially in real-time application, modeling error and unmeasured disturbances can result into steady-state offset. Thus these problems should be considered in the control design. The solution to these problems are so-called offset-free method. The most widely-used way is to

augment the original process model to disturbance model [91, 92]. The disturbance model in general form is considered as the following augmented system.

$$\begin{cases} \begin{pmatrix} x_p(k+1) \\ d(k+1) \end{pmatrix} = \begin{pmatrix} A_p & B_d \\ 0 & I \end{pmatrix} \begin{pmatrix} x_p(k) \\ d(k) \end{pmatrix} + \begin{pmatrix} B_p \\ 0 \end{pmatrix} u(k) \\ y_p(k) = \begin{pmatrix} C_p & D_d \end{pmatrix} \begin{pmatrix} x_p(k) \\ d(k) \end{pmatrix} \end{cases} \tag{5.2}$$

A sufficient condition for reference tracking without offset of given reference is given in [92]. It is that the number of augmented variables should be equal to the number of measured outputs, just as, $dim(d) = dim(y_p)$. Moreover, the augmented system of Eq. (5.2) must be detectable so that the following condition should be satisfied:

$$rank \begin{pmatrix} I - A_p & -B_d \\ C_p & D_d \end{pmatrix} = dim(x_p) + dim(d) \tag{5.3}$$

By this augmented disturbance model, the new states could be used to eliminate the effect of the unmeasured disturbance and model mismatch in the system. The original states and the additional integrating disturbance are estimated by the state observer designed for the augmented system of Eq. (5.2) based on the output measurement in the following section.

5.2.3 State estimate

A Luenberger observer is applied to estimate the states and the disturbance in Eq. (5.2).

$$\begin{pmatrix} \hat{x}_p(k+1) \\ \hat{d}(k+1) \end{pmatrix} = \begin{pmatrix} A_p & B_d \\ 0 & I \end{pmatrix} \begin{pmatrix} \hat{x_p}(k) \\ \hat{d}(k) \end{pmatrix} + \begin{pmatrix} B_p \\ 0 \end{pmatrix} u(k) + \begin{pmatrix} L_1 \\ L_2 \end{pmatrix} \left(y_p(k) - C_p \hat{x_p}(k) - D_d \hat{d}(k) \right) \tag{5.4}$$

5.3 Combined offset-free design

5.3.1 Dynamic state observer

The discrete-time linear model of the diesel engine in real process is considered as

$$\begin{cases} x_p(k+1) = A_p x_p(k) + B_p u(k) + B_w w(k) \\ y_p(k) = C_p x_p(k) + D_w w(k) \end{cases} \tag{5.5}$$

in which $w \in R^q$ is the random noise. All unmeasured disturbances and model mismatch we discussed above are included in $w \in R^q$. In practice, there must be model mismatch between the linear model with matrices (A_p, B_p, C_p) in Eq. (5.1) and the real process.

In general case, and for the match of matrix dimension, the condition that $dim(w) = n + p$ should be assumed. Then the following matrices with parameters are obtained.

$$B_w = \begin{pmatrix} I_n & 0 \end{pmatrix}, D_w = \begin{pmatrix} 0 & I_p \end{pmatrix} \tag{5.6}$$

The state estimate $\hat{x}_p$ and output estimate $\hat{y}_p$ can be obtained by the dynamic observer

$$\begin{cases} \hat{x}\ (k+1) = A_p \hat{x}_p(k) + B_p u(k) + B_v v(k) \\ \hat{y}_p(k) = C_p \hat{x}_p(k) + D_v v(k) \\ \xi(k+1) = A_L \xi(k) + B_L e(k) \\ v(k) = C_L \xi(k) + D_L e(k) \end{cases} \tag{5.7}$$

where $\xi(k)$ is the auxiliary state and $e(k) = y_p(k) - \hat{y}_p(k)$. $e(k)$ is the error between the model output and the estimated output. Then definition of $e(k)$ in this chapter is different from the last chapter. A_L, B_L, C_L and D_L are unknown parameter matrices with appropriate dimensions. Similar to the above assumption, here the condition $dim(v) = n + p$ is considered and that

$$B_v = \begin{pmatrix} I_n & 0 \end{pmatrix}, D_v = \begin{pmatrix} 0 & I_p \end{pmatrix} \tag{5.8}$$

5.3.2 Connection with disturbance models

By the dynamic observer of Eq. (5.7) the following closed-loop augmented system is obtained:

$$\begin{cases} \begin{pmatrix} \hat{x}_p(k+1) \\ \xi(k+1) \end{pmatrix} = \begin{pmatrix} A_p & B_v C_L \\ 0 & A_L \end{pmatrix} \begin{pmatrix} \hat{x}_p(k) \\ \xi(k) \end{pmatrix} + \begin{pmatrix} B_p \\ 0 \end{pmatrix} u(k) + \begin{pmatrix} B_v D_L \\ B_L \end{pmatrix} e(k) \\ e(k) = (I + D_v D_L)^{-1} \left(y_p(k) - \begin{pmatrix} C_p & D_v C_L \end{pmatrix} \begin{pmatrix} \hat{x}_p(k) \\ \xi(k) \end{pmatrix} \right) \end{cases} \tag{5.9}$$

As discussed in [93], the closed-loop system by Eq. (5.9) is treated equivalent to the augmented system by Eq. (5.4). Thus we can get $B_d = B_v C_L$, $D_d = D_v C_L$ and $A_L = I$. The observer gain is also obtained

$$L = \begin{pmatrix} L_1 \\ L_2 \end{pmatrix} = \begin{pmatrix} B_v D_L (I + D_v D_L)^{-1} \\ B_L (I + D_v D_L)^{-1} \end{pmatrix} \tag{5.10}$$

Moreover according to the Theorem 1 in [93], the necessary condition of tracking performance with zero offset is that

$$A_L = I \tag{5.11}$$

5.3.3 Design procedure

Given the engine model of Eq. (5.5) with (A_p, C_p) is detectable, the main target is to design a disturbance model (B_d, D_d) and a state observer gain L so that the predicted output error $(y - \hat{y})$ based on Eq. (5.4) can converge to zero asymptotically for the random noise w.

The design of the dynamic observer of Eq. (5.7) by introducing ideas from linear H_∞ theory is firstly proposed in [93]. Consider the block diagram shown in Figure 5.1, and make

$$\tilde{x}(k) = x_p(k) - \hat{x}_p(k), s(k) = e(k) \tag{5.12}$$

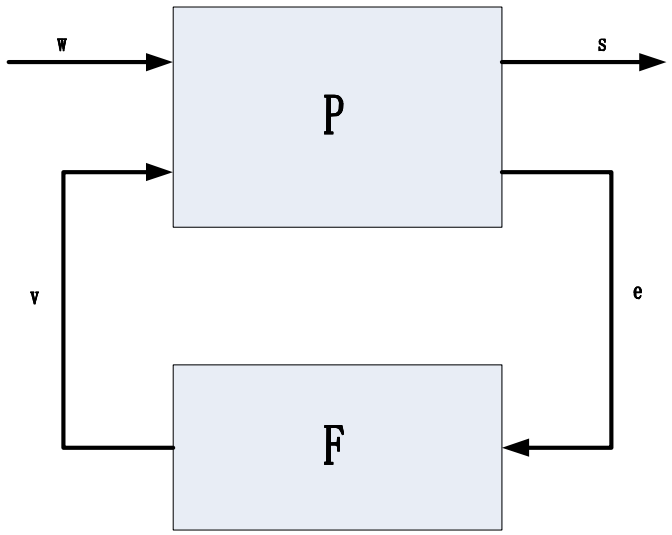

FIGURE 5.1: Closed-loop block diagram (traditional H_∞ theory)

From Eq. (5.5) and Eq. (5.7), we obtain

$$\begin{cases} \tilde{x}(k+1) = A_p\tilde{x}(k) + B_w w(k) - B_v v(k) \\ s(k) = C_p\tilde{x}(k) + D_w w(k) - D_v v(k) \\ e(k) = C_p\tilde{x}(k) + D_w w(k) - D_v v(k) \end{cases} \tag{5.13}$$

The system of block P in Figure 5.1 is described by Eq. (5.13). Equivalently, the system of block P could be presented in terms of discrete-time transfer matrices:

$$\begin{pmatrix} s \\ e \end{pmatrix} = P\begin{pmatrix} w \\ v \end{pmatrix} = \begin{pmatrix} P_{11} & P_{12} \\ P_{21} & P_{22} \end{pmatrix}\begin{pmatrix} w \\ v \end{pmatrix} \tag{5.14}$$

where

$$P(z) = \begin{pmatrix} D_w & -D_v \\ D_w & -D_v \end{pmatrix} + \begin{pmatrix} C_p \\ C_p \end{pmatrix}(zI - A_p)^{-1}\begin{pmatrix} B_w & -B_v \end{pmatrix} \tag{5.15}$$

The relationship between v and e is given:

$$v = Fe \tag{5.16}$$

where F is easily obtained form dynamic observer by Eq. (5.7)

$$F(z) = D_L + C_L(zI - A_L)^{-1}B_L \tag{5.17}$$

At the end, the closed-loop system from w to s expressed by the transfer matrix is shown as

$$G(P,F) = P_{11} + P_{12}F(I - P_{22}F)^{-1}P_{21} \tag{5.18}$$

We wish to design $F\ (A_L, B_L, C_L, D_L)$ in order to satisfy the following two requirement: the above closed-loop system of Eq. (reflooptransfer) is asymptotically stable. Besides this basic requirement, the influence from w to s should be minimized. Here we consider using the H infinity norm as

$$\| G(P,F) \|_\infty < \gamma \tag{5.19}$$

which means that the H_∞ norm of $G(P,F)$ (the maximum gain from w to s) is strictly less than γ. γ is the upper bound for the worst-case performance.

5.3.4 General solution for H_∞ problem

By this procedure, the dynamic observer by Eq. (5.7) is designed from solving the H_∞ problem defined in Eq. (5.19). This kind of problem could be solved efficiently by the method of LMI[94, 95]. A realization of the closed-loop transfer function from w to s is obtained on the assumption that $D_{22} = -D_v = 0$:

$$G(P,F) = D_{cl} + C_{cl}(zI - A_{cl})^{-1}B_{cl} \tag{5.20}$$

where

$$\begin{cases} A_{cl} = \begin{bmatrix} -B_v D_L C_p & -B_v C_L \\ B_L C_p & A_L \end{bmatrix} \\ B_{cl} = \begin{bmatrix} B_w - B_v D_L D_w \\ B_L D_w \end{bmatrix} \\ C_{cl} = \begin{bmatrix} C_p - D_v D_L C_p & -D_v C_L \end{bmatrix} \\ D_{cl} = D_w - D_v D_L D_w \end{cases} \tag{5.21}$$

In Lemma 5.1, if the linear matrix inequality (5.29) is satisfied, $F\ (A_L, B_L, C_L, D_L)$ can solve the H_∞ problem $\| G(P,F) \|_\infty < \gamma$.

However in this thesis, especially in the case of designing the dynamic observer, the parameter D_v is not equal to 0. Thus a linear change of variables is utilized. A fictitious variable is defined:

$$e_f(k) = C_p\tilde{x}(k) + D_w w(k) \tag{5.22}$$

In this condition $D_{22} = 0$, for the system

$$\begin{cases} \tilde{x}(k+1) = A_p\tilde{x}(k) + B_w w(k) - B_v v(k) \\ s(k) = C_p\tilde{x}(k) + D_w w(k) - D_v v(k) \\ e_f(k) = C_p\tilde{x}(k) + D_w w(k) \end{cases} \tag{5.23}$$

the dynamic observer assuming $e_f(k)$ is available for feedback is designed. Inside A_L, B_L, C_L, D_L could be easily obtained. The dynamic observer is given:

$$\begin{cases} \xi(k+1) = A_L\xi(k) + B_L e_f(k) \\ v(k) = C_L\xi(k) + D_L e_f(k) \end{cases} \tag{5.24}$$

Then $e_f(k)$ is replaced by $e(k) + D_v v(k)$. The general dynamic observer is obtained in the following form:

$$\begin{cases} \xi(k+1) = \tilde{A}_L\xi(k) + \tilde{B}_L e(k) \\ v(k) = \tilde{C}_L\xi(k) + \tilde{D}_L e(k) \end{cases} \tag{5.25}$$

where

$$\begin{cases} \tilde{A}_L = A_L - B_L(-D_v)(I + D_L(-D_v))^{-1}C_L \\ \tilde{B}_L = B_L - B_L(-D_v)(I + D_L(-D_v))^{-1}D_L \\ \tilde{C}_L = (I + D_L(-D_v))^{-1}C_L \\ \tilde{D}_L = (I + D_L(-D_v))^{-1}D_L \end{cases} \tag{5.26}$$

Existence of solution

Under the assumption that $D_{22} = -D_v = 0$, $F\ (A_L, B_L, C_L, D_L)$ can solve the H_∞ problem. If $D_v = 0$, the general solution in (5.26) is that $\tilde{A}_L = A_L, \tilde{B}_L = B_L, \tilde{C}_L = C_L, \tilde{D}_L = D_L$. If $D_v \neq 0$, the general solution $\tilde{A}_L, \tilde{B}_L, \tilde{C}_L, \tilde{D}_L$ exists under the assumption that $I + D_L(-D_v) \neq 0$. Thus the general solution in $F\ (\tilde{A}_L, \tilde{B}_L, \tilde{C}_L, \tilde{D}_L)$ is the extension of solution in $F\ (A_L, B_L, C_L, D_L)$.

Remark 5.1 *As discussed in this section, the dynamic observer is designed based on the idea of H_∞ theory which can be efficiently solved by the method of LMI. But with additional condition for tracking control without steady error by Eq. (5.11), $\tilde{A_L}$ should be identity matrix. With this nonlinear equality constraints, the LMI convex optimization problem becomes complicated and even unsolvable. Here we try to solve this problem in a simple but efficient way. The constraints are equivalent to the following two requirements:(1) $A_L = I$; (2) minimize $D_L(-D_v)$ under the minimization of B_L and C_L. The numerical details are discussed in section 5.6.*

Discussion

The necessary condition of offset-free tracking is that $\tilde{A}_L = I$. In order to make sure that $\tilde{A}_L = A_L - B_L(-D_v)(I + D_L(-D_v))^{-1}C_L = I$, here we try to solve this nonlinear equality by (1) $A_L = I$; (2) $B_L(-D_v)(I + D_L(-D_v))^{-1}C_L = 0$. Since the condition (2) is still nonlinear equality. So we try to solve this problem by minimizing $D_L(-D_v)$ under the minimization of B_L and C_L.

In section 5.3.2, we know the relation between the disturbance model and dynamic observer. we can get $B_d = B_v C_L$, $D_d = D_v C_L$ and $A_L = I$. The observer gain is also obtained

$$L = \begin{pmatrix} L_1 \\ L_2 \end{pmatrix} = \begin{pmatrix} B_v D_L (I + D_v D_L)^{-1} \\ B_L (I + D_v D_L)^{-1} \end{pmatrix}$$

So B_L, C_L and D_L should not be equal to 0. In order to make $B_L(-D_v)(I+D_L(-D_v))^{-1}C_L \approx 0$, we just minimize $D_L(-D_v)$ under the minimization of B_L and C_L. Based on Eq. (5.25) and Eq. (5.26), the following system is considered

$$\begin{cases} \xi(k+1) = \xi(k) + \tilde{B}_L e(k) \\ \quad v(k) = \tilde{C}_L \xi(k) + \tilde{D}_L e(k) \end{cases}$$

The system is very special since $\tilde{A}_L = I$. B_L, C_L and D_L are in really small values. As a result, $\tilde{B}_L, \tilde{C}_L, \tilde{D}_L$ are in really small values, but not equal to zero matrices.

From the above discussion we can see the solution proposed here is one kind of compromise. The best solution is A_L, B_L, C_L, D_L that directly make $\tilde{A}_L = I$. In the future, it will be a hot topic to solve this nonlinear equality.

5.4 Reduced-order design

A sufficient condition for reference tracking without offset is given in section 5.2.2 that the number of the integrating variables of the augmented system should be equal to the number of the measured outputs, just as, $dim(d) = dim(y_p)$. As for the system by Eq. (5.2) and the equivalent system by Eq. (5.9), we find that the order of the dynamic observer should be equal to the number of integrating disturbances, $dim(A_L) = dim(d)$. In order to achieve the reference tracking without offset, the order of the dynamic observer must be designed equal to the number of the measured outputs, which might be less than the order of the system by Eq. (5.13). Thus when we solve the H_∞ control problem of the system by Eq. (5.13), reduced-order design is really needed.

The design of solving reduced-order problems has received great attention in recent years. And the reduced-order design is a very challenging issue in the robust control theory, since it has been proved to be a non-convex problem. Many different strategies have been applied to solve it. [94, 96–100]. In this chapter, the two-step algorithm initiated with HIFFO is presented for solving the non-convex reduced-order problem [101, 102]. HIFFO is a toolbox of Matlab for fix-order H_∞ controller design. A structure for introducing the slack matrix variable is used for relaxing the LMI. Then an iterative procedure for updating the slack matrix variables from the initial solution of reduced-order problem is conducted to decrease the upper bound of the H_∞ norm.

Lemma 5.1 *From the bounded real lemma [94, 95], internal stability and the H_∞ norm constraint by Eq. (5.19) are equivalent to the existence of $X_{cl} = X_{cl}^T > 0$ such that*

$$\begin{pmatrix} -X_{cl}^{-1} & A_{cl} & B_{cl} & 0 \\ A_{cl}^T & -X_{cl} & 0 & C_{cl}^T \\ B_{cl}^T & 0 & -\gamma I & D_{cl}^T \\ 0 & C_{cl} & D_{cl} & -\gamma I \end{pmatrix} < 0 \tag{5.27}$$

Then the above inequality is pre-multiplied and post-multiplied in both sides by

$$\begin{pmatrix} I & 0 & 0 & 0 \\ 0 & X_{cl}^{-1} & 0 & 0 \\ 0 & 0 & I & 0 \\ 0 & 0 & 0 & I \end{pmatrix} \tag{5.28}$$

Letting $M = X_{cl}^{-1} = M^T$, the following matrix inequality is obtained,

$$\begin{pmatrix} -M & A_{cl}M & B_{cl} & 0 \\ MA_{cl}^T & -M & 0 & MC_{cl}^T \\ B_{cl}^T & 0 & -\gamma I & D_{cl}^T \\ 0 & C_{cl}M & D_{cl} & -\gamma I \end{pmatrix} < 0 \tag{5.29}$$

The main method in this section is to transfer matrix variables M with slack variable α inside. This is done to solve the non-convex problems by LMI relaxing. Now, M is designed in the following structure,

$$M = \begin{pmatrix} \alpha I_n & 0 \\ 0 & \alpha I_p \end{pmatrix} M_0 \tag{5.30}$$

where scalar α is the decision variable.

Suppose that there exists an initial solution of order $dim(A_L)$ with the H_∞ norm requirement $\| G(P,F) \|_\infty < \gamma$ I condition in Eq. (5.29) is satisfied when γ is equal to γ_0. Note that if we assign that $\alpha = 1$, we can get that the matrix M is equal to M_0. Based on Eq.(5.21) and Eq.(5.34), we define

$$\begin{cases} \overline{A}_{cl} = \begin{pmatrix} \alpha A_p - B_v \overline{D}_L C_p & -B_v \overline{C}_L \\ \overline{B}_L C_p & \overline{A}_L \end{pmatrix} \\ \overline{B}_{cl} = \begin{pmatrix} \alpha B_w - B_v \overline{D}_L D_w \\ \overline{B}_L D_w \end{pmatrix} \\ \overline{C}_{cl} = \begin{pmatrix} \alpha C_p - D_v \overline{D}_L C_p & -D_v \overline{C}_L \end{pmatrix} \\ \overline{D}_{cl} = \alpha D_w - D_v D_L D_w \end{cases} \tag{5.31}$$

where

$$\overline{A}_L = \alpha A_L, \overline{B}_L = \alpha B_L, \overline{C}_L = \alpha C_L, \overline{D}_L = \alpha D_L \tag{5.32}$$

Then based on the above definition the following theorem for the reduced-order controller design could be obtained.

Theorem 5.1 *Suppose that matrices M_0 is given. Then the inequality $\| G(P,F) \|_\infty < \gamma$ holds if there exist scalar α such that*

$$\begin{pmatrix} -M & \overline{A}_{cl}M_0 & \overline{B}_{cl} & 0 \\ M_0\overline{A}_{cl}^T & -M & 0 & M_0\overline{C}_{cl}^T \\ \overline{B}_{cl}^T & 0 & -\alpha^2\gamma I & \overline{D}_{cl}^T \\ 0 & \overline{C}_{cl}M_0 & \overline{D}_{cl} & -\gamma I \end{pmatrix} < 0 \tag{5.33}$$

is feasible. where

$$M = \begin{pmatrix} \alpha I_n & 0 \\ 0 & \alpha I_p \end{pmatrix} M_0 \tag{5.34}$$

Proof. Since the calculation procedure is obvious by the assumption of the parameter matrix, the proof is omitted here. □

It can be seen that there exists a term α^2 in Eq. (5.33). It will make the inequality unsolvable. Thus it is necessary to make a line search for finding the upper bound γ of the H_∞ norm. It is obvious to see that if $\alpha = 1$, the inequality in Theorem by Eq. (5.33) is equivalent to the LMI of Lemma by Eq. (5.29). This fact implies that the initial solution will always satisfy the inequality in the Theorem. As a consequence, the calculated upper-bound γ in Eq. (5.33) should be equal or less than γ_0 from the initial solution. The decreasing of the upper bound γ of the H_∞ norm can be guaranteed by solving the LMI problem Eq. (5.33) when $\alpha = 1$. Then the line search of α is finally released.

The reduced-order design is conducted as the following procedure:

Step 1: The initial reduced-order controller is given by discrete time HIFFO [103].

Step 2: For an initial given controller, M_0 is calculated according to the LMI by Eq. (5.33), when α is assumed to be 1.

Step 3: The first-step for decreasing of the upper bound on the H_∞ performance is designed by Theorem 5.3 in consideration of $\alpha = 1$. The value of γ is updated in each iteration.

Step 4: The second-step is that the line search over α is performed under the Theorem by Eq. (5.33) after the suitable γ is obtained in step 3.

Remark 5.2 *The reduced-order procedure in this paper is designed from Step 1 to Step 4. The reduced-order controller is initially given by discrete time HIFFO in Step 1. It is worth mentioning that the two step algorithm from Step 2 to Step 4 is not capable of reduce the order of the solution. However this two-step algorithm started by discrete time HIFFO is really suitable for the satisfaction of Eq. (5.11) and the additional condition in the section 5.3.4.*

5.5 Controller design

The model predictive control algorithm for general used in this thesis is described in details.

5.5.1 MPC algorithm

The discrete-time MPC problem in general case can be formulated as:

$$\min_{U} \sum_{k=0}^{N-1} (x(k)^T Q x(k) + u(k)^T R u(k)) + x(N)^T Q_N x(N) + \sum_{k=1}^{N-1} \Delta u(k)^T P \Delta u(k) \tag{5.35}$$

where:

$$U = (u(0), u(1), \cdots, u(N-1))^T \tag{5.36}$$

s.t.

$$x(k+1) = Ax(k) + Bu(k) \tag{5.37}$$

$$\Delta \underline{u} \leq \Delta u(k) \leq \Delta \overline{u} \tag{5.38}$$

$$\underline{u} \leq u(k) \leq \overline{u} \tag{5.39}$$

$$\Delta u(k) = 0, k > n_c \tag{5.40}$$

Eq. (5.37) is used to describe the general model for controller design. x and u are the states and manipulated variables for the general model. A and B are the parameter matrices with appropriate dimensions.Q, Q_N and P are positive semidefinite matrices and R is a positive definite matrix. Q and Q_N are the weight matrices for the states and R is the weight matrix for inputs. Q and R here are different from the ones defined in Chapter 4. P is the weight matrix for inputs rates. N is the prediction horizon. n_c is the control horizon.

5.5.2 Solving quadratic programming problem

The MPC problem from Eq. (5.35) to Eq. (5.40) needs to be solved at each sampling time. In this paper, an open source software named as *qpOASES* [104] is used to solve the quadratic programming (QP) problem in the following form:

$$\begin{aligned} \min_{x} \quad & \frac{1}{2}x^T Hx + x^T g(\omega_0) \\ s.t. \quad & lbA(\omega_0) \leq Ax \leq ubA(\omega_0) \\ & lb(\omega_0) \leq x \leq ub(\omega_0) \end{aligned} \tag{5.41}$$

where the Hessian matrix H is symmetric and positive (semi-)definite. The gradient vector g and the constraint vectors lb, ub is affinely related to the parameter ω_0. The main idea of *qpOASES* is inspired to deal with the problem of quadratic programming. The condition of applying this method which is called online strategy is that there is not too much change for the active set of QP between each sampling time. It will be really fast and efficient when *qpOASES* is applied to solve the problem of quadratic programming for model predictive control.

The problem arises on how to transfer this MPC problem by Eq. (5.35) to the QP form by Eq. (5.41).

Remark 5.3 *The variable x in Eq. (5.41) is just the optimization target of QP problem that is different from the state variable in Eq. (5.37). For the MPC design in this paper, the optimization target is the calculation of the manipulated variables u.*

Based on the current state $x(0)$ and the model by Eq. (5.37), we can predict the future state:

$$\begin{cases} x(0) = x(0) \\ x(1) = Ax(0) + Bu(0) \\ x(2) = A^2x(0) + ABu(0) + Bu(1) \\ \vdots \\ x(N) = A^Nx(0) + A^{N-1}Bu(0) + A^{N-2}Bu(1) + \cdots + Bu(N-1) \end{cases} \tag{5.42}$$

Then we can easily write this to matrix form:

$$\begin{pmatrix} x(0) \\ x(1) \\ x(2) \\ \vdots \\ x(N) \end{pmatrix} = \begin{pmatrix} I \\ A \\ A^2 \\ \vdots \\ A^N \end{pmatrix} x(0) + \begin{pmatrix} 0 & & & & \\ B & 0 & & & \\ AB & B & 0 & & \\ \vdots & & & \ddots & \\ A^{N-1}B & A^{N-2}B & A^{N-3}B & \cdots & B \end{pmatrix} \begin{pmatrix} u(0) \\ u(1) \\ u(2) \\ \vdots \\ u(N-1) \end{pmatrix} \tag{5.43}$$

then Eq. (5.43) could be transferred to:

$$\overline{X} = \overline{A}x(0) + \overline{B}U \tag{5.44}$$

where:

$$\overline{X} = \begin{pmatrix} x_0 \\ x_1 \\ x_2 \\ \vdots \\ x_N \end{pmatrix} \quad \overline{A} = \begin{pmatrix} I \\ A \\ A^2 \\ \vdots \\ A^N \end{pmatrix} \quad \overline{B} = \begin{pmatrix} 0 & & & & \\ B & 0 & & & \\ AB & B & 0 & & \\ \vdots & & & \ddots & \\ A^{N-1}B & A^{N-2}B & A^{N-3}B & \cdots & B \end{pmatrix} \tag{5.45}$$

The cost function in MPC is:

$$J = \sum_{k=0}^{N-1} (x(k)^T Qx(k) + u(k)^T Ru(k)) + x(N)^T Q_N x(N) + \sum_{k=1}^{N} \Delta u(k)^T P \Delta u(k) \tag{5.46}$$

Writing Eq. (5.46) to the vector form:

$$J = \frac{1}{2}\overline{X}^T \overline{QX} + \frac{1}{2}U^T \overline{R}U \tag{5.47}$$

where:

$$\overline{Q} = \begin{pmatrix} Q & & & & \\ & Q & & & \\ & & \ddots & & \\ & & & Q & \\ & & & & Q_N \end{pmatrix} \tag{5.48}$$

$$\overline{R} = \begin{pmatrix} R+P & -P & & & \\ -P & R+2P & -P & & \\ & -P & \ddots & -P & \\ & & -P & R+2P & -P \\ & & & -P & R+P \end{pmatrix} \tag{5.49}$$

Then the MPC problem by Eq. (5.35) is obtained as:

$$\begin{aligned} \min_U J &= \min_U \frac{1}{2}\overline{X}^T\overline{QX} + \frac{1}{2}U^T\overline{R}U \\ &= \min_U \frac{1}{2}U^T\left(\overline{B}^T\overline{QB} + \overline{R}\right)U + U^T\overline{B}^T\overline{QA}x(0) \end{aligned} \tag{5.50}$$

Eq. (5.50) is the form of Eq. (5.41), where:

$$\begin{aligned} H &= \overline{B}^T\overline{QB} + \overline{R} \\ g(\omega_0) &= \overline{B}^T\overline{QA}x(0) \end{aligned} \tag{5.51}$$

By introducing the constraints of input rate, the transform procedure becomes more complicated especially the definition of $\overline{R}$. With input rate constraints, the input constraints by Eq. (5.41) need to be updated every sampling time to take the input rate limitations into consideration.

5.5.3 Tracking control

To achieve the tracking control of diesel engine in this chapter, the disturbance model by Eq. 5.2 is augmented with a new state $x_e(k) = y_p(k) - y_{ref}(k)$, where $y_{ref}(k)$ is the reference for tracking. This state represents the error between real measured output and

setpoint.

$$\begin{pmatrix} x_p(k+1) \\ d(k+1) \\ x_e(k+1) \end{pmatrix} = \begin{pmatrix} A_p & B_d & 0 \\ 0 & I & 0 \\ C_pA_p - C_p & C_pB_d & I \end{pmatrix} \begin{pmatrix} x_p(k) \\ d(k) \\ x_e(k) \end{pmatrix} + \begin{pmatrix} B_p \\ 0 \\ C_pB_p \end{pmatrix} u(k) \tag{5.52}$$

The tracking control is achieved by applying this augmented form into the MPC design of Eq. (5.37):

$$x(k) = \begin{pmatrix} x_p(k) \\ d(k) \\ x_e(k) \end{pmatrix} \qquad B = \begin{pmatrix} B_p \\ 0 \\ C_pB_p \end{pmatrix} \qquad A = \begin{pmatrix} A_p & B_d & 0 \\ 0 & I & 0 \\ C_pA_p - C & & I \end{pmatrix} \tag{5.53}$$

At each sampling time, the state x_p and d are estimated by the Luenberger observer by Eq. 5.9. And the output y_p can be measured.

We can clearly see that the augmented disturbance d is not affected by the manipulated variables u. But because the disturbances are observable, the bad influence can be removed from the control performance based on the estimates.

5.6 Experimental results

The parameters of the MPC are designed as Table 5.1 shows.

TABLE 5.1: Parameters of MPC with second-order model

Q	diag{0,0,0,0,0,0,1,0.01}
R	diag{10,1,1,1}
P	P={10,10,10,10}
Control horizon	3
Prediction horizon	5
Injection quantity	$680 \leq u_1 \leq 700$
Injection timing	$708 \leq u_2 \leq 714$
Injection pressure	$100 \leq u_3 \leq 110$
EGR valve	$9 \leq u_4 \leq 17$

The control objective in this thesis is to operate the engine to meet drivers speed demand and reduce NOx emission. Thus the accurate tracking control for engine speed with no offset is needed. Since the NOx emission is inevitable in the cycle of diesel engine working, we try to reduce the NOx emission instead of offset-free tracking of reference

zero. So the reference of NOx emission is set as 50 ppm and the weight on the output of NOx emission is chosen as 0.01. As Table 5.1 shows, since the prior control target is the engine speed tracking, the weight on engine speed tracking is chosen as 1 and NOx emission 0.01. The weights on the other states are set to zeros. In consideration of fuel consumption, the weight on injection quantity is chosen as 10 which is bigger than other manipulated variables. The constraints of u_2 and u_4 are expanded from the original ones applied for linear system identification. Thus the tested diesel engine can be working in a wider nonlinear operation region.

The three control systems is different in the chosen disturbance model and related state observer. The details are shown as follows, .

MPC 1: the second order model is identified in Chapter 3, and state estimate by Kalman filter is applied in MPC design.

MPC 2: the disturbance model by Eq. (5.2) is chosen as $B_d = 0$ and $D_d = I$ in general case, with state estimate by steady-state Kalman filter.

MPC 3: the disturbance model and state observer are given by the proposed method. Using the method in Remark 1, the following parameter can be obtained

$$\begin{aligned} A_L = I, \tilde{A}_L &= \begin{pmatrix} 0.9992 & 0.0010 \\ -2.9131 * 10^{-4} & 1.0000 \end{pmatrix} \approx I \\ B_d &= \begin{pmatrix} 0.0035 & -1.6024 * 10^{-4} \\ 0.0044 & 0.0012 \end{pmatrix} \\ D_d &= \begin{pmatrix} -4.4463 & 9.1777 \\ -23.5656 & -8.2174 \end{pmatrix} \end{aligned} \tag{5.54}$$

5.6.1 Simulation results

The simulation results are demonstrated in this section. The control system of MPC1, MPC2 and proposed MPC3 are built in the simulink. The reference of engine speed make a step from 2300 rpm to 2400 rpm. The reference of NOx stays at 50 ppm.

MPC with second-order model

The model mismatch between the model used for controller and target model is set in Figure 5.2. The steady disturbance is added into the system as Figure 5.3. The simulation results of control variables and manipulated variables are shown in Figure 5.5. From the results, we can see that under the influence of model mismatch and

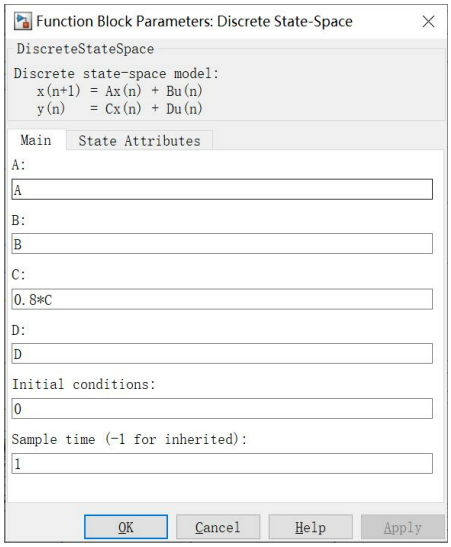

FIGURE 5.2: Condition of model mismatch

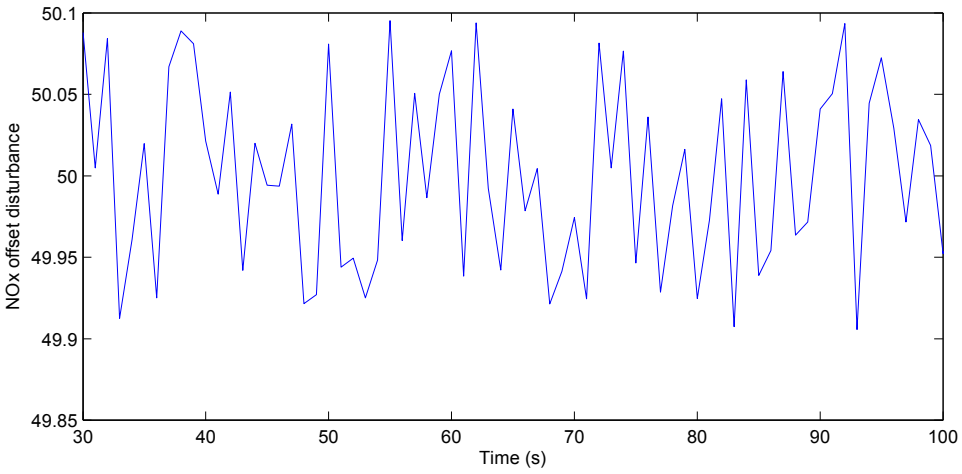

FIGURE 5.3: Unmeasured steady disturbance

steady disturbance, the response time is similar by three methods. Comparing with the MPC2 with normal disturbance model, MPC3 by the proposed method shows smaller overshoot and settling time. There is steady offset in the tracking results by MPC1. With the better transient performance, the NOx value is lower by the proposed method.

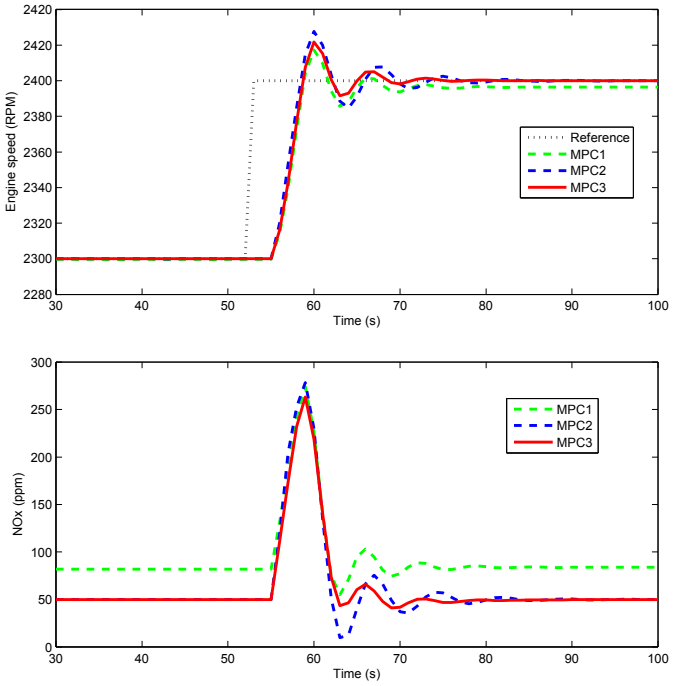

FIGURE 5.4: Simulation results of control variables with second-order model

MPC with fourth-order model

The model used in this case is fourth-order identified in Chapter 3. By the reduced-order design method proposed in this chapter, the simulation results are similar to the ones with second-order model. It is proved that the proposed condition for general case and reduced-order design are effective. The comparison is shown is Table 5.3.

TABLE 5.2: Comparison of simulation results

	MPC 1	MPC 2	MPC 3
Settling time(s)	19	30	19
Overshoot(rpm)	5	21	12
Steady tracking error (MSE from 25s to 50s)	33.36	0.0683	0.0163
NOx value (ppm/point)	89.6124	62.8376	62.7812

5.6.2 Real-time test results

The real-time test results are demonstrated in this section.

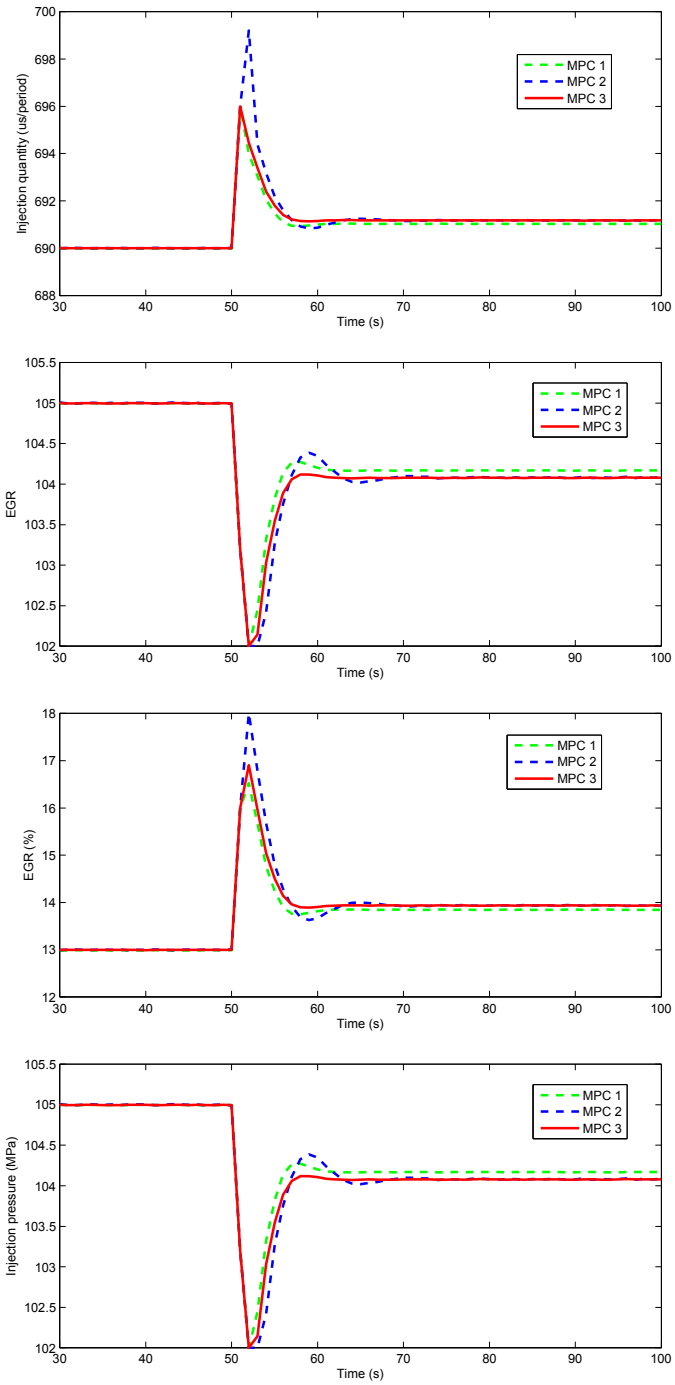

FIGURE 5.5: Simulation results of manipulated variables with second-order model

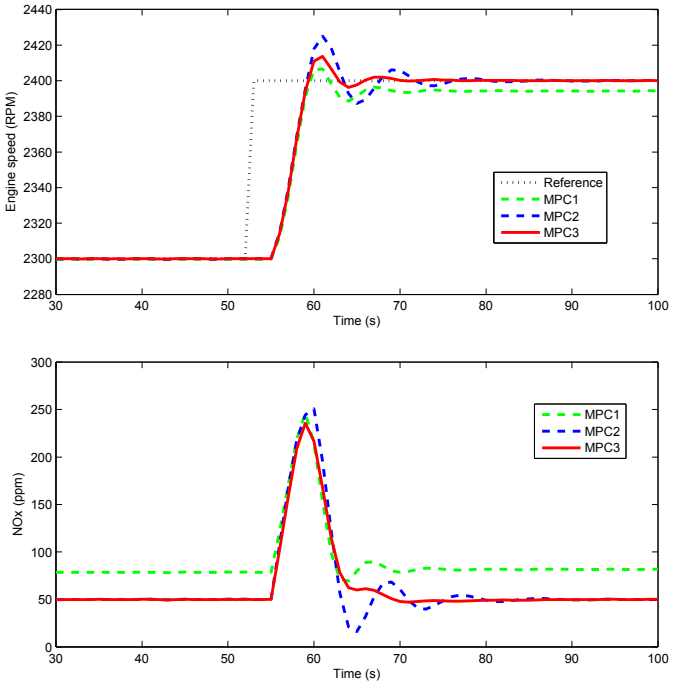

FIGURE 5.6: Simulation results of control variables with fourth-order model

MPC with second-order model

The proposed control system is also implemented in the dSPACE system. The control performance is evaluated in the real-time application. All the experiments are done in the test bench described in Chapter 3 which is fully warmed.

In this section we consider two case. In the first case, the engine speed reference changes in the working range where the system identification is done in Chapter 3. In Case 2, the engine speed range is almost the entire normal operation range of the tested diesel engine. The second case analyzes how efficient the proposed control system can be applied during the working range of diesel engine expands. The NOx reference remains at 50 for each case. This is done to ensure the exhaust emission is as low as possible when the engine speed is changing.

$$Case1:$$

$$\begin{cases} y_1^{ref} = 2300, y_2^{ref} = 50, 0 \le t \le 20 \\ y_1^{ref} = 2500, y_2^{ref} = 50, 20 \le t \le 70 \\ y_1^{ref} = 2300, y_2^{ref} = 50, 70 \le t \le 110 \end{cases}$$

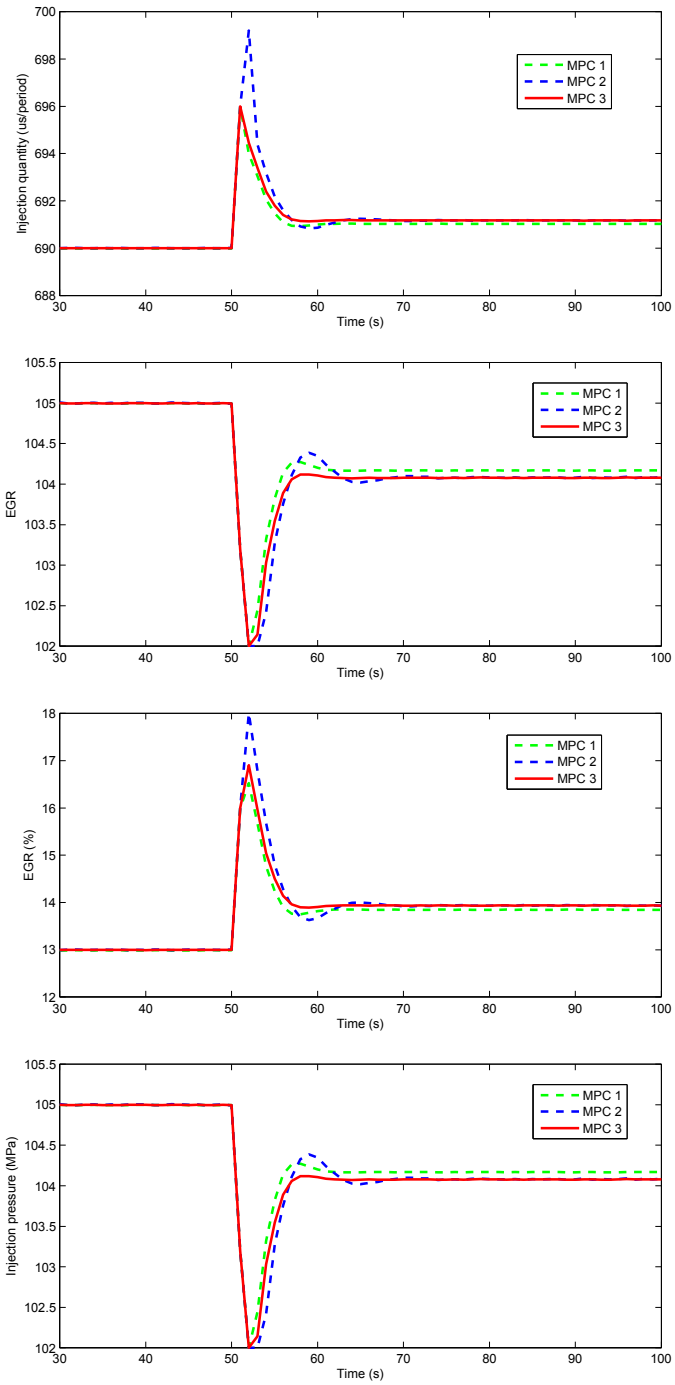

FIGURE 5.7: Simulation results of manipulated variables with fourth-order model

$$Case2:$$
$$\begin{cases} y_1^{ref} = 2150, y_2^{ref} = 50, 0 \le t \le 20 \\ y_1^{ref} = 2650, y_2^{ref} = 50, 20 \le t \le 70 \\ y_1^{ref} = 2150, y_2^{ref} = 50, 70 \le t \le 120 \end{cases}$$

The experimental results of all the cases are summarized in Figure 5.8 and Figure 5.9. In these figures, (a) show the control variables and (b) depict the manipulated variables. The red solid lines show the results of the proposed method, the blue dashed lines show the results of MPC 2, and the green dotted lines show the results of MPC 1.

The results shown here clearly indicate that the closed-loop control performance is significantly influenced by the disturbance model and the related state observer together especially if there is model mismatch and nonlinearity in the system.

In Figure 5.8 we can see that the tracking performance of engine speed by MPC 1, MPC 2 and MPC 3 is similar for case 1. But for MPC 3, designed with the proposed method, the offset of tracking is least. Also, the exhaust emission of NOx is lower than the other methods. Due to the fixed-structure of the observer (steady-state Kalman filter), it seems like that MPC 2 has a worse performance. While the combine design of MPC 3 can realize its priority to choose the observer gain.

For case 2, the working range expands as the nonlinearities and model mismatch increase. It can be obviously seen that the tracking performance of MPC 3 is much better than the other two methods. It seems like that the offset-free tracking is achieved quickly for the proposed method. In another word, the estimate error of the outputs can go to zero more quickly by the proposed method. As a results, the manipulated variables can be used more quickly and efficiently. Since the proposed method can deal with wider working range, it is less time-consuming when the MPC in the sub-zone is extended to the entire working range by gain schedule technique.

MPC with fourth-order model

The parameters of MPC regulators are the same except for

$$Q = diag\{0,0,0,0,0,0,1,0.01\} \tag{5.55}$$

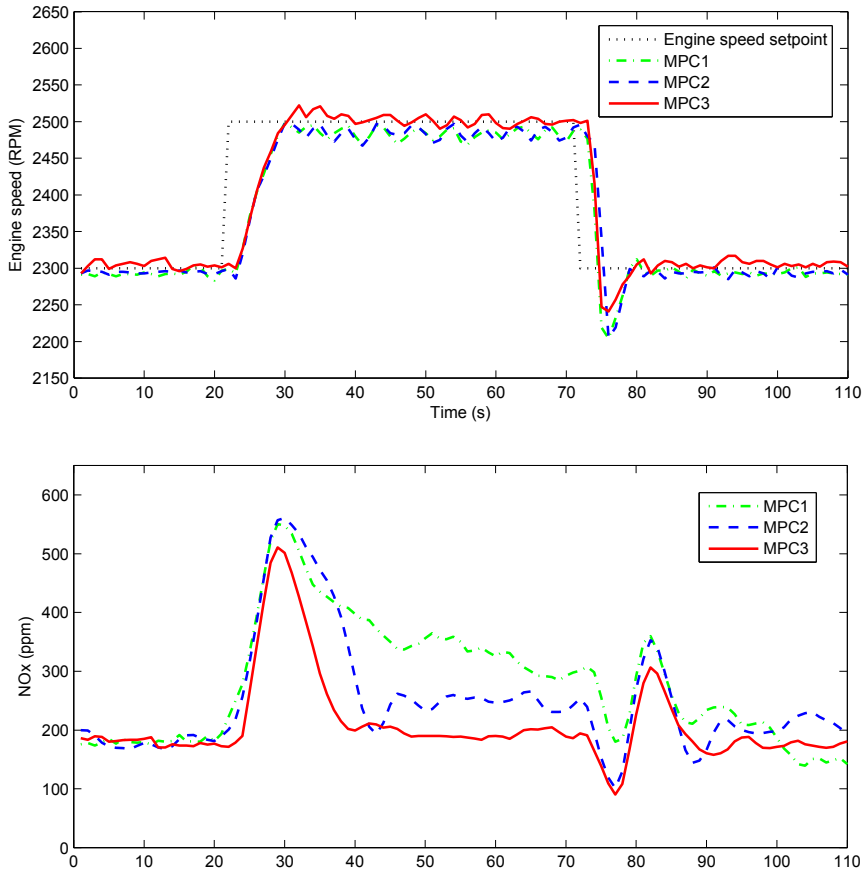

(a) Control variables

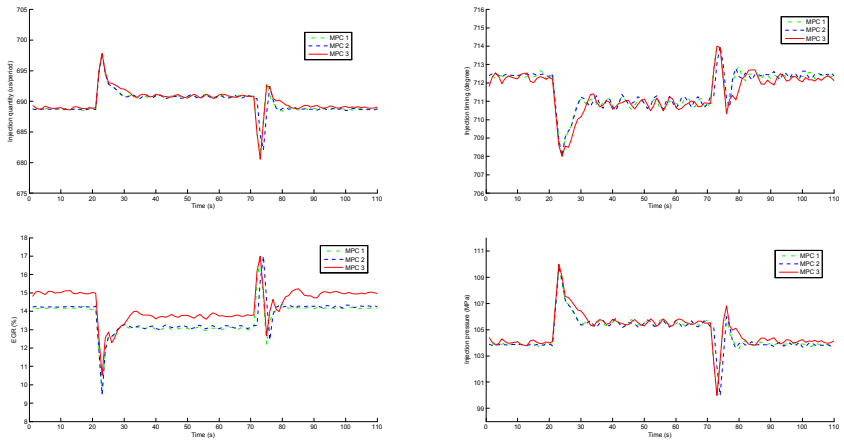

(b) Manipulated variables

FIGURE 5.8: Step response test by second-order model for case 1

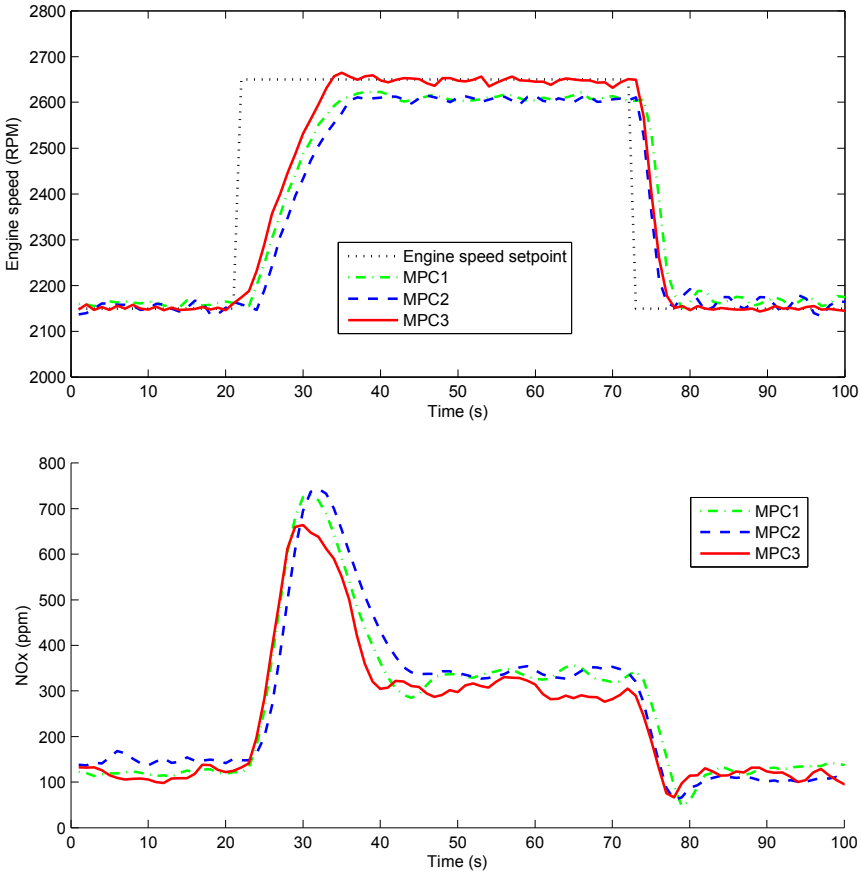

(a) Control variables

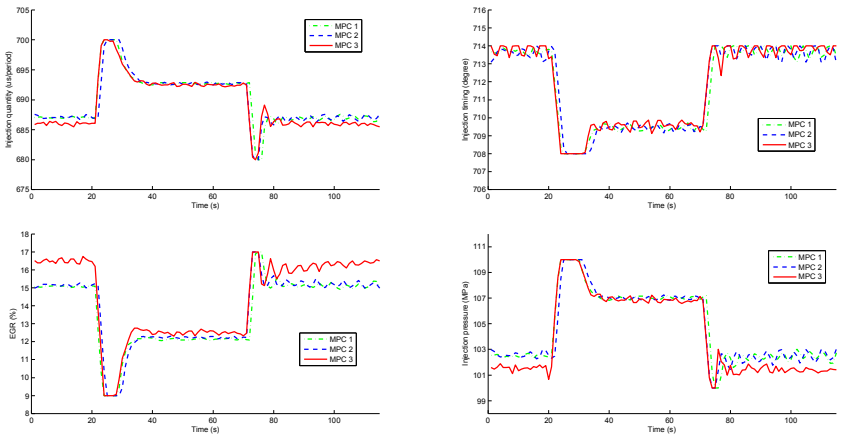

(b) Manipulated variables

FIGURE 5.9: Step response test by second-order model for case 2

With the fourth order model, the dimension of the states increases. The disturbance model and state observer used in MPC 3 is designed by the proposed reduced-order method. By the method in Remark 5.1 and 5.2, the following parameter can be obtained

$$
\begin{aligned}
A_L = I, \tilde{A}_L &= \begin{pmatrix} 0.9987 & -9.1583 * 10^{-5} \\ -0.0159 & 1.0011 \end{pmatrix} \approx I \\
B_d &= \begin{pmatrix} 0.0012 & -1.1909 * 10^{-4} \\ -0.0083 & 3.1866 * 10^{-4} \\ 0.0149 & -0.0021 \\ -0.0112 & 0.0017 \end{pmatrix} \\
D_d &= \begin{pmatrix} 14.0414 & -1.0719 \\ -9.9634 & 0.7216 \end{pmatrix}
\end{aligned}
\tag{5.56}
$$

The solution could be obtained after 5 times in which the total iteration is 100. The initial bound on the H_∞ performance is $\gamma_0 = 1.5762 * 10^8$. By the search procedure proposed, $\alpha = \beta = 100$, we get the updated H_∞ performance $\gamma = 1.3110 * 10^6$. The lower bound is obtained. More optimized solution to the reduced-order problem is obtained to ensure a better dynamic performance for the controller.

In this section the same two cases of experiment are considered. The experimental results are summerized in Figure 5.10 for the first case and in Figure 5.11 for the second case.

The realtime test results obviously prove that the design of the control system by the reduced-order method are also efficient. In Figure 5.10 and 5.11, the tracking performance of MPC 3 designed by the proposed reduced-order method is better than MPC 1 and MPC 2. The tracking error is obviously less than the other two methods. Also the NOx value is maintained in a lower level by the method designed in this paper. The comparison of experiments results for each case is shown in Table 5.3. *

5.6.3 More real-time results

The above real-time experiments were done on 20th and 22th November 2017. As a matter of fact, many real-time tests were done before. The real-time tests on 18th and 19th are shown in Figure 5.12 and 5.13. The comparison between three methods from different days is shown in Table 5.4. As for MPC 2 which is the normal offset-free

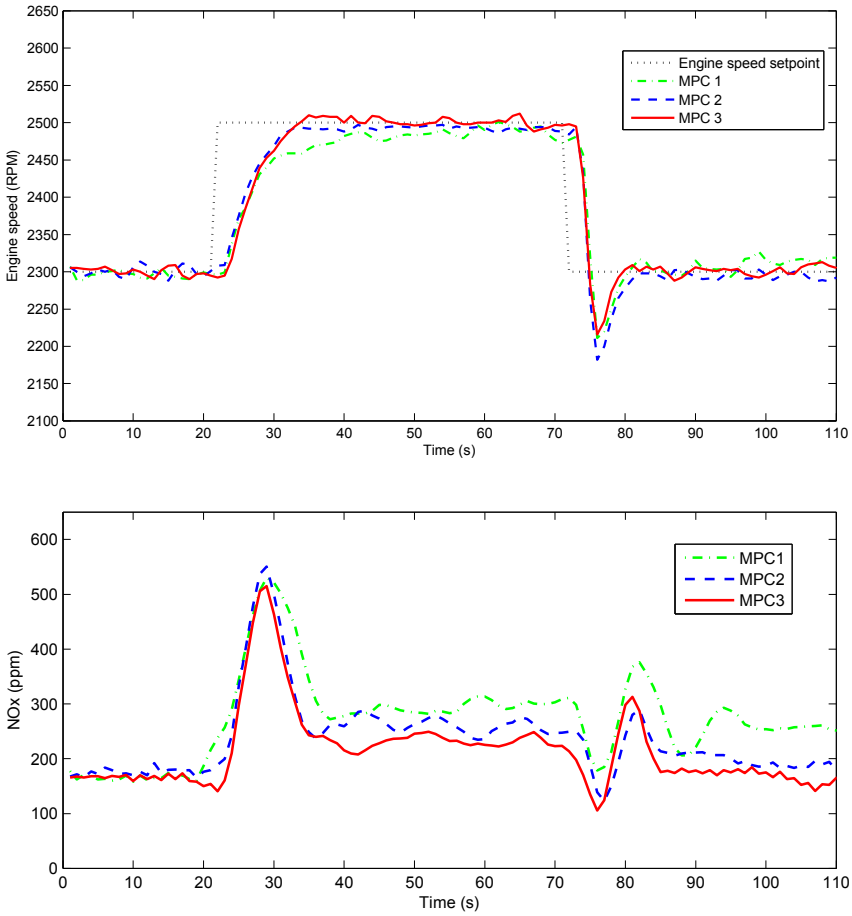

(a) Control variables

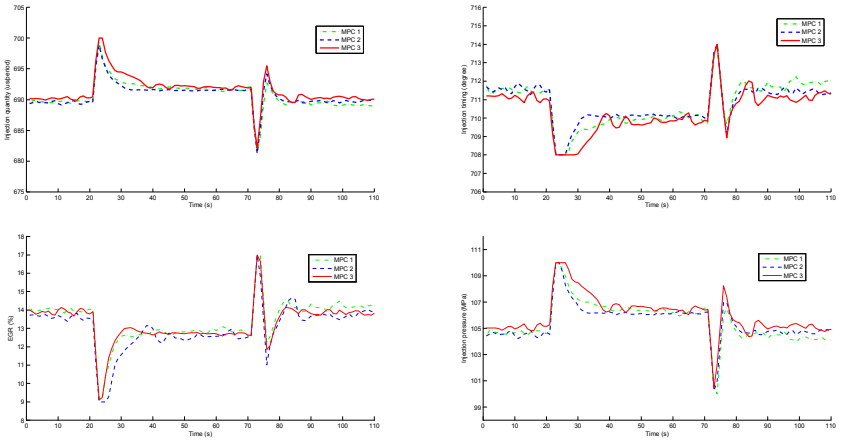

(b) Manipulated variables

FIGURE 5.10: Step response test by fourth-order model for case 1

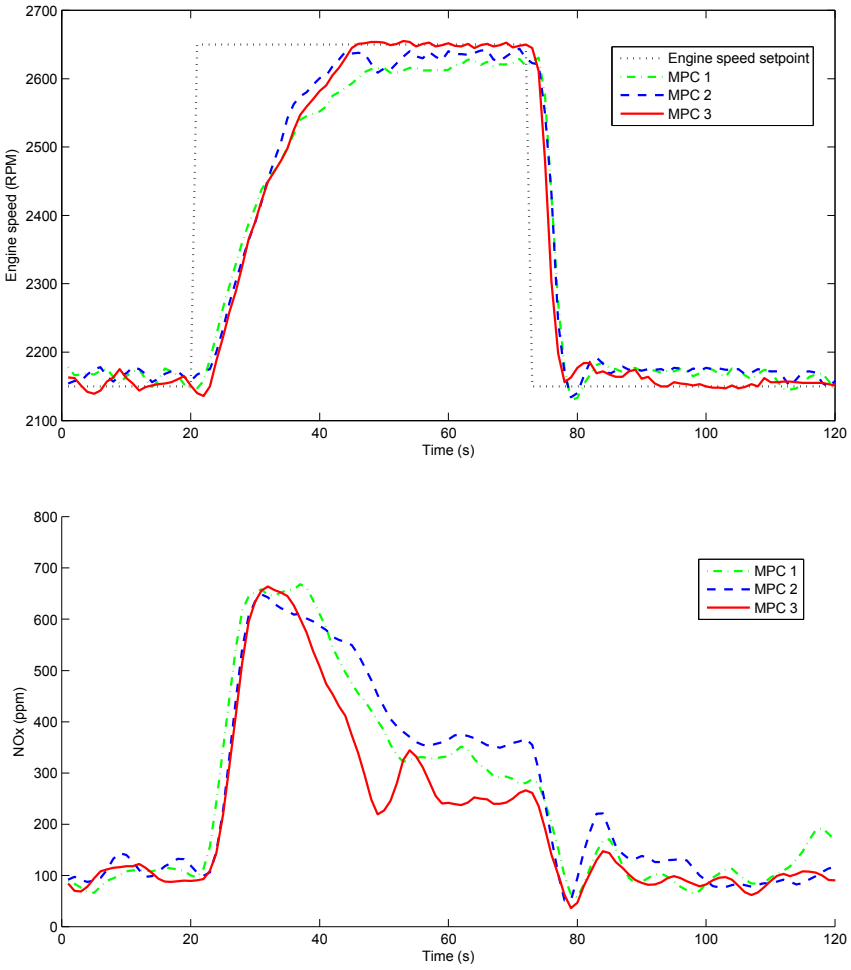

(a) Control variables

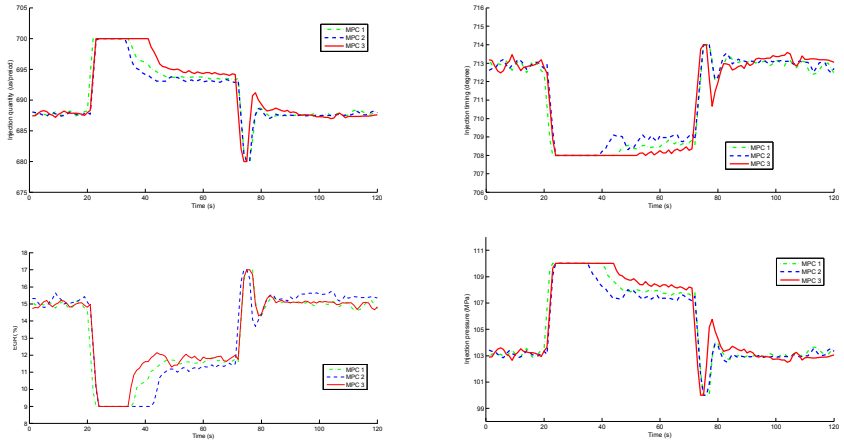

(b) Manipulated variables

FIGURE 5.11: Step response test by fourth-order model for case 2

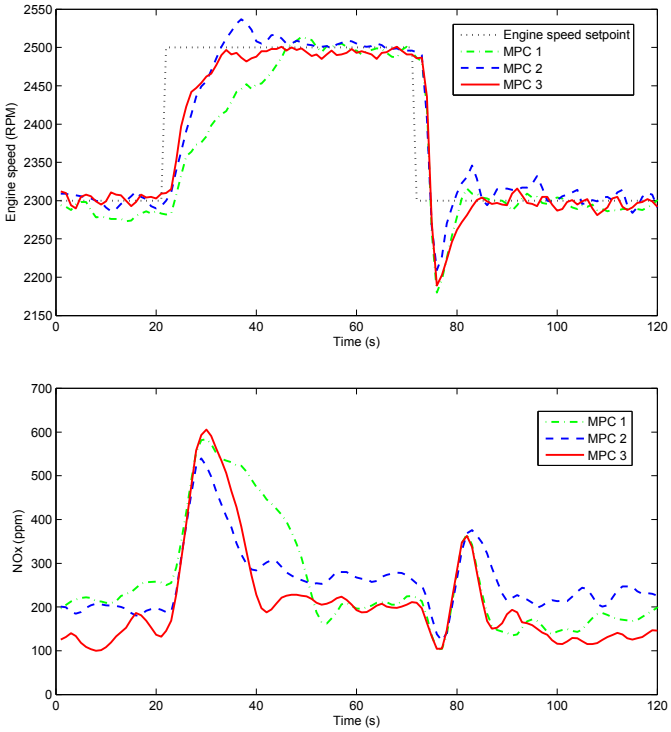

FIGURE 5.12: Control variables of case 1 on 11.18.2017

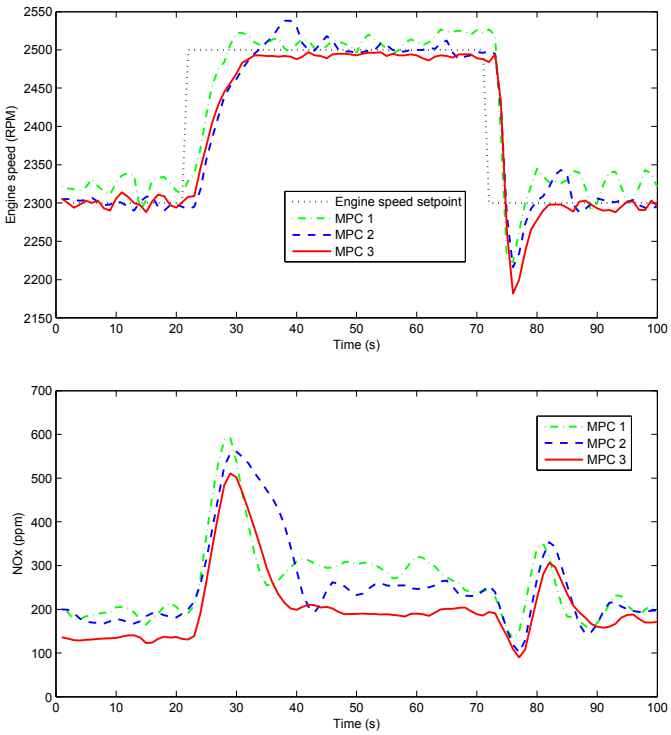

FIGURE 5.13: Control variables of case 1 on 11.19.2017

T -time results for 2 cases

Case 1	MPC 1	MPC 2	MPC 3
Settling time(s)	25	24	19
Overshoot(rpm)	0	0	0
Steady tracking error (MSE from 25s to 50s)	214.8462	56.5385	44.0000
NOx value (ppm/point)	283.0822	233.5020	197.0302
Case 2			
Settling time(s)	40	32	26
Overshoot(rpm)	0	0	0
Steady tracking error (MSE from 25s to 50s)	999.1875	158.6875	46.8125
NOx value (ppm/point)	255.5243	248.0755	225.3903

MPC, we can see that the average value of settling time and overshoot are bigger than MPC 1 which is the normal MPC. But with the offset-free design, the steady tracking error of MPC 2 is smaller than MPC 1. The proposed method MPC 3 has the best performance including the engine speed tracking and NOx value. The dynamic and static performance are both satisfied. In details of Table 5.4, for case 1 by fourth-order model

TABLE 5.4: Comparison of real-time results for different days

Case 1	MPC 1 (11.18)	MPC 1 (11.19)	MPC 1 (11.20)	average value
Settling time(s)	30	19	25	24.67
Overshoot(rpm)	0	25	0	8.33
Steady tracking error (MSE in the middle 25s)	354.3591	501.4739	214.8462	356.8931
NOx value (ppm/point)	325.7407	306.8257	283.0822	305.2162
Case 1	MPC 2 (11.18)	MPC 2 (11.19)	MPC 2 (11.20)	average value
Settling time(s)	30	28	24	27.33
Overshoot(rpm)	47	48	0	31.67
Steady tracking error (MSE in the middle 25s)	184.5092	174.9709	56.5385	138.6729
NOx value (ppm/point)	302.8231	288.3870	233.5020	274.9040
Case 1	MPC 3 (11.18)	MPC 3 (11.19)	MPC 3 (11.20)	average value
Settling time(s)	21	19	19	19.67
Overshoot(rpm)	0	0	0	0
Steady tracking error (MSE from 25s to 50s)	212.5983	158.7482	44.0000	138.4488
NOx value (ppm/point)	194.7924	202.4092	197.0302	198.0773

in the defined linear working region, the tracking performance for engine speed is similar, but the settling time and tracking error are least by the proposed method and average

value of NOx emission decreases by 26.7% ((274.9040-201.6374)/274.9040) comparing with MPC 2 which is designed by normal offset-free method. Comparing with MPC 1 which is the normal MPC without disturbance model, the tracking error of engine speed is decreased by 61.2% ((356.8931-138.4488)/356.8931) and NOx emission decreases by 35.1% ((305.2162-198.0773)/305.2162) by the proposed method. In details of Table 5.3, for case 2 by fourth-order model with bigger working region, comparing with MPC 2,the tracking error for engine speed by the proposed method decreases by 70.5% ((158.6875-46.8125)/158.6875) and NOx emission value decreases by 9.1% ((248.0755-225.3903)/248.0755). Comparing with MPC 1, the tracking error for engine speed by the proposed method decreases by 95.3% ((999.1875-46.8125)/999.1875) and NOx emission value decreases by 11.8% ((255.5243-225.3903)/255.5243).

Remark 5.4 *The offset-free design is the modification of normal MPC itself. In this research, there are two control target. At first, we choose the engine speed as the main target which has priority. So weight of engine speed in the cost function in Table 5.1 is 1 which is bigger than the weight of NOx 0.01. As for the second target, the NOx is inevitable which means we cannot control it as zero. To make a compromise, we set the reference value of NOx as 50 ppm. As a result, we can have a good performance of engine speed tracking and NOx in a low level.*

5.7 Summary

This chapter presents an offset-free model predictive control of diesel engine with input constraints. Coupling relationship between the setting variables and nonlinear behavior of the system make the problem difficult to solve by classical control design methods especially with the input constraints. Compared with traditional offset-free tracking control, the disturbance model and state estimate gains are given from a combined design. Furthermore the general solution and method of reduced-order design for H-infinity problem are addressed. A two-step algorithm is presented for the reduced-order controller design which is suitable for additional condition of offset-free tracking. The realtime test results prove that the reference of engine speed can be tracked precisely and the emissions can be reduced feasibly by the proposed method.

MPC has the ability to deal with input constraints. However the limitation of MPC is the computation speed. The simple structure of state feedback control in prior chapter makes it has no such concern.

Chapter 6

Conclusions

6.1 Conclusion

In order to comply with increasingly stringent emission regulations and fuel efficiency standards, the performance of diesel engine should be further improved, especially during the transient condition. In the research, dynamic model-based control method is applied on a real-time diesel engine for satisfying the driver's demand and reducing the exhaust emission. In addition, the techniques for improving the closed-loop performance of model-based control system are developed. The performance is satisfied with following requirement.

- Faster response of engine speed;
- Smaller overshoot of variables during the transient condition of engine speed;
- Accurate tracking of engine speed without steady offset;
- With better transient performance, the NOx value is reduced.

The research is included in one model and two control algorithms.

- Dynamic model of diesel engine by state space equation including air loop and fuel loop together;
- Extended guaranteed cost control algorithm;
- Modified model predictive control algorithm with no steady error.

Finally the designed control algorithms have been tested for the real-time application. The main work of the thesis has been described in Chapter 3, 4, and 5.

In Chapter 3, we develop the diesel engine test bench for investigating the characteristics of diesel engine. It is used for collecting data for modeling and real-time test of control algorithm. After getting data by designed experiment, the linear system identification is applied for model including air loop and fuel loop. The modeling fit for engine speed and NOx for controller design in Chapter 4 is 69.7% and 81.2%. As for controller design in Chapter 5, the second modeling fit for engine speed and NOx is 77.4% and 80.3%. For further discussion of dimension problem, the forth-order model is raised with similar fit. It is proved that the identified dynamic model in state space form can be used for the controller design and real-time test in the following chapters.

In Chapter 4, the guaranteed cost state-feedback tracking control for the diesel engine system with input constraints is presented. The engine process is fast and uncertain. In order to achieve the real-time application, the combustion uncertainties and nonlinear behavior are expressed by parameter uncertainties based on linear state space equations identified in chapter 3. For controller design, the quadratic performance with uncertainty, the inputs constraints and the demand of tracking are guaranteed by three linear matrix inequalities (LMIs). The state feedback and estimate gains are given from feasible solution of an augmented LMI simultaneously. Then the simulation is done to prove the priority of the proposed method with faster response speed and smaller overshoot of engine speed. Furthermore the NOx is reduced at the same time. Finally the real-time test of the proposed control system is applied on our test bench. The experimental results prove that the proposed control system achieve a better performance in precise reference tracking, meanwhile NOx is in a lower level as well. For case 1 in the defined linear working range, the tracking error for engine speed by the proposed method decreases by 37.2% and NOx emission value decreases by 19.2%. For case 2 with bigger working region, the overshoot for engine speed by the proposed method decreases by more than 68.8% and NOx emission value decreases by 38.3%. For case 3 with the biggest working range, the results are similar to case 2.

The main contributions related to this chapter are shown as follows:

- The process of diesel engine through both air and fuel loop is expressed by linear state space equations with parameter uncertainties
- Compared with traditional guaranteed cost control, the state feedback and estimate gains are given from feasible solution of an augmented LMI simultaneously.

- To deal with tracking problem and physical constraints, more LMI conditions are discussed.

Chapter 5 raises an model predictive control for the diesel engine process with no steady error. Since the application of input constraints in the prior chapter is not so convenient, the MPC method becomes an attractive choice. As MPC has more robustness to uncertainties, the main problem is the steady error in real-time application. In order to solve this problem, the definition of disturbance model and state estimate is firstly given. Then the parameters of disturbance model and state estimate gains are obtained from a combined design based on H_∞ theory. For the solution to H_∞ problem, there will be two challenges.

Firstly for general application of H_∞ theory, the general solution is put forward. And the additional condition of offset-free tracking based on this solution is discussed. Secondly with the dimension of the model increasing, the reduced-order design for H_∞ problem is needed. Then a two-step algorithm is presented for the solution which is suitable for the the additional condition of offset-free tracking. Finally the obtained disturbance model and state estimate gain are applied in the solver (qpOASES) of quadratic programming (QP) problem, which is the core of MPC problem. The real-time test by the proposed approach is also done in our test bench. For case 1 in the defined linear working range (2300 2500rpm), the tracking error for engine speed by the proposed method MPC 3 decreases by 61.2 % and NOx emission value decreases by 35.1% comparing with MPC 1 which is designed by normal MPC method. For case 2 with bigger working range (2150 2650rpm), comparing with MPC 1,the tracking error for engine speed by the proposed method decreases by 95.3% and NOx emission value decreases by 11.8%. The experimental results prove that the designed control system can achieve the reference tracking control of engine speed precisely and affectively, meanwhile the emissions can be reduced feasibly. The control performance by forth-order model proves the effectiveness of the proposed reduce-order design. The main contributions related to this chapter are shown as follows:

- Compared with traditional offset-free tracking control, the disturbance model and state estimate gains are given from a combined design based on H_∞ theory.
- The general solution of H_∞ problem is put forward. The additional condition of offset-free tracking based on this solution is discussed.

- With the dimension of the model increasing, the reduced-order design for H_∞ problem is presented.
- A two-step algorithm is presented for the reduced-order design problem which is suitable for the the additional condition of offset-free tracking.

In summary, the relations between traditional methods and proposed methods are shown as follows:

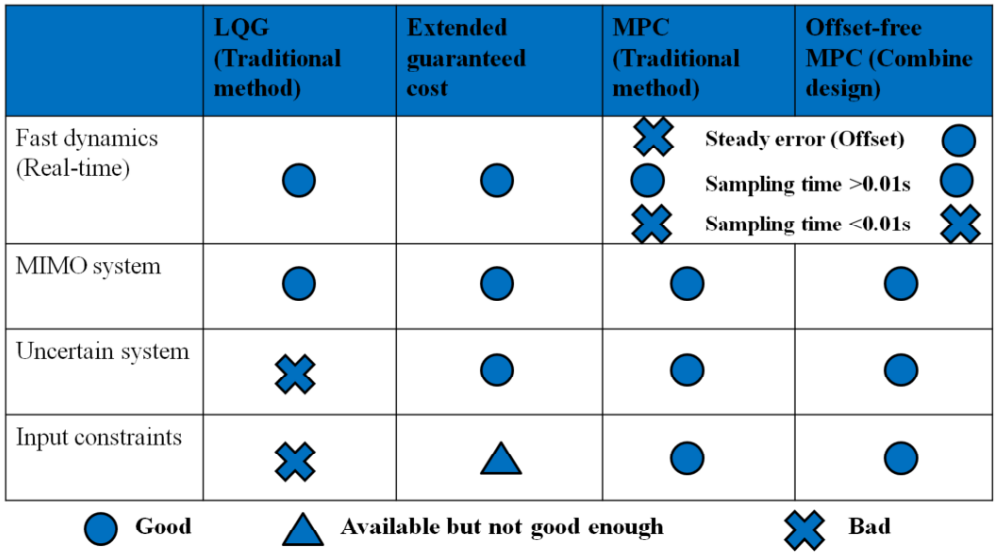

FIGURE 6.1: Relations between traditional methods and proposed methods

As it shows, we can see that the method proposed in Chapter 5 has better ability of handling input constraints than extended guaranteed cost control in Chapter 4. But when sampling time is smaller than $0.01s$, the method of guaranteed cost shows great advantage with simple structure.

6.2 Topics for future research

Despite several progress that has been made in these research, there are still many aspects that needs further investigations. There are two main aspects.

6.2.1 Transient performance between each sub-zone

In order to describe the nonlinear behavior of a diesel engine, the wide operating region is divided into several sub-zone. [54, 62–65]. One example is shown is Figure 6.2 in Chapter 2.

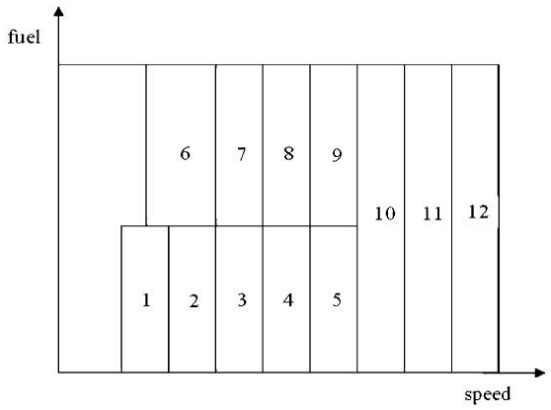

FIGURE 6.2: One example for segmentation of the engine operation region

So it is interesting to see how the performance will be by the proposed method when the diesel engine is working across each sub-zone. But it is not suitable for our test bench currently. The one-cylinder diesel engine we test is YANMAR TF70V-E. Its normal working range is from 1600 to 2700 rpm. It was firstly implemented in our lab in 2002. After so many years and some reform by the company of FC-design and ourselves, its normal working range is currently from 2000 to 2700 rpm. When the engine speed is under 2000 rpm, the engine will flameout itself. So almost the entire normal working range is tested in our experimental results. If possible, I hope that the proposed method could be tested when the engine is working across the sub-zones.

The proposed methods could be easily applied into multiple sub-zones.

- **Gain scheduling method**
  Different from [52, 68, 105], the gain scheduling method discussed here is not

based on LPV model. The state feedback gain and state estimate gain are obtained by the strategy proposed in Chapter 4 in each sub-zone. W

-zones will be much less than the original linear methods. The logic of gain scheduling is that it depends on the engine speed. For example, there are two sub-zones, one is from 1000 rpm to 2000 rpm, and the other one is from 2000 rpm to 3000 rpm. When engine speed is changing from 1900 rpm to 2500 rpm, the state feedback gain and state estimate gain change at the point of 2000 rpm. The transient performance will be an interesting topic to discuss.

- **Multi-MPCs**
  The MPC algorithm could be easily extended into Multiple MPCs. In simulink of MATLAB, there are tools of multiple MPCs that can switch between multiple implicit MPC controllers. In each linear sub-zone, one MPC controller could be obtained by the strategy proposed in Chapter 5. Also the transient performance between each sub-zone needs to be further studied.

6.2.2 Nonlinear control method

With the development of hardware, the computation speed will be satisfied to apply the nonlinear method for diesel engine control. The neural network-based nonlinear model predictive control will be an interesting choice. The whole working range of the engine can be described by the neural network. And the QP solver for NMPC will be used for on-line application. The structure of neural network-based nonlinear model predictive control is shown in Figure 6.3.

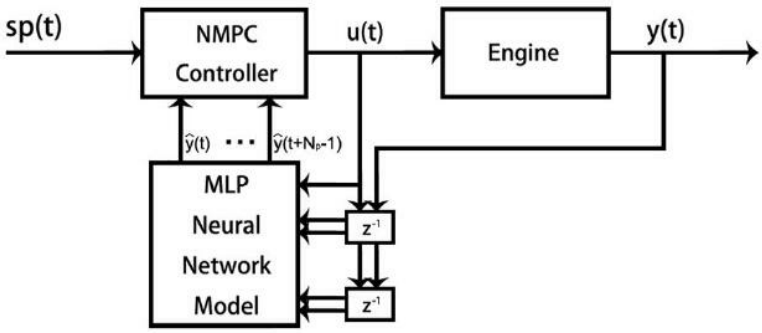

FIGURE 6.3: Structure of neural network-based nonlinear model predictive control

The challenge of this method consists of the following two parts:

- **Neural network model**
  Just as the Figure 6.3 shows, the model here is with the simple structure of MLP for fast computation speed. As for the parameters in neural network such as number of neurons, the number of delays, it needs further study in consideration of computation speed and model prediction accuracy.

- **NMPC solver**
  The computation speed of NMPC solver is a critical issue. It is very important for real-time application of neural network-based nonlinear model predictive control. The research on NMPC solver has been a very hot topic. As far as I am concerned, the parallel algorithm will be a solution of increasing speed of computation.

6.2.3 Application in production diesel engine

Since our research is focused on real-time test in engine test bench, the application and improvement of production diesel engine are worth looking forward to. I will work in the research center in company of DENSO. DENSO is a company that is world-top of engine technology. There are many research about transient control of engine. I hope my knowledge will be useful in the development of engine technology, and I will try my best to make contribution to the society for a better world in the future.

Bibliography

[1] A. Alagumalai, "Internal combustion engines: Progress and prospects," *Renewable and Sustainable Energy Reviews*, vol. 38, pp. 561–571, 2014.

[2] M. Hannan, F. Azidin, and A. Mohamed, "Hybrid electric vehicles and their challenges: A review," *Renewable and Sustainable Energy Reviews*, vol. 29, pp. 135–150, 2014.

[3] A. Gurney, H. Ahammad, and M. Ford, "The economics of greenhouse gas mitigation: Insights from illustrative global abatement scenarios modelling," *Energy Economics*, vol. 31, pp. S174–S186, 2009.

[4] W. Knecht, "Diesel engine development in view of reduced emission standards," *Energy*, vol. 33, no. 2, pp. 264–271, 2008.

[5] L. Guzzella and A. Amstutz, "Control of diesel engines," *IEEE control systems*, vol. 18, no. 5, pp. 53–71, 1998.

[6] L. Guzzella and C. Onder, *Introduction to modeling and control of internal combustion engine systems*. Springer Science & Business Media, 2009.

[7] I. Park, S. Hong, and M. Sunwoo, "Robust air-to-fuel ratio and boost pressure controller design for the egr and vgt systems using quantitative feedback theory," *IEEE Transactions on Control Systems Technology*, vol. 22, no. 6, pp. 2218–2231, 2014.

[8] E. J. Bissett, "Mathematical model of the thermal regeneration of a wall-flow monolith diesel particulate filter," *Chemical Engineering Science*, vol. 39, no. 7-8, pp. 1233–1244, 1984.

[9] V. Rapp, N. Killingsworth, P. Therkelsen, and R. Evans, "Lean-burn internal combustion engines," in *Lean Combustion (Second Edition)*. Elsevier, 2016, pp. 111–146.

[10] H. Stuhler, T. Kruse, A. Stuber, K. Gschweitl, W. Piock, H. Pfluegl, and P. Lick, "Automated model-based gdi engine calibration adaptive online doe approach," SAE Technical Paper, Tech. Rep., 2002.

[11] S. J. Korn, "An advanced diesel fuels test program," *SAE Transactions*, pp. 79–95, 2001.

[12] N. Tietze, U. Konigorski, C. Fleck, and D. Nguyen-Tuong, "Model-based calibration of engine controller using automated transient design of experiment," in *14. Internationales Stuttgarter Symposium*. Springer, 2014, pp. 1587–1605.

[13] E. Millich, C. Bohn, H. Braun, and M. Schultalbers, "A highly efficient simulation-based calibration method exemplified by the charge control," SAE Technical Paper, Tech. Rep., 2005.

[14] M. R. Kianifar, F. Campean, and A. Wood, "Application of permutation genetic algorithm for sequential model building–model validation design of experiments," *Soft Computing*, vol. 20, no. 8, pp. 3023–3044, 2016.

[15] S. Mosbach, A. Braumann, P. L. Man, C. A. Kastner, G. P. Brownbridge, and M. Kraft, "Iterative improvement of bayesian parameter estimates for an engine model by means of experimental design," *Combustion and Flame*, vol. 159, no. 3, pp. 1303–1313, 2012.

[16] R. G. Prucka, "An experimental characterization of a high degree of freedom spark-ignition engine to achieve optimized ignition timing control." 2008.

[17] H. Borhan and E. Hodzen, "A robust design optimization framework for systematic model-based calibration of engine control systems," *Journal of Engineering for Gas Turbines and Power*, vol. 137, no. 11, p. 111601, 2015.

[18] E. G. Giakoumis, C. D. Rakopoulos, A. M. Dimaratos, and D. C. Rakopoulos, "Exhaust emissions of diesel engines operating under transient conditions with biodiesel fuel blends," *Progress in Energy and Combustion Science*, vol. 38, no. 5, pp. 691–715, 2012.

[19] B. Berger, "Modeling and optimization for stationary base engine calibration," Ph.D. dissertation, Technische Universität München, 2012.

[20] D. Wu, M. Ogawa, Y. Suzuki, H. Ogai, and J. Kusaka, "Modified multi-objective particle swarm optimization: Application to optimization of diesel engine control parameter," *SICE Journal of Control, Measurement, and System Integration*, vol. 3, no. 5, pp. 315–323, 2010.

[21] T. Lee and R. D. Reitz, "Response surface method optimization of a hsdi diesel engine equipped with a common rail injection system," in *2001 Fall Technical Conference of the ASME Internal Combustion Engine Division*, vol. 1, 2002, pp. 89–95.

[22] B. Wahono and H. Ogai, "Construction of response surface model for diesel engine using stepwise method," in *The 6th International Conference on Soft Computing and Intelligent Systems, and The 13th International Symposium on Advanced Intelligence Systems*. IEEE, 2012, pp. 989–994.

[23] B. Wahono, H. Ogai, M. Ogawa, J. Kusaka, and Y. Suzuki, "Diesel engine optimization control methods for reduction of exhaust emission and fuel consumption," in *2012 IEEE/SICE International Symposium on System Integration (SII)*. IEEE, 2012, pp. 722–727.

[24] T. Ganapathy, R. Gakkhar, and K. Murugesan, "Optimization of performance parameters of diesel engine with jatropha biodiesel using response surface methodology," *International Journal of Sustainable Energy*, vol. 30, no. sup1, pp. S76–S90, 2011.

[25] J. B. Hirkude and A. S. Padalkar, "Performance optimization of ci engine fuelled with waste fried oil methyl ester-diesel blend using response surface methodology," *Fuel*, vol. 119, pp. 266–273, 2014.

[26] M. Pandian, S. Sivapirakasam, and M. Udayakumar, "In - fect of injection system parameters on performance and emission characteristics of a twin cylinder compression ignition direct injection engine fuelled with pongamia biodiesel–diesel blend using response surface methodology," *Applied Energy*, vol. 88, no. 8, pp. 2663–2676, 2011.

[27] Z. Qiangqiang, L. Bolan, S. Xiaochen, C. Zhang, and H. Jingchao, "Model based calibration for improving fuel economy of a turbocharged diesel engine." *Thermal Science*, vol. 22, no. 3, 2018.

[28] S. Park, Y. Kim, S. Woo, and K. Lee, "Optimization and calibration strategy using design of experiment for a diesel engine," *Applied Thermal Engineering*, vol. 123, pp. 917–928, 2017.

[29] F -
chine learning tool for diesel engine air path calibration," SAE Technical Paper, Tech. Rep., 2014.

[30] M.-B. C. T. User's, "Guide. the mathworks," *Inc., Natick, MA, USA*, 2004.

[31] J. M. Desantes, J. J. López, J. M. García, and L. Hernández, "Application of neural networks for prediction and optimization of exhaust emissions in a hd diesel engine," *SAE Transactions*, pp. 1993–2002, 2002.

[32] Q. Zhou, A. Gullitti, J. Xiao, and Y. Huang, "Neural network–based modeling and optimization for effective vehicle emission testing and engine calibration," *Chemical Engineering Communications*, vol. 195, no. 6, pp. 706–720, 2008.

[33] M. Akcayol, C. Cinar, H. I. Bulbul, and A. Kilicarsalan, "Artificial neural network based modeling of injection pressure in diesel engines," in *4th WSEAS Int. Conf. on Information Science, Communications and Applications (ISA 2004)*. Citeseer, 2004, pp. 21–23.

[34] E. Samadani, A. H. Shamekhi, M. H. Behroozi, and R. Chini, "A method for pre-calibration of di diesel engine emissions and performance using neural network and multi-objective genetic algorithm," *Iranian Journal of Chemistry and Chemical Engineering (IJCCE)*, vol. 28, no. 4, pp. 61–70, 2009.

[35] K. Razmjooei and G. Nagarajan, "Optimization of di diesel engine operating parameters using a response surface method," SAE Technical Paper, Tech. Rep., 2010.

[36] J. H. Holland, "Genetic algorithms and the optimal allocation of trials," *SIAM Journal on Computing*, vol. 2, no. 2, pp. 88–105, 1973.

[37] J. M. Alonso, F. Alvarruiz, J. M. Desantes, L. Hernández, V. Hernández, and G. Molto, "Combining neural networks and genetic algorithms to predict and reduce diesel engine emissions," *IEEE transactions on evolutionary computation*, vol. 11, no. 1, pp. 46–55, 2007.

[38] T. Hiroyasu, M. Miki, J. Kamiura, S. Watanabe, and H. Hiroyasu, "Multi-objective optimization of diesel engine emissions and fuel economy using genetic algorithms and phenomenological model," SAE Technical Paper, Tech. Rep., 2002.

[39] T. Hiroyasu, "Diesel engine design using multi-objective genetic algorithm," in *Japan/US Workshop on Design Environment 2004*. Citeseer, 2004.

[40] H. Hiroyasu, H. Miao, T. Hiroyasu, M. Miki, J. Kamiura, and S. Watanabe, "Optimization of diesel engine emissions and fuel efficiency using genetic algorithms and phenomenological model with egr, injection timing and multiple injections," in *5th Stuttgart Symposium, Stuttgart (Germany)*, 2003.

[41] T. Hiroyasu, M. Miki, S. Nakayama, and Y. Hanada, "Multi-objective optimization of diesel engine emissions and fuel economy using spea2+," in *Proceedings of the 7th annual conference on Genetic and evolutionary computation*. ACM, 2005, pp. 2195–2196.

[42] R. Eberhart and J. Kennedy, "Particle swarm optimization," in *Proceedings of the IEEE international conference on neural networks*, vol. 4. Citeseer, 1995, pp. 1942–1948.

[43] P. Karra and S.-C. Kong, "Application of particle swarm optimization for diesel engine performance optimization," SAE Technical Paper, Tech. Rep., 2010.

[44] P. K. Karra and S.-C. K

–903, 2010.

[45] R. S. Benson, J. Ledger, N. D. Whitehouse, and S. Walmsley, "Comparison of experimental and simulated transient responses of a turbocharged diesel engine," SAE Technical Paper, Tech. Rep., 1973.

[46] D. Winterbone, C. Thiruarooran, and P. Wellstead, "A wholly dynamic model of a turbocharged diesel engine for transfer function evaluation," SAE Technical Paper, Tech. Rep., 1977.

[47] S. S. Shamsi, "Development of a real-time digital computer simulation of a turbocharged diesel engine," SAE Technical Paper, Tech. Rep., 1980.

[48] G. Gissinger, R. Renard, and M. Hassenforder, "Model based design and control of diesel engines," SAE Technical Paper, Tech. Rep., 1989.

[49] M. Kao and J. J. Moskwa, "Turbocharged diesel engine modeling for nonlinear engine control and state estimation," *Journal of dynamic systems, measurement, and control*, vol. 117, no. 1, pp. 20–30, 1995.

[50] E. Hendricks, "Mean value modelling of large turbocharged two-stroke diesel engines," SAE Technical Paper, Tech. Rep., 1989.

[51] J.-P. Jensen, A. Kristensen, S. C. Sorenson, N. Houbak, and E. Hendricks, "Mean value modeling of a small turbocharged diesel engine," SAE Technical Paper, Tech. Rep., 1991.

[52] M. Jung, "Mean-value modelling and robust control of the airpath of a turbocharged diesel engine," Ph.D. dissertation, University of Cambridge, 2003.

[53] R. Omran, R. Younes, and J.-C. Champoussin, "Optimal control of a variable geometry turbocharged diesel engine using neural networks: Applications on the etc test cycle," *IEEE Transactions on Control Systems Technology*, vol. 17, no. 2, p. 380, 2009.

[54] D. Zhao, C. Liu, R. Stobart, J. Deng, E. Winward, and G. Dong, "An explicit model predictive control framework for turbocharged diesel engines," *IEEE Transactions on Industrial Electronics*, vol. 61, no. 7, pp. 3540–3552, 2014.

[55] M. Ammann, N. P. Fekete, L. Guzzella, and A. H. Glattfelder, "Model-based control of the vgt and egr in a turbocharged common-rail diesel engine: theory and passenger car implementation," SAE Technical Paper, Tech. Rep., 2003.

[56] S. Billings, S. Chen, and R. Backhouse, "The identification of linear and nonlinear models of a turbocharged automotive diesel engine," *Mechanical Systems and Signal Processing*, vol. 3, no. 2, pp. 123–142, 1989.

[57] J. Saint-Donat, N. Bhat, and T. J. McAvoy, "Neural net based model predictive control," *International Journal of Control*, vol. 54, no. 6, pp. 1453–1468, 1991.

[58] Y. Zhai, "Advanced neural network based control for automotive engines," Ph.D. dissertation, Liverpool John Moores University, 2009.

[59] L. Cheng, W. Liu, Z.-G. Hou, J. Yu, and M. Tan, "Neural-network-based nonlinear model predictive control for piezoelectric actuators," *IEEE Transactions on Industrial Electronics*, vol. 62, no. 12, pp. 7717–7727, 2015.

[60] A. Afram, F. Janabi-Sharifi, A. S. Fung, and K. Raahemifar, "Artificial neural network (ann) based model predictive control (mpc) and optimization of hvac systems: A state of the art review and case study of a residential hvac system," *Energy and Buildings*, vol. 141, pp. 96–113, 2017.

[61] S. Wang, D. Yu, J. Gomm, G. Page, and S. Douglas, "Adaptive neural network model based predictive control for air–fuel ratio of si engines," *Engineering Applications of Artificial Intelligence*, vol. 19, no. 2, pp. 189–200, 2006.

[62] H. J. Ferreau, P. Ortner, P. Langthaler, L. Del Re, and M. Diehl, "Predictive control of a real-world diesel engine using an extended online active set strategy," *Annual Reviews in Control*, vol. 31, no. 2, pp. 293–301, 2007.

[63] X. Wang, H. Waschl, D. Alberer, and L. Del Re, "A design framework for predictive engine control," *Oil & Gas Science and Technology–Revue d'IFP Energies nouvelles*, vol. 66, no. 4, pp. 599–612, 2011.

[64] P. Ortner, P. Langthaler, J. G. Ortiz, and L. Del Re, "Mpc for a diesel engine air path using an explicit approach for constraint systems," in *Proc. IEEE International Conference on Control Applications*, 2006, pp. 2760–2765.

[65] P. Ortner and L. Del Re, "Predictive control of a diesel engine air path," *IEEE transactions on control systems technology*, vol. 15, no. 3, pp. 449–456, 2007.

[66] D. Liu, H. Javaherian, O. Kovalenko, and T. Huang, "Adaptive critic learning techniques for engine torque and air–fuel ratio control," *IEEE Transactions on Systems, Man, and Cybernetics, Part B (Cybernetics)*, vol. 38, no. 4, pp. 988–993, 2008.

[67] M. Herceg, T. Raff, R. Findeisen, and F. Allgowe, "Nonlinear model predictive control of a turbocharged diesel engine," in *Computer Aided Control System Design, 2006 IEEE International Conference on Control Applications, 2006 IEEE International Symposium on Intelligent Control, 2006 IEEE*. IEEE, 2006, pp. 2766–2771.

[68] P. Ortner, R. Bergmann, H. J. Ferreau, and L. Del Re, "Nonlinear model predictive control of a diesel engine airpath," *IFAC Proceedings Volumes*, vol. 42, no. 2, pp. 91–96, 2009.

[69] M. Karlsson, K. Ekholm, P. Strandh, R. Johansson, and P. Tunestal, "Lqg control for minimization of emissions in a diesel engine," in *2008 IEEE International Conference on Control Applications*. IEEE, 2008, pp. 245–250.

[70] F -path systems for advanced diesel engines," in *ASME 2009 Dynamic Systems and Control Conference*. American Society of Mechanical Engineers, 2009, pp. 281–287.

[71] J. D. López, J. J. Espinosa, and J. R. Agudelo, "Lqr control for speed and torque of internal combustion engines," *IFAC Proceedings Volumes*, vol. 44, no. 1, pp. 2230–2235, 2011.

[72] M. Karlsson, K. Ekholm, P. Strandh, R. Johansson, and P. Tunestal, "Multiple-input multiple-output model predictive control of a diesel engine," *Advances in Automotive Control*, pp. 131–136, 2010.

[73] L. Ljung, *System identification: theory for the user*. Prentice-hall, 1987.

[74] T. Söderström and P. Stoica, "System identification," 1989.

[75] L. Ljung, *System Identification: Theory for the User*. Pearson Education, 1998.

[76] Y. Zhu, *Multivariable system identification for process control*. Elsevier, 2001.

[77] N. T. Hung, I. Ismail, N. B. Saad, L. Tufa, and M. Irfan, "Design of optimal gbn sequences for identification of mimo systems," in *Control Conference (ASCC), 2015 10th Asian*. IEEE, 2015, pp. 1–6.

[78] L. Ljung, "System identification toolbox for use with {MATLAB}," 2007.

[79] M. KOTHARE, "Robust constrained model predictive control using linear matrix inequalities," *Automatica*, vol. 32, no. 10, pp. 1361–1379, 1996.

[80] J. Wu, S. K. Nguang, J. Shen, G. J. Liu, and Y. G. Li, "Guaranteed cost nonlinear tracking control of a boiler-turbine unit: an lmi approach," *International Journal of Systems Science*, vol. 41, no. 7, pp. 889–895, 2010.

[81] L. Yu and F. Gao, "Optimal guaranteed cost control of discrete-time uncertain systems with both state and input delays," *Journal of the Franklin Institute*, vol. 338, no. 1, pp. 101–110, 2001.

[82] L. Yu, Q.-L. Han, and M.-X. Sun, "Optimal guaranteed cost control of linear uncertain systems with input constraints," *International Journal of Control, Automation, and Systems*, vol. 3, no. 3, pp. 397–402, 2005.

[83] J. Xu, Y. Wang, and H. Wu, "Lmi based tracking guaranteed cost control," in *Mechatronics and Automation, Proceedings of the 2006 IEEE International Conference on*. IEEE, 2006, pp. 1037–1042.

[84] H. Mukaidani, Y. Ishii, N. Bu, Y. Tanaka, and T. Tsuji, "Lmi-based neurocontroller for state-feedback guaranteed cost control of discrete-time uncertain system," *IEICE transactions on information and systems*, vol. 88, no. 8, pp. 1903–1911, 2005.

[85] F

Information and Automation (ICIA), 2010 IEEE International Conference on. IEEE, 2010, pp. 335–339.

[86] X. Yang and H. Gao, "Guaranteed cost output tracking control for autonomous homing phase of spacecraft rendezvous," *Journal of Aerospace Engineering*, vol. 24, no. 4, pp. 478–487, 2010.

[87] C.-H. Lien, "Robust observer-based control of systems with state perturbations via lmi approach," *IEEE Transactions on Automatic Control*, vol. 49, no. 8, pp. 1365–1370, 2004.

[88] H. Lens and J. Adamy, "Observer based controller design for linear systems with input constraints," in *Proceeding of the 17th World Congress, The International Federation of Automatic Control*, 2008.

[89] S. Boyd, L. El Ghaoui, E. Feron, and V. Balakrishnan, *Linear matrix inequalities in system and control theory*. Siam, 1994, vol. 15.

[90] G. Stewart and F. Borrelli, "A model predictive control framework for industrial turbodiesel engine control," in *2008 47th IEEE conference on decision and control*. IEEE, 2008, pp. 5704–5711.

[91] K. R. Muske and T. A. Badgwell, "Disturbance modeling for offset-free linear model predictive control," *Journal of Process Control*, vol. 12, no. 5, pp. 617–632, 2002.

[92] G. Pannocchia and J. B. Rawlings, "Disturbance models for offset-free model-predictive control," *AIChE journal*, vol. 49, no. 2, pp. 426–437, 2003.

[93] G. Pannocchia and A. Bemporad, "Combined design of disturbance model and observer for offset-free model predictive control," *IEEE Transactions on Automatic Control*, vol. 52, no. 6, pp. 1048–1053, 2007.

[94] P. Gahinet and P. Apkarian, "A linear matrix inequality approach to h_∞ control," *International journal of robust and nonlinear control*, vol. 4, no. 4, pp. 421–448, 1994.

[95] P. Gahinet, "Explicit controller formulas for lmi-based h_∞ synthesis," *Automatica*, vol. 32, no. 7, pp. 1007–1014, 1996.

[96] H. D. Tuan, P. Apkarian, and T. Q. Nguyen, "Robust and reduced-order filtering: new lmi-based characterizations and methods," *IEEE Transactions on Signal Processing*, vol. 49, no. 12, pp. 2975–2984, 2001.

[97] P. Apkarian, D. Noll, and H. Duong Tuan, "Fixed-order h_∞ control design via a partially augmented lagrangian method," *International Journal of Robust and Nonlinear Control: IFAC-Affiliated Journal*, vol. 13, no. 12, pp. 1137–1148, 2003.

[98] P. Apkarian, D. Noll, J.-B. Thevenet, and H. D. Tuan, "A spectral quadratic-sdp method with applications to fixed-order h_2 and h_∞ synthesis," *European Journal of Control*, vol. 10, no. 6, pp. 527–538, 2004.

[99] A. Molina-Cristobal, I. Griffin, P. Fleming, and D. Owens, "Multiobjective controller design: Optimising controller structure with genetic algorithms," *IFAC Proceedings Volumes*, vol. 38, no. 1, pp. 51–56, 2005.

[100] F

-3, pp. 542–575, 2006.

[101] C. M. Agulhari, R. C. Oliveira, and P. L. Peres, "Lmi relaxations for reduced-order robust h_∞ control of continuous-time uncertain linear systems," *IEEE Transactions on Automatic Control*, vol. 57, no. 6, pp. 1532–1537, 2012.

[102] A. Sadeghzadeh, "Robust reduced-order controller synthesis: a dilated lmi approach," *IMA Journal of Mathematical Control and Information*, vol. 34, no. 2, pp. 479–499, 2015.

[103] A. P. Popov, H. Werner, and M. Millstone, "Fixed-structure discrete-time h_∞ controller synthesis with hifoo," in *49th IEEE Conference on Decision and Control (CDC)*. IEEE, 2010, pp. 3152–3155.

[104] H. J. Ferreau, C. Kirches, A. Potschka, H. G. Bock, and M. Diehl, "qpoases: A parametric active-set algorithm for quadratic programming," *Mathematical Programming Computation*, vol. 6, no. 4, pp. 327–363, 2014.

[105] X. Wei and L. Del Re, "Gain scheduled h_∞ control for air path systems of diesel engines using lpv techniques," *IEEE transactions on control systems technology*, vol. 15, no. 3, pp. 406–415, 2007.

Publication List

Journal Paper

1. G.Yu, H.Ogai and H.Deng, "Extended Guaranteed Cost Control of Diesel Engine via LMI Approach", *IEEJ Trans. on Electrical and Electronic Engineering, Vol.13, No.3*, pp.496-504, 2018.

2. G.Yu, H.Ogai and H.Deng, "Offset-free model predictive control of diesel engine by combined design of disturbance model and observer", *IEEJ Trans. on Electrical and Electronic Engineering, Vol.14, No.1*, pp.116-129, 2019.

International Conference Paper

1. G.Yu and H.Ogai, "Transient control for diesel engine based on dynamic mathematical model", *SICE Annual Conference (SICE 2014) Proceedings of the IEEE (Sapporo)*, 2014, pp.446-451.

2. G.Yu, H.Ogai and H.Deng, "Offset-free model predictive control of diesel engine by combined design of disturbance model and observer", *SICE Annual Conference (SICE 2017), Proceedings of the IEEE (Kanazawa)*, 2017, pp.1577-1582.

Domestic Conference Paper

1. H.Deng, G.Yu, H.Zhang, Y.Shimizu and H.Ogai, "Diesel Engine Transient Control of RPM Tracking and Emission Decreasing using Model Predictive Control", *The 3rd Multi-s (MSCS 2016) (Nagoya)*, 2016, pp.527-533.